UNIVERSITÀ DEGLI STUDI DI TRIESTE

UNIVERSITÀ ARISTOTELE DI SALONICO

XXXIII CICLO DEL DOTTORATO DI RICERCA

IN

METODOLOGIE DI BIOMONITORAGGIO DELL' ALTERAZIONE AMBIENTALE

MEDITERRANEAN FOREST SPECIES MAPPING

USING HYPERSPECTRAL IMAGERY

Settore scientifico-disciplinare: BIO/07

DOTTORANDA
GIORGIA GALIDAKI

COORDINATORE
Chiar.mo Prof. ALBERTO PALLAVICINI

SUPERVISORE DI TESI
Chiar.mo Prof. ENRICO FEOLI

CO-SUPERVISORE DI TESI
Chiar.mo Prof. IOANNIS GITAS

ANNO ACCADEMICO 2011 / 2012

This academic journey started when I was feeling sad and empty in soggy northern London, and....

- Pr. Gitas told me "come back in the lab, there is always a place for you here!"
- Pr. Feoli told me "I would love to work with you!"
- my family said "go ahead and do what you love, we are always here for you!"
- my friends said "PhD, why not? I will start one too!"

....and was kept alive by all the "you can do it, I am sure you can! go on!" by all these people, my extended family, my husband, my new family, my fellow researchers, and by my deep childhood love for research and academia!

I tried hard to complete this project but nothing would have been possible without the support of the people that surround me. This study is their accomplishment too and their name should be noted if not in the first page, at least in the second!

Without any further literary delirium, here are my colleagues in this study. Each of them had a unique and irreplaceable contribution and each one of them deserves my honest respect and deep gratitude:

Marina Galidaki, Nikos Galidakis, Giannis Galidakis, Thomas Lagkas, my sweet endless love Giorgos Lagkas , Pr. Ioannis Gitas, Pr. Enrico Feoli, Dr. Dragan Massimo, Pr. Mauro Tretiach, Dr. Andrea Nardini, Pr. Pier Luigi Nimis, Dr. Pierluigi Barbieri, Pr. Alberto Pallavicini, Dr. Piero Giulianini, Evi Fasouli, Elena Benedetti, Simona Silva, Fabio Strechelli, Stefania Arabito, Dr. Michela Sesso, Dr. Elisa Malisana, Dr. Claudia Blason, Luca Dorigo, Tassoula Lagka, Giorgos Lagkas, Lina Lagka, Iliana Fylla, Giorgos Fyllas, Lina Fylla, Sparti Katsigaraki, Rudolf, Maria Dimitropoulou, Katerina Valta, Danae Georgakopoulou, Nikos Androutsopoulos, Kimon Fasoulas, Nikolas Dalianis, Dr. Jim Stavrakoudis, Eleni Dragozi, Maria Tompoulidou, Dr. Anastasia Polychronaki, Chara Minakou, Pr. Giorgos Mallinis, Pr. Dimitris Karamanolis, Pr. Michalis Karteris, Dr. Vassilis Giannakopoulos, Dr. Giannis Stergiopoulos, Dinos Dimitrakopoulos, Dr. Periklis Toukiloglou, Dimitra Papadopoulou, George Panourgias, Thanos Jovico, Giorgos Buikis, Capriccios, Patty Roma.

This study took me 5 long years, in which many wonderful things happened, however always in its shadow! I am glad it has finished and I can now focus on something new, carrying this study neatly packed in my luggage...

I feel strong and I feel ready! Further research here I come!

Table of Contents

List of Figures

List of Tables

List of Abbreviations

ANN	Artificial Neural Network
EEA	European Environmental Agency
EFI	European Forest Institute
EUFORGEN	European Forest Genetic Resources Programme
GEOBIA	Geographic Object Based Image Approach
JRC	Joint Research Centre (European Commission)
KIA	Kappa Index of Agreement
LDA	Linear Discriminant Analysis
LR	Linear Regression
MDC	Minimum Distance Classifier
MhDC	Mahalanobis Distance Classifier
MLC	Maximum Likelihood Classifier
MNF	Minimum Noise Fraction
MTMF	MixtureTuned Matched Filtering
NCWI	National Coastal Wetlands Inventory (United States)
NN	Nearest Neighbor
OA	Overall Accuracy
PCA	Principal Components Analysis
RA	Regression Analysis
SAM	Spectral Angle Mapper
SCBD	Secretariat of the Convention on Biological Diversity
SCM	Spectral Correlation Mapper
SMM	Spectral Mixture Modeling
SVM	Support Vector Maschines
UNCBD	UN Convention on Biological Diversity
UNFCCC	UN Framework Convention on Climate Change
UN-REDD	UN Collaborative Programme on Reducing Emissions from Deforestation and Forest Degradation in Developing Countries

1

INTRODUCTION

Forest has been a natural resource of vital importance to mankind through history, and its sustainable management is a core objective with numerous aspects. Forests are increasingly recognized as ecological systems of fundamental importance for environmental protection not only at the regional level but also on the global scale.

The value of forests is largely related to their **environmental and social functions.** Forests regulate local and global climate, ameliorate weather events, and regulate the hydrological cycle. Among other services they provide timber, fuelwood and non-timber forest products, flora and fauna biodiversity and genetic information and insurance, watershed protection, carbon storage and sequestration, as well as grounds for recreation and research (SCBD, 2001).

Mediterranean forest is found in five widely separated regions, characterized by **Mediterranean-type climates.** Although they represent a **small fraction of the world's forest** cover, they are very important because they are **hotspots** for plant and animal diversity (Myers et al., 2000), but also because these regions are hotspot of human population growth (Corona and Mariano, 1992; Cowling et al., 1996).

The Mediterranean rim, in particular, has been colonized by men for possibly more than 10,000 years (Di Castri, 1981), and this coevolution of man and forest formed and kept a dynamic equilibrium at least until the Second World War (Caravello and Giacomin, 1993). Over the last half century, plains are being increasingly utilized, hilly and mountain areas are being abandoned and naturally reforested, and agricultural land and human settlements are quickly increasing along the coastline (MacDonald et al., 2000), forcing uneven pressures on Mediterranean forests.

Also, the Mediterranean area is especially sensitive to any climate change because it represents a transition zone between the arid and humid regions of the world (Scarascia-Mugnozza et al.,

2000). The effects of climate change are mainly anticipated though an increase in fire frequency and other processes driven by drought stress (Fyllas et al., 2008).

The aforementioned rapid and abrupt human induced stresses, compound with the presumed climatic change, which is expected to drastically modify growing conditions for trees, is very likely to diminish forested areas within the Mediterranean basin and to replace them by fire prone shrub communities (de Rios et al., 2007).

As it is apparent, Mediterranean forests need to be understood, described, monitored and preserved. In all these cases, **spatial information**, regarding geographic location, spatial extent, structure and biodiversity among others, is essential and traditionally collected with all means available.

In particular, forest species mapping is an objective and a prerequisite in various applications that span in the fields of **ecology, biology, forestry** and **agriculture**, such as resource inventories, biodiversity assessment, fire hazard assessment, conservation planning, pest and environmental stress management, monitoring changes, and assessing per-species carbon sequestration.

Adding to that, forest species information is also essential for the national reporting obligations towards national and international policies, such as the UN Framework Convention on Climate Change (UNFCCC) and its Kyoto Protocol, the UN Convention on Biological Diversity (UNCBD), the UN Collaborative Programme on Reducing Emissions from Deforestation and Forest Degradation in Developing Countries (UN-REDD), the Ministerial Conference on the Protection of Forests in Europe (MCPFE), and the Streamlining European 2010 Biodiversity Indicators (SEBI2010).

Remote Sensing that provides systematic, repetitive and consistent observations has long proven to be valuable in forest management, as it allows for reduction in the costs of forest inventories and improvement in the accuracy of the fieldwork results (Muinonen and Tokola 1990; Tomppo, 1993; MacDonald et al., 2000; Wulder et al., 2003; Remmel et al., 2005; McRoberts and Tomppo, 2007; Tomppo et al., 2008). Turner et al. (2001), also commented that, although at the landscape scale remote sensing is a handy tool, at regional and global scales is almost a necessity.

Remote sensing data are valuable in forest studies and management and have been used for various types of forest maps and forest inventories, in scales form local to global (Hyyppä et al., 2000; Myeni et al., 2001; Dong et al., 2003; Frankenberg et al., 2005; Gibbs et al., 2007).

However, use of multispectral imagery, which has been available for more than 30 years, has necessarily focused on landcover and broad vegetation types (Loveland, 2000) rather than discrimination of vegetation at a species level. Plant species composition, unlike other vegetation attributes, is difficult to detect with traditional remote sensing techniques (Schmidtlein and Sassin, 2004) and it is conventionally collected with typically expensive and time-consuming field based investigations, which can only provide information from sparse points of collection.

Advances in **hyperspectral technology**, which is capable of resolving the spectrum in continuous narrow bands and allow detection of subtle spectral changes of various targets, overcome such limitations and provide means for in depth analysis of forest species (Nagendra and Rocchini, 2008; Heumann, 2011a). Further, the availability of hyperspectral data has led to the investigation and development of innovative techniques for their exploitation (Nagendra and Rocchini, 2008; Heumann, 2011a).

Airborne hyperspectral sensors such as AVIRIS, CASI, HyMap and PROBE-1 have been used with success in species level vegetation mapping (Martin et al. 1998; Schmidt and Skidmore, 2001; Aspinal, 2002; Parker Williams and Hunt, 2002; Buddenbaum et al., 2005; Chom et al., 2010; Dalponte et al., 2012). While they present many advantages, like fine spatial resolution and minimum atmospheric influence, their high cost limits their operational use in regional scales.

On the other hand, **spaceborne** hyperspectral sensors, such as Hyperion onboard NASA's EO1, though they provide moderate spatial resolution and introduce error related to the long pathway of radiation between target feature and sensor, they have appealing advantages, such as the broad scale, low cost and repeatable collection, which make them applicable to real world problems.

Since hyperspectral imagery in general and Hyperion imagery specifically has given promising results in species discrimination studies (Townsend and Foster, 2003; Ramsey III et al., 2005; Pengra et al., 2007; Tsai et al., 2007; Vyas et al., 2011), it is very challenging to assess its applicability in **Greek forest**.

Two typical Mediterranean type forest areas, Thassos Island covered with pines and Taxiarchis covered with both pines and deciduous species, have been chosen to study the use of EO1 Hyperion imagery in species level mapping. The **challenge** is to provide a methodology for cost effective, repetitive, regional mapping of forest species, which could be implemented in standard remote sensing systems.

To exploit the opportunities mentioned above and address the aforementioned needs, this study aims to investigate the potential of employing satellite hyperspectral imagery in Mediterranean forest species mapping, in two typical Greek forests. The specific objectives are:

I. To investigate the performance of Spectral Angle Mapper (SAM), a traditional remote sensing classification technique used with hyperspectral data, in Mediterranean forest species mapping and, assess the accuracy of the produced maps with field survey data.
II. To investigate the performance of Support Vector Machines (SVM), an advanced supervised learning technique, in Mediterranean forest species mapping and, assess the accuracy of the produced maps with field survey data.
III. To investigate the potential of a geographic object based image approach (GEOBIA), which considers geographic object as a unit of analysis, in Mediterranean forest species mapping and, assess the accuracy of the produced maps with field survey data.

2

LITERATURE REVIEW

Chapter 1 discussed the importance of forest mapping and the need for further exploring the value that can be added in species level mapping with the exploitation of hyperspectral data.
This chapter:

- *illustrates the importance of the Mediterranean forests and describes the forests in Greece as well as the forest species found in the study areas (section 2.1),*
- *discusses the use and value of remote sensing in forest mapping as well as in forest species mapping in particular (section 2.2), and*
- *reviews the image analysis techniques used with hyperspectral data and their application, particularly considering the ones used in this study (section 2.3).*

2.1 MEDITERRANEAN FORESTS

2.1.1 Description of Mediterranean forest

About a century ago, Schimper (1903) while studying plant adaptation recognized the biological similarities between five widely separated regions characterized by **Mediterranean-type climates**. These regions comprise the Mediterranean basin itself, a major portion of California, Central Chile, and parts of the Southwestern and Southern Australia as shown in Figure 2.1.

The main characteristic of the Mediterranean climate, as suggested by Köppen (1931), is bi-seasonality in temperature and precipitation - cool winters with low solar irradiance and hot dry summers with high solar irradiance. In his climatic classification system, Mediterranean climates are restricted to areas where the mean temperature of the coldest month is between 0 and 18^{o}C, and the mean temperature of the warmest month exceeds 10^{o}C.

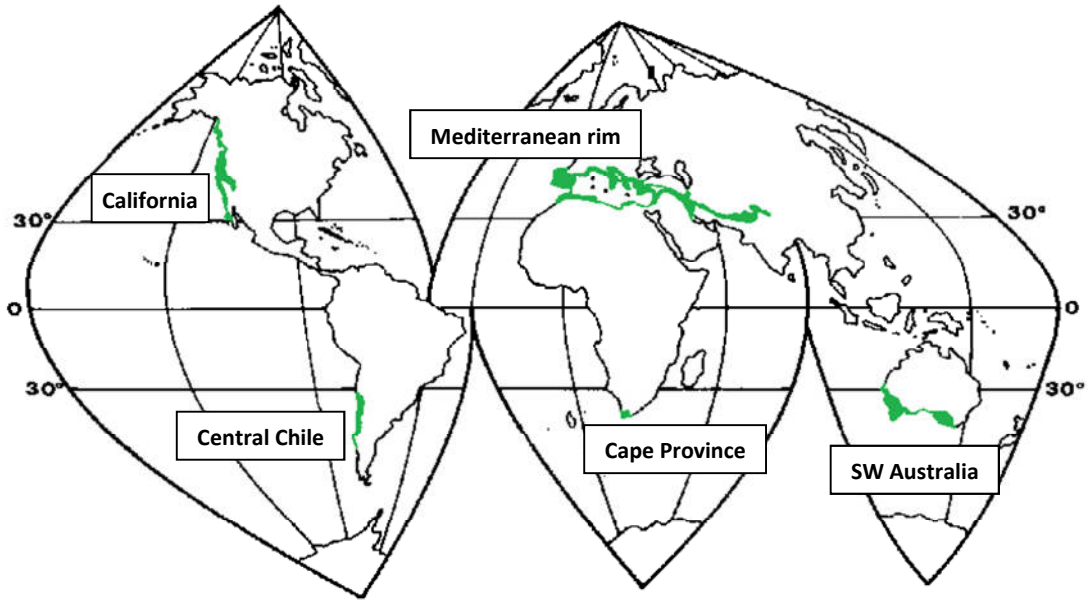

Figure 2.1 The five Mediterranean-climate regions of the world, based on the climatic zones of Köppen (1931).

Leisz (1982) described the **Mediterranean ecosystem** as the one influenced by Mediterranean climate. Mediterranean ecosystems have a very restricted distribution but occur in five widely separated parts of the world, all centered between 30^{o} and 40^{o} north or south of the equator and all influenced by similar oceanic and atmospheric circulation systems (Archibold, 1995; Hobbs et al., 1995).

The natural **vegetation** of the Mediterranean region is closely related to the typical features of the Mediterranean **climate and geomorphology** that cause climatic conditions to vary considerably even over short distances, **and it is** decisively controlled by anthropogenic induced stresses such as fire, grazing and logging.

The Mediterranean area, ranked first out of the five Mediterranean regions of the world in terms of the plant species diversity, hosts approximately 25,000 vascular plants (Cowling et al., 1996) whereas in central and northern Europe, a region four times greater, only 6000 flowering plants and ferns can be found. **Forest trees** represent an important component of the Mediterranean flora. The number of tree species is quite large compared to the trees living in central Europe (100 vs. 30, respectively; Scarascia-Mugnozza et al., 2000). Mediterranean forests are characterized by a **high proportion of broadleaf** (60%) relative to coniferous forests, varying from 76% in Italy to 49% in Portugal (Dafis, 1997).

The value of Mediterranean forests is largely related to their **environmental and social functions** (Figure 2.2). Forests play a major role in protecting soil, **stabilizing** slopes and reducing water runoff in the mountainous and hilly watersheds, preventing **erosion, landslides and floods.** Further, wood has traditionally been a basic **source of energy** in many Mediterranean countries, therefore large areas of broadleaf forests are managed as coppices in order to fulfil the local fuelwood needs. **Biodiversity** of Mediterranean forests is also of particular interest, not only because they are hotspots of plant diversity with high inter- and intra-species **genetic variability**, but also because the broader area is hotspot of human population growth (Cowling et al., 1996; Corona and Mariano, 1992).

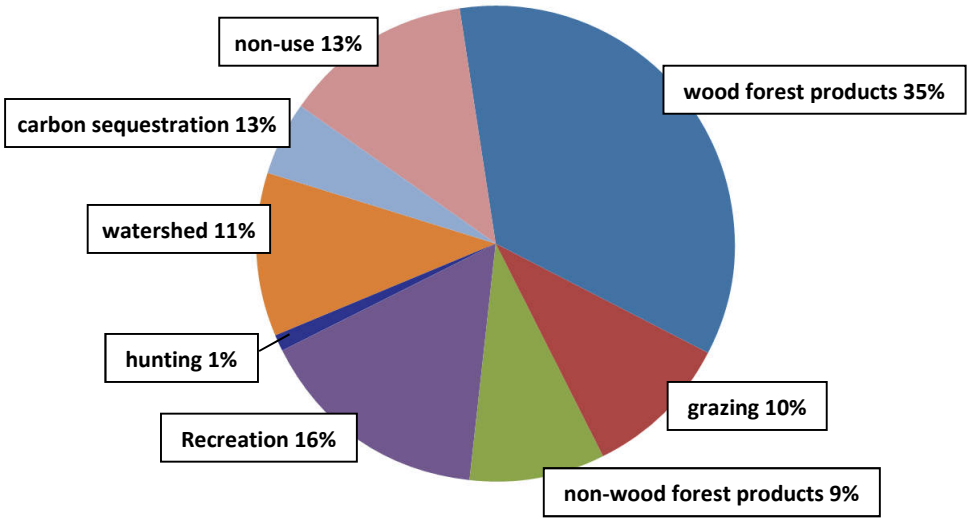

Figure 2.2 Mediterranean Forest Research Agenda (MFRA) 2010-2020, data from Merlo and Croitoru, 2005.

In the Mediterranean basin has a long history of **human** presence and activity for over perhaps a period of >10,000 years (Di Castri, 1981). According to Myers et al. (2000), the Mediterranean basin is one of the four most significantly **altered** hotspots on Earth. **Human has been stressing** forest structures and functions with practices like agriculture and animal husbandry (Naveh and Dan, 1973; Le Houerou, 1981; Naveh, 1998) together with deforestation practices and fire management. The different forms of **over-exploitation** caused the virtual disappearance of most **climax** forest types from the Mediterranean region (Quezel, 1977). The remaining so-called natural forests are altered woods, more or less intensively managed by man, that often correspond to different stages of regressive succession of the original forest (Scarascia-

Mugnozza et al., 2000). The extent of the forest cover is reduced, resulting in progressively open and degraded woods and, in several cases, bare land with eroded slopes, especially in mountain areas (Thirgood, 1981).

However, the integration of natural ecosystems and traditional **human** activities, what Romans called *ager-saltus-silva,* is one of the reasons for the high environmental diversity that characterizes the region (Cowling et al. 1996; Preiss et al., 1997; Blondel and Aronson, 1999; Heywood 1999).

The anthropogenic modification of the Mediterranean environment, along with the variable **geomorphological** conditions, results in finely grained combinations of different types of vegetation, varying from intensively cultivated fields to almost natural forest tree and shrubs communities, generally referred to with the term of landscape (Naveh and Lieberman, 1993).

Mediterranean landscapes are characterized by high **spatiotemporal heterogeneity of vegetation patterns** that cannot be regarded as a simple mixing of life-forms over large areas but, rather, the formation of transitional zones of varying mixtures resulting from disturbance and recovery cycles (Shoshany, 2000). This heterogeneity has both horizontal and vertical directions, as well as a temporal dimension (Di Castri, 1981), due to the micro biotopes, irregular terrain and seasonal changes respectively.

Typical trends in the Mediterranean region over the last half century is that natural forest vegetation in coastal zones, riparian belts and suburban spaces is increasingly jeopardised by land development for agriculture, tourism, industry, transportation infrastructures or may be subjected to an irreversible degradation, while mountain areas are being abandoned and naturally reforested (MacDonald et al., 2000). Forest and shrub vegetation is **expanding** in marginal and remote areas.

In addition, during the last century, extensive **reforestations** have been conducted by national forest services all over the Mediterranean region; with soil protection and runoff control as primary objectives, while production of timber is usually considered supplementary.

The aforementioned forest fragmentation and degradation has also produced a variety of low density, woody vegetation as the **maquis and phrygana**, which are regarded as typical vegetation of the Mediterranean ecosystems.

Although Mediterranean forests have historically evolved under the aforementioned influences, the modern anthropogenic pressures, expressed by land use and landcover changes along with the presumed climatic change, happen in such a hasty and 'anarchic' manner that threatens the what appears to be fragile equilibrium. The Mediterranean area is a **transition zone** between arid and humid regions of the world and as such is especially sensitive to any climate change.

The objectives of maintaining biological diversity and providing for renewable natural resources in a changing climate represent an enormous challenge to scientists and land managers.

Forests are increasingly recognized as **ecological systems of fundamental importance** for environmental protection, not only at the regional level but also on the global scale. They seem to play a key role in global bio-geochemical cycles as the carbon and water **cycles**, regulating regional and global climates and because of this have become a chief research focus.

Although Mediterranean forest and shrub ecosystems represent a **small fraction of the world's forest** cover, their characteristics make them interesting **model systems** for the study of effects of global change on terrestrial ecosystems (Scarascia-Mugnozza et al., 2000).

2.1.2 Greek forest and forest species

The Greek forest vegetation has been described by Dafis (1976) and classified in five **vegetation zones**, based on the phytosociology system units of Braun-Blanquet (1952) (class, ordne, alliance, association, subassociation) and the South East European vegetation classification system proposed by Hovart et al. (1974) (table 2.1).

Greece has approximately 6,000 plant taxa, a very high degree of endemism (-20%) but unfortunately a high number of plant taxa considered as threatened (900; 600 of them endemics) (Georghiou and Delipetrou, 2000; Kokkoris and Arianoutsou, 2001). Mediterranean-type ecosystems constitute 40% of the terrestrial ecosystems of Greece (Arianoutsou, 2001).

The main **forest types** existing in Greece are:

- thermophilous conifers forests of altitudes up to 1000m,
- deciduous forests, dominated by *Quercus ssp, Acer ssp, Tilia ssp* and *Fagus sylvatica*
- and boreal conifer forests, dominated by *Abies cephalonica*, *Pinus nigra* and *Fagus sylvatica*

Table 2.1 Greek vegetation zones

Zone	Sub-zone	Growth space	Thassos	Taxiarchis
Quercetalia ilicis	Oleo-Ceratonion	Oleo-Ceratonietum		
		Oleo-Lentiscetum	x	
	Quercion ilicis	Adrachno-Quercetum ilicis		
		Orno-Quercetum ilicis	x	x
Quercetalia pubescentis	Ostryo-Carpinion	Cocciferetum		x
		Coccifero-Carpinetum	x	x
		Carpinetum orientalis		
	Quercion frainetto	Quercetium frainetto		x
		Tilio-Castanetum		x
		Quercetum montanum		x
Fagetalia	Abietion cephalonicae	Abietum cephalonicae		
	Fagion moesiacae	Abietum borisii regis	x	
		Abieti-Fagetum		
		Fagetum moesiacae		X
Vaccinio-Picetalia	Vaccinio-Piceion	Pinetum silvestris		
		Picetum abies		
	Pinion heldreichii			
Astragalo-Acantholimonetalia	Astragalo-Daphnion			
	Junipero-Daphnion			

Pines are substantial components of the vegetation surrounding the Mediterranean Basin (Barbero et al., 1998). Traits characteristic of these species, such as high light demands, strong drought tolerances, and relatively fast growth-rates (Hanley and Fenner, 1997; Richardson and Rundel, 1998), enable them to thrive in harsh Mediterranean conditions. The high genetic variability and/or phenotypic plasticity exhibited by Mediterranean pines explains their high colonising ability and the central role they play in vegetation dynamics in the Mediterranean region (Barbero et al., 1998).

Pine species that grow in Europe are *P. brutia, P. cembra, P. halepensis, P. heldreichii, P. mugo, P. uncinata, P. nigra, P. peuce, P. pinaster, P. pinea* and *P. sylvestris*. Only four of them (*P. cembra, P. mugo, P. uncinata, P. pinaster*) are not found in Greece (Gaussen et al., 1993). It is interesting to note that Greece is the only European country in which there is natural distribution of *P. halepensis* and *P. brutia*. Besides the natural pine stands, pine species are massively used in reforestation plantations. In the two study areas of this study *Pinus brutia* and *Pinus nigra* are dominant species.

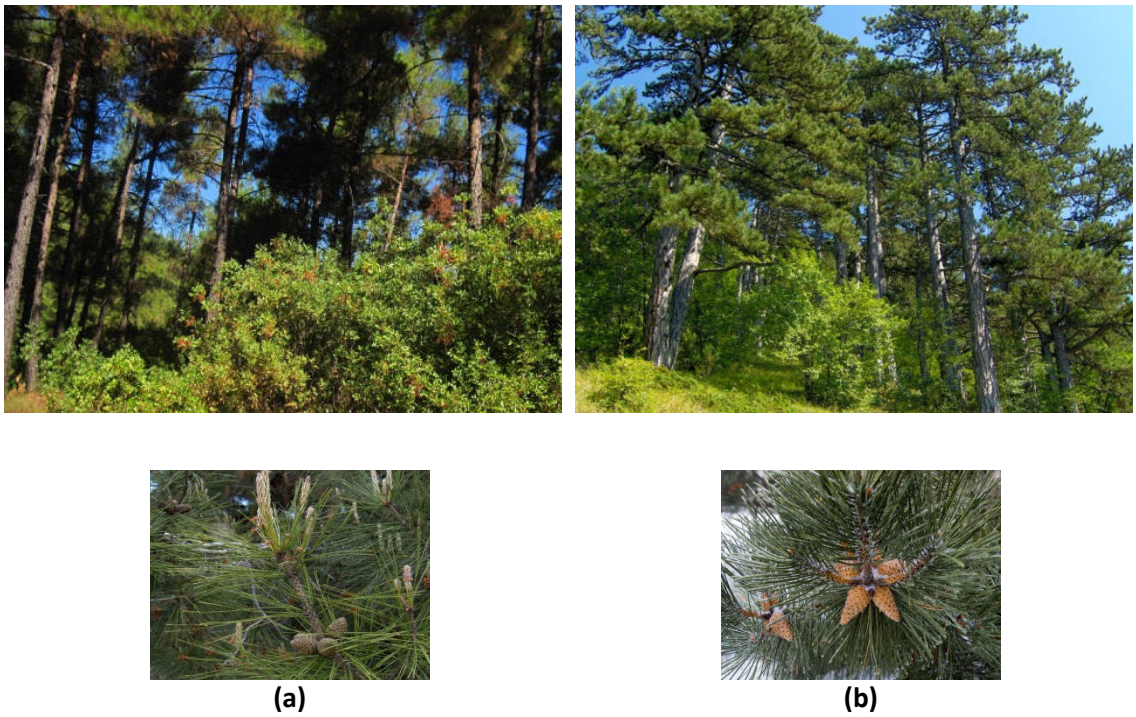

Figure 2.3 Stands and branches of *P. brutia* (a) and *P. nigra* (b).

More specifically, ***Pinus brutia* Ten**. (Figure 2.3.a) is a tree of great ecological and economic importance for the Eastern Mediterranean region (Panetsos, 1981; Nahal, 1983) and a significant forest tree species of the north-eastern coast and several Aegean Sea islands of Greece.

It is 15- 20m high, very rarely grows up to 30m and has sessile cones and strong, dark green needles 10–18 cm long. It is wind-pollinated, allogamous and monoecious. It is an extremely prolific seed disperser and can colonize open and disturbed areas easily, withstanding prolonged drought and the absence of summer rainfall. Because it is adapted to forest fires, it usually regenerates well after fire, using the seed bank released from serotinous cones (Boydak, 2004). *Pinus brutia* forests can grow on all bioclimates of the Mediterranean region and although they can grow on all substrates they particularly favor dry sands and light calcareous soils. They can be found at altitudes between sea level and 600m in the northern Mediterranean, and between sea level and 1400m in the southern Mediterranean.

***Pinus nigra ssp. pallasiana* Arn**. (Figure 2.3.b) is widely abundant in mountainous Mediterranean areas, ranging from the western part of Greece to the Taurus Mountain in Turkey, and it is usually found at the earlier stages of succession. It can grow in thermo-

Mediterranean to oro-Mediterranean conditions, and it presents an increased ecological plasticity that enables it to compete with evergreen Mediterranean species (Quezel, 1977). *Pinus nigra* is adapted to many soil types and topographic habitats and appears to do well on the poorer limestone soils. It is monoecious, with staminate and ovulate strobili borne separately on the same tree. Minimum seed bearing age is 15 to 40 years. It is 15- 25m high with initially spherical crown that eventually gets conical and it has grey and black bark with splits along the trunk (Athanasiadis, 1986). It is the pine that bears whit shade more than any other pine found in Greece and it is known to experience difficulties in successfully regenerating after large wildfires (Trabaud and Campant, 1991). In terms of production, it is used as a construction material as well as for resin collection.

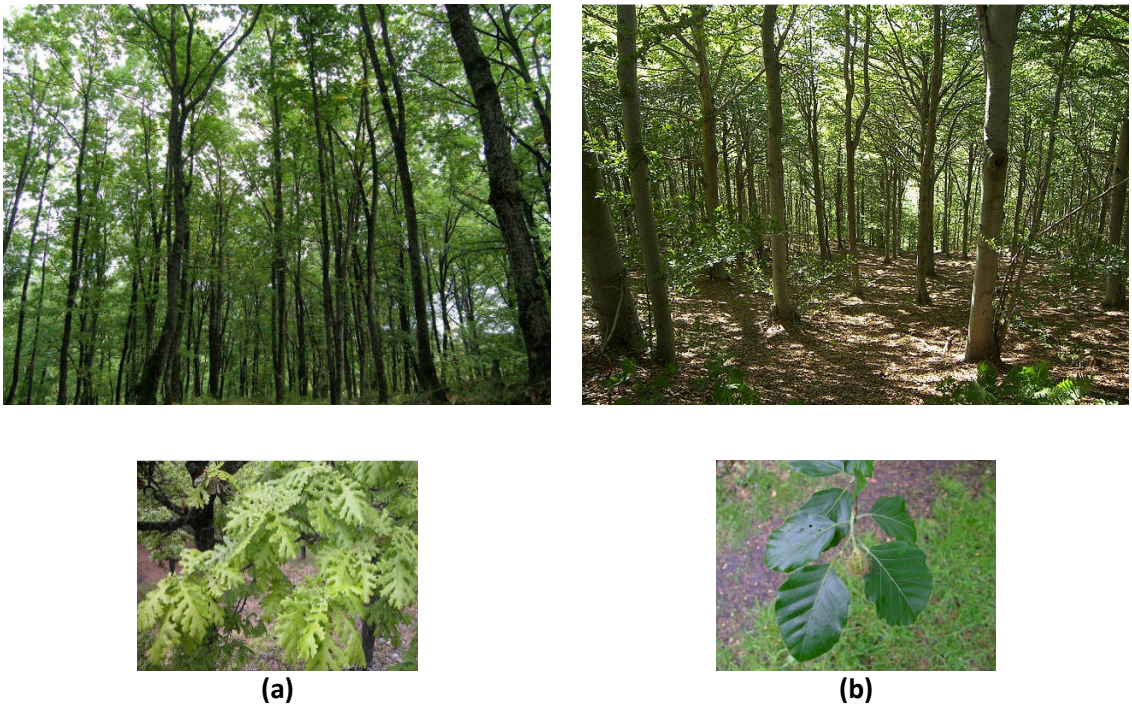

Figure 2.4 Stands and branches of *Q. frainetto* (a) and *F. sylvatica* (b).

Oak forests account for 23% of the total forest area in Greece and are adapted to the extremely dry summers that characterize this Mediterranean region (Radoglou, 1996). About 75% of the oak forests are degraded, low productivity coppice forests (Dafis, 1982) commonly grazed by sheep or cattle. In fact, the proportion of pasture woods in the thermophilous deciduous forest is much higher than in beech, fir and pine forests (Bergmeier and Dimopoulos, 2008). Oaks found in Greece include *Q. frainetto, Q. dalechampii, Q. penducolata, Q. pendiculiflora, Q.*

macrolepis, Q. euboica, Q, infectoria, Q. coccifera, Q. petraea, Q. cerris, Q. pubescens, Q. ilex and *Q. trojana* (Athanasiadis, 1986). Besides the evergreen *Q. coccifera* that is a core component in maquis, the most frequently dominating deciduous oak species of mainland Greece is ***Quercus frainetto Ten***., formerly known as *Quercus conferta* Kit. (Valentini et al., 1992; Athanasiadis 1986; Bergmeier and Dimopoulos, 2008) (Figure 2.4.a). It creates 80% of the deciduous oak forests of the country and it occurs in the entire semi-mountainous area of mainland Greece (Dafis and Kakouros, 2006). It also dominates a large part of the Taxiarchis study area. *Q. frainetto* is a deciduous species that shows lower tolerance to drought and high temperatures than other oak species, and has a high demand for soil water. It grows to a height of 35m and trunk diameter may exceed 1m.

Another very important species in Greek forests is ***Fagus sylvatica* L.**, (Figure 2.4.b) which forms natural stands in higher altitudes. According to Pignatti the mountains, from the ecological point of view not always can be considered as belonging to the true Mediterranean type ecosystem, however in the versatile Mediterranean terrain, mountains and lowlands mix in a continuous way. *F. sylvatica* is an important tree for forestry in Europe and one of the most represented tree genera of the continent. Its taxonomic history in western Eurasia is complicated and controversial (Papageorgeiou et al., 2008). According to the latest and most accepted taxonomic classification, one beech species exists in western Eurasia (*Fagus sylvatica*) with two subspecies: *F. sylvatica ssp. sylvatica* and *F. sylvatica ssp. orientalis* (Denk 2003). Greece contains the trailing edge of the *Fagus* ssp. range, and is within the contact zone between the two subspecies (*F. sylvatica* and *F. orientalis*). The occurrence of *F. sylvatica* forest in Greece is described as patchy (Horvat et al., 1974; Bergmeier, 1990). *F. sylvatica* is a large tree with slow growth rate, typically 25–35m tall and up to 1.5m trunk diameter. Its appearance varies according to its habitat but it tends to have a long, slender light-gray trunk with a narrow crown and erect branches. The leaves are alternate, simple, and entire or with a slightly crenate margin. Leaves are often not abscised in the autumn and instead remain on the tree until the spring.

Figure 2.5 shows the distributions of *P. brutia*, *P. nigra* and *F. sylvatica* according to EUFORGEN.

Besides forests, other typical Mediterranean vegetation includes maquis and phrygana. **Maquis** (synonyms: macchia - Italy, chaparral - California, fynbos - S. Africa, matorral – Chile, kwongan-heath-mallee - Australia) represent a tall evergreen broadleaved shrub community (2-5 m and up to 9 m) that presumably represents a phase in succession to secondary deciduous woodland. The most typical dominant species are evergreen oaks, such as *Quercus ilex*, *Q.*

rotundifolia and *Q. coccifera*. **Maquis** vegetation is very important, as it protects soils from erosion and provides habitat to many animal species. Phrygana (synonyms: garrigue – French, tomillares - Spain, batha - Israel, coastal sage - California, renosterbos - S. Africa) are open vegetation communities dominated by cushion-shaped shrubs up to 0.50 m in height usually separated from each other by open, eroded stony patches. Although, in most cases they are stages of manmade degradation of the original Mediterranean forest (Raus 1979) they can also represent natural ecosystems of dry and shallow primary sites well adapted to the severe drought.

Almost one fourth of Greece's area is covered by forests, primarily natural and of high ecological value. Another 24% is covered by woodlands or forested lands, which often result from the degradation of forests adjacent to urban or tourist areas. Despite their great value, Greek forests face many dangers and threats. Wildfires and encroachment as a result of urban expansion and uncontrolled human activity are definitely the most important threats. Greek forests are gradually replaced by urban, suburban and tourist areas. The absence of a coherent and efficient national forest policy, lack of forestry management and the degeneration of the Forest Service are factors that stress these problems and withhold sustainable development.

A key factor of forest studies that needs to be addressed is the absence of required information, both spatial or other. Currently the main national forest map products date back to 1960, are kept dispersed in several forest service authorities, are in paper form, are produced with inconsistent methodology, are not easily accessible, and may date back to 1960. Table 2.2 summarizes the national spatial forest-related information, available for Greek forests. Greece is also covered by several European mapping forest products, as shown in table 2.3.

(a)

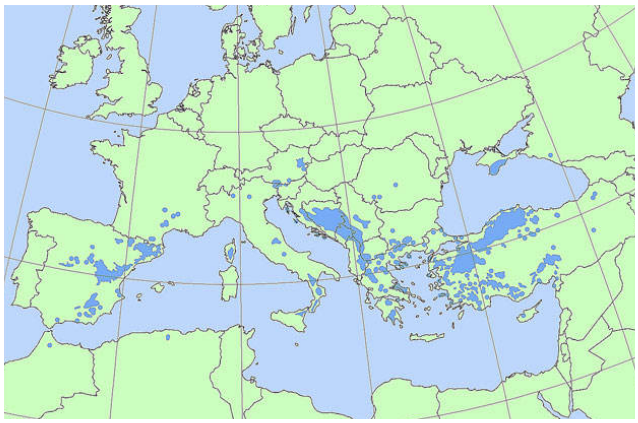

(b)

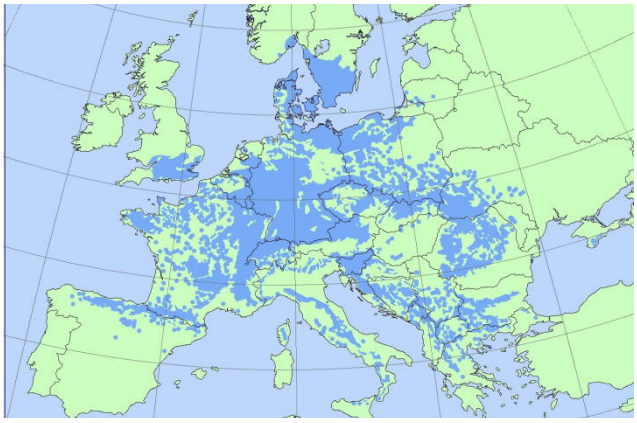

(c)

Figure 2.5 Distribution of *P. brutia* (a), *P. nigra* (b) and *F. sylvatica* (c) (source: EUFORGEN – European Forest Genetic Resources Programme).

Table 2.2 National spatial forest-related data.

product	owner	production method	scale	format	information	date	access
LPIS	OPEKEPE	aerial or satellite orthoimagery	1:5,000	vector	Land use (all forest areas are grouped)	2009	
Management plans	52 forest services	variable – field visits or digitizing on available imagery	1:20,000 (rarely 1:5,000)	variable – paper of vector	forest species	variable	under restri-ctions
Forest and woodland delineation	Ktimatologio S.A.	visits or digitizing on aerial imagery	50m apoklisi	vector	3 classes: forest, woodland, other	1945 and 1996	no
WWF	WWF	object based classification of Landsat 5TM imagery	1:60,000	vector	9 land use/cover (2 forest classes)	1987/ 2007	upon request
Forest map of Greece	Foremen Ministry of Agriculture	Composition of maps of 1976 (unknown pr. method)	1:500,000	paper	16 forest pieces	1976	open
Vegetation map of Greece	Foremen Ministry of Agriculture	unknown	1:1,000,000	paper	10 vegetation formations	1978	open
Prefecture forest map	Foremen Ministry of Agriculture	Digitizing on aerial photography	1:200,000	paper	8 forest species and other landcover	1960	open
Phytosociolo-cigal map of Greece		unknown	1:1,000,000	paper	9 vegetation subzones	1973	open
Forest inventory maps	Foremen Ministry of Agriculture	digitizing on aerial orthoimagery imagery	1:20,000	vector		1960-1983	no

Table 2.3 International spatial forest-related data available for Greece

product	owner	production method	scale	format	information	date	access
Forest map of Europe	EFI	earth observation data / forest inventory statistics	1x1km	raster	% of forest cover	2006	open
Maps for Forest Tree Species in Europe	JRC-IES-CCU - EC	transnational survey and compositional kriging	1x1km	raster	distribution of 20 tree species	2001	open
Forest cover map 2000/2006	JRC	earth observation data	25x25m	raster	forest cover	2006	open
CLC2000	EEA	digitizing on earth observation data	1:100,000	raster/ vector	44 landcover classes	2006	open

2.2 REMOTE SENSING OF FORESTS

2.2.1 Forest mapping

There are numerous aspects of forest mapping, as forest is a part of a broad range of functions. It is a biodiverse ecosystem with numerous values, components, inhabitants, and interactions that need to be understood, described, monitored and preserved. Among other, it is an asset with great economic value that needs to be sustainable managed in terms of production. In all these cases, spatial data are essential and traditionally collected with all available means.

Over the past few decades, remote sensing has been a valuable source of information for forest resource monitoring and management, as it provides means for solving various types of problems. It is an effective and economical method for gathering spatially distributed data over a broad range of scales. Remotely sensed imagery is frequently used to map forest parameters for use in a variety of resource assessment, land management, and modeling applications. The use of remote sensing has increased significantly, because it introduces methodologies for providing cost effective forest inventory data, such as **geographic location, spatial extent, forest structure, and health condition** among other (Figure 2.6).

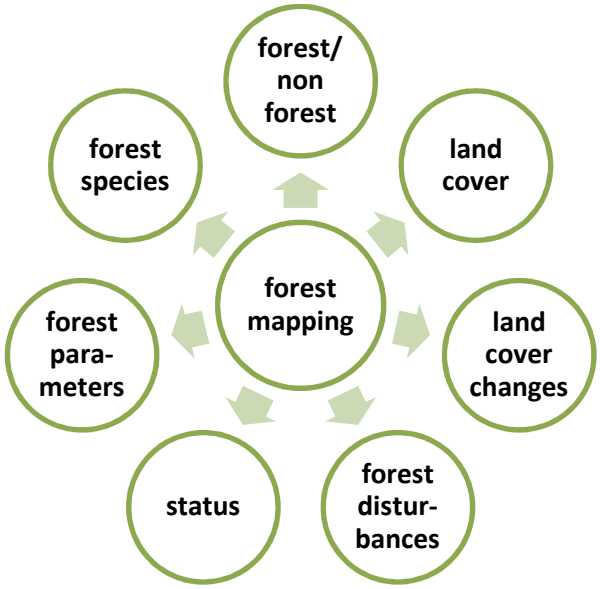

Figure 2.6 Common fields of forest studies.

Forest classifications have traditionally used multispectral data (Franklin, 1994). Loveland, 2000 reported that mapping from **coarse spectral resolution** images has focused on **landcover** and **broad vegetation types**. Numerous studies have been carried out to generate landcover maps of various forest ecosystems with the help of multispectral data (Tucker et al., 1985; Rogan et al., 2002; Pal and Mather, 2003; Sedano et al., 2005; Knorn et al., 2009). Further, multispectral imagery has been used in studies including **forest growth** (Helmer et al., 2000; Nelson et al., 2000**), forest stress** (Hanger and Rigina, 1998; Govender et al., 2009), fuel mapping (Riano et al., 2002), **above ground biomass** (AGB) estimation (Scholes et al., 1996; Maselli and Chiesi, 2006), **forest successional stages** (Vieira et al., 2003; Falkowski et al., 2009), **forest degradation and deforestation** (Duveiller et al., 2008; Asner et al., 2009),

Nevertheless, optical remote sensing has expanded from the use of panchromatic and multispectral sensors to off-nadir looking instruments and imaging spectrometers (Asner, 1998). Imagery has advanced in both spectral and spatial resolution. As sensors and associated technologies evolve, new types of remote sensing data provide further opportunities in remote sensing applications and intriguer research to constantly pursue novel goals. Figure 2.7 summarizes the available types of remotely sensed data.

High spatial resolution multispectral imagery has been employed during the last two decades. There have been studies which examined the use of high spatial resolution satellite imagery to: **map LULC** (Roberts et al., 2003b; Rodriguez and Feller, 2004; Kim et al., 2009), automate extraction of detailed **forest parameters** (Mallinis et al., 2004; Hay et al., 2005; Mallinis et al., 2008; Song et al., 2010), estimate various **biophysical parameters** (Roberts et al., 2003; Kovacs et al., 2005; Boggs, 2010; Peuhkurinen et al., 2008).

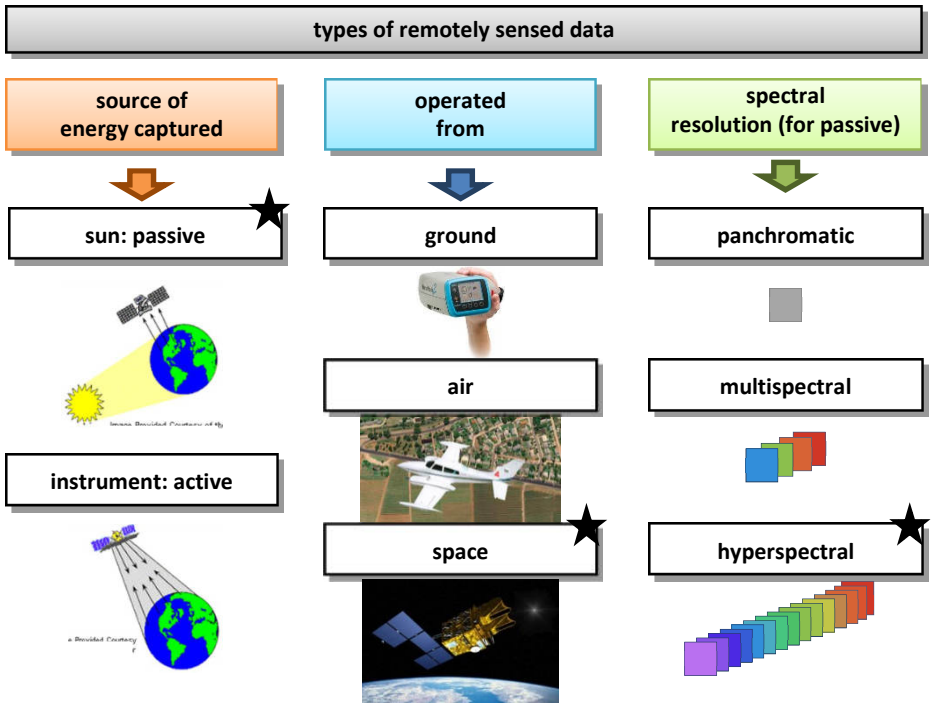

Figure 2.7 Types of remotely sensed data. Stars indicate the types that Hyperion imagery belongs to.

Over the past few decades, the emergence of hyperspectral sensors has certainly had significant impacts on our ability to map forest (Pu, 2009). However, the efficacy of hyperspectral data for forest research and monitoring rests in understanding the sources of variance in spectral signatures at different biophysical, taxonomic, community and ecosystem levels of organization (Asner, 2008).

The use of hyperspectral imagery has been evaluated in numerous studies, including among other **canopy biodiversity** (Carlson et al., 2007), **stress** (Campbell et al., 2004; Peña and Altmann, 2009; Hatala et al., 2010), **foliar chemistry** (Zarco-Tejada et al., 2004; Asner and Martin, 2008; Martin et al., 2008; Kokaly et al., 2009), **species mapping** (Ustin et al., 2002; Goodenough et al., 2003; Lucas et al., 2008b; Kamal and Phin, 2011; Vyas et al., 2011;), **AGB** (Thenkabail et al., 2004;

Lucas et al., 2008a), **landcover** (Thenkabail et al., 2004; Koetz et al., 2008; Pignatti et al., 2009; Oldeland et al., 2010), **biophysical parameters** (Lee et al., 2004; Pu et al., 2005; Schlerf et al., 2005,), **wildfire management** (Keramitsoglou et al., 2008). Wu and Peng (2011), reviewed advances in researches on hyperspectral remote sensing technology in forestry information extraction and the unresolved problems.

Studies comparing multispectral and hyperspectral data have typically documented the advance results of the later (Blackburn, 1999; Thenkabail et al., 2000; Goodenough et al., 2003; Thenkabail et al., 2004; Pu et al., 2005).

It is worth pointing out that high spatial resolution imagery, both multispectral and hyperspectral has been typically used in local scale studies, while satellite imagery with coarser spatial resolution and wider cover has been employed in regional or smaller scale studies.

In the case of hyperspectral remote sensing, it is also noteworthy that imagery from aerial sensors is more widely used, because of its longer history and success in various applications. However, satellite imagery has also gained much attention and provided many successful applications. Goodenough et al., (2004) summarized the forest information products obtainable from satellite hyperspectral sensing and the important features of hyperspectral remote sensing involved in forest information extraction. At the moment, EnMAP, a new satellite hyperspectral sensor, is under construction and scheduled to launch in 2015 by German Aerospace Center – DLR. The Canadian Space Agency is also developing technologies and mission concepts for an operational hyperspectral mission called HERO (Bergeron et al., 2008).

Besides passive remote sensing, that includes the above mentioned types of sensors, there have also been extensive studies using active remote sensing sensors. An active sensor, instead of capturing energy that is naturally available, provide their own energy source for illumination toward the target, and detect and measure the radiation that is reflected or backscattered from the target. Among other, Radar and LiDAR are the most commonly used in forest studies. Radars have been used to estimate forest structure parameters (Hyde et al., 2005; Hyde et al., 2006), map deforestation (Papathanassiou and Cloude, 2001; Sun et al., 2008; Neumann et al., 2010) or estimate biomass (Ranson et al., 1994), among other applications. LiDAR have also been used to estimate forest structure parameters (Ranson et al., 1994; Hudak et al., 2002; Hill and Thomson, 2005; Lefsky et al., 2005; Hyde et al., 2006; McRoberts and Tomppo, 2007) and biomass (Boudreau et al., 2008; Goetz et al., 2009).

All terrestrial biomes have been investigated in a lesser or greater extent. Among them, Mediterranean forests have been extensively studied, because of their unparalleled importance. Key promoters of these studies are the factors that shape the Mediterranean landscape such as wildfires, soil erosion and land use or cover change.

Some of the foci of these studies include: **burned area mapping** (Gitas et al., 2004; Polychonaki and Gitas, 2010; Mallinis and Koutsias, 2012) **fuel mapping** (Riano et al., 2002; Roberts et al., 2003a; Arroyo et al., 2006, Jia et al., 2006)**, desertification** (Dragan et al., 2005; Mallinis et al., 2009)**, forest regeneration** (Wittenberg et al., 2007; Mitri and Gitas, 2010; Veraverbeke et al., 2012)**, land use/cover mapping** (Koetz et al., 2008; Pignatti et al., 2009)**,** and **change detection mapping** (Berberoglu and Akin, 2009; Dragozi et al., 2012).

What is special with Mediterranean forests, as Lucas et al., 2008b stressed, is that recognition techniques, that may be suitable for wide forest stands (i.e., limited numbers of species, stands spatially organized in large homogeneous patches), have limited success in Mediterranean regions with more complex landscapes, where landcovers and forest types vary frequently over small areas.

Shoshany, (2000) also argues that assessments of multispectral and multi-temporal images have shown limitations in their applicability over wide regions, due mainly to the heterogeneity of Mediterranean regions.

2.2.2 Forest species mapping

Plant species is the main building block of almost all ecosystems, and sustainable management of any ecosystem requires a comprehensive understanding of species composition and distribution (Nagendra, 2001). Timely and accurate mapping of vegetation species is an objective and a prerequisite in various applications that span in the fields of **ecology, biology, forestry** and **agriculture**, such as resource inventories, biodiversity assessment, fire hazard assessment, conservation planning, pest and environmental stress management, monitoring changes, and assessing per-species carbon sequestration. Moreover, **forest growth models**, such as the biogeochemical process Forest-BGC model (Running and Coughlan, 1988), parameterize model input variables depending on tree species (Baker and Robinson, 2010). Adding to that, species level composition information is critical for a better understanding and modeling of ecosystem functioning, since many species exhibit differences in functional attributes or decomposition rates (Huber et al., 2008). Adding to that, forest species information

is also essential for the national reporting obligations towards national and international policies, such as (a) the UN Framework Convention on Climate Change (UNFCCC) and its Kyoto Protocol, as means to quantify changes in CO_2, particularly in relation to land use (Rosenqvist et al., 2000; Goodenough et al., 2001), land use change and forestry (LULUCF) activities, (b) the UN Convention on Biological Diversity (UNCBD) and (c) the UN Collaborative Programme on Reducing Emissions from Deforestation and Forest Degradation in Developing Countries (UN-REDD), as species information can be used in conjunction with allometric models to estimate AGB (Rosenqvist et al., 2003).

Mapping forest species is usually based on **field surveys** and **manual interpretation** of large scale aerial photography (Gong and Yu, 2001). However, field surveys are expensive and time-intensive while aerial photo interpretation is dependent on the experience of photo interpreters, which is documented that allows for large inconsistencies between different interpreters (Biging et al., 1991, Davis et al., 1995). In the contrary, spectral and spatial analysis of remotely sensed imagery, may provide detailed and accurate species level products, in a time and cost effective manner, as in numerous other applications

It has been a long standing objective of **remote sensing** working within forest ecosystems to provide species level results that are the near equivalent of ground-based forest inventory efforts (Anderson et al., 2008). Franklin (2001), argued that no one had succeeded in duplicating this level of description in identifying forest tree species using digital data and methods.

Multispectral image classification (Walsh, 1980; Vieira et al., 2003), **multi-temporal** analysis (Wolter et al., 1995; Key et al., 2001; Brown de Colstoun et al., 2003), and **multi-sensor** data fusion (Goodenough et al., 2005) have been investigated in species level mapping, reporting moderate success. Ke et al., 2010 used synergy of Quickbird and LiDAR in an OBIA environment and discriminated between 5 species with high accuracy. Coleman et al. (1990), used Landsat TM data to differentiate large stands of four pine species and concluded that pine species stands have highly similar reflectance and are not separable using Landsat TM imagery. Although **fine spatial resolution multispectral images** have proven very successful in various applications, in the case of forest species level mapping fine spatial resolution alone was not sufficient for accurate discrimination (Asner et al., 2002; Carleer and Wolff, 2004; Johansen and Phinn, 2006).

Compared to many other vegetation attributes, plant species composition is **difficult to detect** with remote sensing techniques (Schmidtlein and Sassin, 2004). This is because of the very

similar spectral response of vegetation species. In particular, in the visible range of the electromagnetic spectrum spectral variability among species is low due to strong absorption by chlorophyll (Poorter et al., 1995; Cochrane, 2000), while In short-wave infrared range water absorption tends to obscure absorption by lignin and cellulose (Gausman, 1985; Asner, 1998). The reflectance of vegetation from discerned species is highly correlated due to their common chemical composition (Portigal et al., 1997).

With the **advent of hyperspectral imaging**, there has been an expanding potential for spectral discrimination between species (Nagendra and Rocchini, 2008; Heumann, 2011a). Back in 1999, Yu et al. reported that advances in hyperspectral data processing and advanced recognition algorithms are beginning to overcome similarities in spectral properties and variability in lighting conditions, two of the main problems in species recognition when using aerial hyperspectral imagery. At the time, there was not any satellite hyperspectral sensor available.

The range of spectroscopic sensors allows for **data collection is various scales**, and also offers the opportunity to explore the spatial-scale dependency of spectral reflectance in the remote identification of species (Figure 2.8). There are several studies of the value of hyperspectral data, at scales such as leaf, brunch, crown, canopy and landscape.

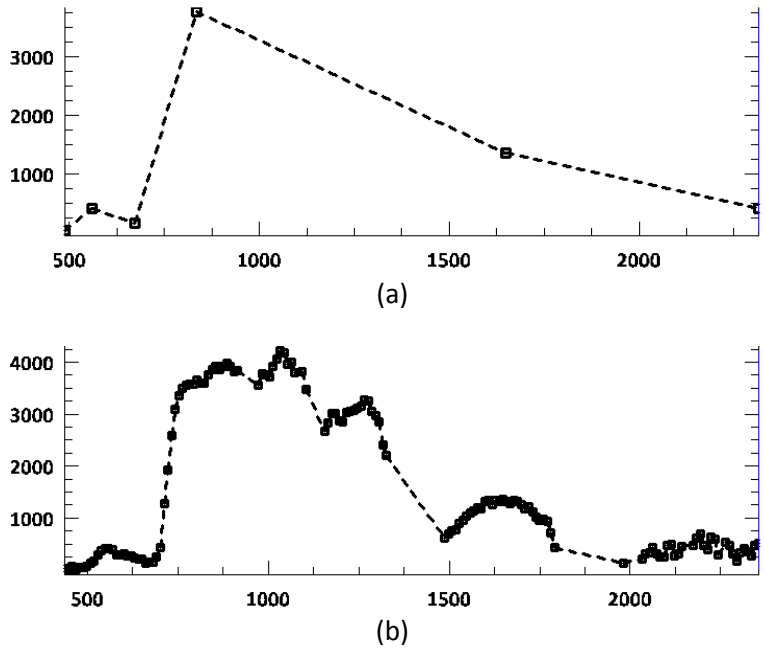

Figure 2.8 Spectral signature of a vegetation pixel (a) from a 6 band multispectral Landsat TM image and (b) from a 141 band hyperspectral Hyperion image.

A number of studies have evaluated the use of ***in situ*** or **laboratory data**, in species discrimination at the **leaf scale**. Gong et al., (1997) used *in situ* measurements of sunlit crown areas discriminated between six conifer species with accuracies high as 79%. Pu (2009), used *in situ* measurements of 11 broadleaved species, in urban environment, and achieved overall accuracy of 89%. He advocated that with current remote sensing techniques, including high spatial and spectral resolution data, it is still difficult but possible to identify similar species with an acceptable accuracy.

Other studies have investigated the relationship between **leaf and canopy spectra**. van Aardt and Wynne (2001) concluded that accurate spectral discrimination of three pine species (*Pinus taeda, Pinus virginiana, Pinus echinata*) can be extended from field-based measurements to airborne hyperspectral data. This was confirmed by accuracies as high as 85% when 3.4 m AVIRIS data were used. Clark et al., 2005 used HYDICE to discriminate tropical rain forest tree species at **leaf to crown** scales and although they reported advanced accuracies, they also found that overall classification accuracy decreased from leaf scales measured in the laboratory to pixel and crown scales measured from the airborne sensor. On the contrary, when Cochrane (2000) used laboratory spectra from 11 tree species to simulate branch and crown scales he found that discrimination was possible at crown scales, but declined at branch and leaf scales. Lee et al., 2007 also found that leaf-level reflectance spectra of pine needles and oak leaves did not quite correspond with the canopy-level spectral of the respective forest stands.

Studies have revealed that leaf-scale reflectance spectra **are controlled** by leaf biochemical properties and leaf morphology (Woolley, 1971; Tucker and Garrett, 1977; Asner, 1998; Grant, 1987; Roberts et al., 2004). On the other hand, research in the spectral variability of canopies has shown that canopy-scale spectra are mediated by factors such as gap fraction, leaf area index (LAI), leaf angle distribution (LAD), soil and vegetation cover, and least on foliar properties (Baret et al. 1995; Asner, 1998; Asner, 2008). To date, we still do not know the precise relative importance of leaf and canopy properties determining the hyperspectral signatures of forest canopies (Asner, 2008).

Asner, (1998) showed that the capabilities of vegetation remote sensing are ecosystem dependent (e.g., grasslands, shrub-lands, and woodlands); that is, the structural attributes of ecosystems determine the relative contribution of leaf, canopy, and landscape factors driving variation in a reflectance signal. In agreement with that, research applications that have incorporated **LiDAR** measurements to model canopy, found that insights of canopy **structural**

parameters provide considerable flexibility and analytical potential for studies of terrestrial ecosystems and the species contained within them (Asner et al., 2008; Dalponte et al., 2008; Waslsh et al. 2008; Jones et al., 2010; Ke et al., 2010; Leuther et al., 2012). These imply that in the diverse, disturbed and fragmented **Mediterranean forest**, structural rather than species spectral differences may predominate in imagery, rendering mapping of this type of ecosystem very challenging.

A number of studies have been conducted on species-level mapping using remotely sensed imagery in a variety of biomes (Martin et al., 1998; Roberts et al., 1998; Ustin and Xiao, 2001; Parker- Williams and Hunt, 2002; Kokaly et al., 2003; Underwood et al, 2003; Stavrakoudis et al., 2012a), mostly driven by the needs to detect **invasive species** threatening native ecosystem biodiversity, as this is a major environmental and ecological concern (Clark et al., 2005; Ramsey III et al., 2005; Pengra et al., 2007; Tsai et al., 2007; Walsh et al., 2008; Miao et al., 2011). The difference between invasion species and inventory species mapping is that in the second case more than one species is the main target, thus multiplying the importance of misclassification.

Airborne hyperspectral sensors such as AVIRIS, CASI, HyMap, PROBE-1 AND hYsPEX have been mostly successful in mapping vegetation at the species level (Schmidt and Skidmore, 2001; Parker Williams and Hunt, 2002; Kamal and Phin, 2011; Dalponte et al., 2012; Zhang and Xie, 2013). Martin et al. (1998) used AVIRIS data and MLC to classify 11 forest cover types based on relative basal area and reported accuracies higher that 75%, for coniferous species, while deciduous species were inseperable, mainly because of the mixture pattern. Aspinal (2002) found that high spatial resolution hyperspectral imagery has great potential for separating the three closely related and visually similar *Populus* species. More recently, Buddenbaum et al. (2005) used Hymap to classify 3 conifer species with overall accuracy between 60% and 78%, using geostatisical measures. Chom et al. (2010) found that intra-species variability was higher in deciduous rather than evergreen species in a savannah environment, and suggested that a multitemporal approach would be essential to improve the classification results in this environment. van Aardt and Wynne (2001), used AVIRIS data and discriminal techniques to measure the separability between 3 species and found cross-validation accuracies between 65% and 85%. Youngentob et al., 2011 used a Hypam image to map 9 *Eucalyptus* species using multiple endmember spectral mixture analysis and continuum-removed and achieved overall classification accuracies between 75% and 83%.

While aerial imagery is mostly used to take advantage of the fine high spatial resolution, the high cost and limited coverage of airborne sensors is a barrier to their use for wider scale management and research. In the contrary, satellite platforms provide other advantages, such as wider view, broader scale, repeatable collection of data and lower cost, which are very appealing for both research and operational applications.

However, **satellite** hyperspectral remote sensors will always be at a disadvantage relative to aerial sensors with similar spectral resolution in that they are further from the reflecting surface receiving less reflected energy, adding to the distortion and loss of signal as the energy passes through the full extent of the atmosphere (Pengra et al., 2007). Adding to that, as image pixels tend to be **mixed** rather than pure (Settle and Drake, 1993), the coarser spatial resolution of satellite imagery makes mixture more influencing than in aerial imagery. Foody and Hill (1996), further argued that **topography** is one of the primary sources of perceived spatial variation in an image of 30 x 30 m spatial resolution. The above prefigure that forest species mapping using satellite data focuses in smaller scale (regional to national) studies than when using aerial sensors.

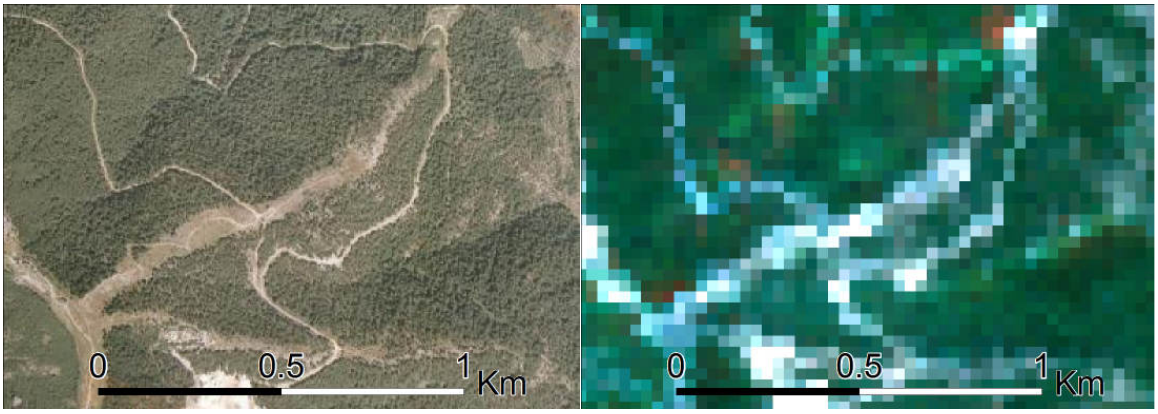

Figure 2.9 (a) A forest area in Thassos, with fire brakes and dirt roads as seen in (a) an aerial image with 4m spatial resolution and (b) Hyperion image with 30m spatial resolution.

Hyperion is the first hyperspectral sensor to operate from space and has been contributing to vegetation studies since its early days (Datt et al., 2003; Goodenough et al., 2003; Ramsey III et al., 2005). Hyperion is capable of resolving 242 spectral bands (from 0.4 to 2.5 μm) and has a moderate spatial resolution of 30 by 30 meters (Figure 2.9). This is in agreement with spatial

resolution requirements for land use applications, which were determined in the 1970's in preparation for the Landsat Thematic Mapper.

Other satellite hyperspectral sensors are:

- MODIS. MODIS imagery has 250 to 1,000m spatial resolution and 1 to 2 day temporal resolution, and due to these characteristics it is typically used in multitemporal studies, in regional or smaller scales (Beck et al., 2006; Houborg et al., 2007; Chuvieco et al., 2008). This spatial resolution does not allow for species level mapping in such heterogeneous landscapes as the Mediterranean.

- ASTER. ASTER sensor captures 14 spectral bands with spatial resolution between 15 and 90m depending on the band. It can provide imagery for regional to national scale vegetation mapping and has been used for landcover studies (Sharma et al., 2004; Ghanbari et al., 2008), species mapping (Keramitsoglou et al., 2005; Hassan et al., 2011) and various studies of mangrove environments (Saito et al., 2003; Heumann, 2011a), however on the whole is used in a lesser extent that Hyperion imagery.

- CHRIS/PROBA. CHRIS/PROBA with 20m spatial resolution and 19 spectral bands has been mostly used in mapping forest structural parameters, as it allows for a multi-angle view of the area under investigation (Goodenough et al., 2006; Rautiainen et al., 2008; Schlerf et al., 2012).

Table 2.4 Results of published species mapping studies with Hyperion imagery.

study	number of species	OA	classifiers	environment
Goodenough et al., 2003	5	83%-92%	MLC	temperate
Galvao et al., 2005	5	87.5%	MDA	agricultural
Pengra et al., 2007	1	81%	SCM	wetland
Tsai et al., 2007	3	up to 86%	ML	tropical
Rao, 2008	12	86%	SAM	agricultural
Walsh et al., 2008	1	Not assessed	SMA	tropical
Pignatti et al., 2009	3	approx. 70%	ML, MD, SAM, MhD	Mediterranean
Vyaz et al. 2011	6	81%, 66%, 71%	ANN, SAM, SVM	tropical

Species level studies with Hyperion imagery (table 2.4) have focused on examining spectral separability and identifying optimal band combination (Thenkabail et al., 2004; Ramsey III et al., 2005; Papes et al., 2010; Somers and Asner, 2012), estimating biochemical properties (Townsend

et al., 2003; Smith et al., 2003b; Martin et al., 2008; Somers and Asner, 2012) or developing novel techniques (Stavrakoudis et al., 2012a, 2012b).

Fewer studies have focus on actual mapping of a vegetation area. Between those, some aimed to map species in agricultural environments (Galvao et al., 2005; Rao, 2008), in wetlands (Pengra et al., 2007), in tropical rainforest (Tsai et al., 2007; Walsh et al., 2008; Vyaz et al. 2011), in temperate conifer forest (Goodenough et al., 2003) and Mediterranean forest (Pignatti et al., 2009). Synergy between Hyperion and other type of data has been also examined to improve mapping results (Mitri and Gitas, 2010).

Valuable conclusions of these studies suggest that Hyperion has enormous advantage over ETM+ multispectral imagery in species mapping (Goodenough et al., 2003), especially in the case of conifers (Townsend and Foster, 2003), and that using image spectra to train a classifier provides more accurate results that using spectra form *in situ* measurements (Rao, 2008). Both these conclusions are consistent with Cho et al., (2010) findings.

It is interesting to note that the aforementioned studies incorporated data dimensionality reduction techniques in their methodologies, such as spectral indices (Galvao et al., 2005), MNF (Goodenough et al., 2003; Pengra et al., 2007; Walsh et al., 2008; Pignatti et al. 2009), PCA (Tsai et al., 2007) and SDA (Vyaz et al. 2011). Another interesting point is that several studies addressed the exploitation of vegetation phenology either through multitemporal analysis (Somers and Asner, 2011) or by taking advantage of the senescence phase of the plant under investigation (Walsh et al., 2008).

Vyaz et al., 2011 and Pignatti et al., 2009 compared between different classifiers and they found that classification accuracy varied according to species and technique used, but in most cases accuracies over 70% were achieved. Pengra et al., (2007) found some barriers in mapping an invasive plant, *Phragmites australis*, in coastal wetlands using the EO-1 Hyperion hyperspectral sensor mostly because of the small size and linear arrangement of *Phragmites* stands relative to the sensor resolution, which did not allow for capturing of pure pixels. Townsend and Foster (2003) also reported that mixed species composition remained an issue due to 30-metre resolution. Ramsey III et al., (2005) although they studied the occurrence of an invasive species in regional scale, they did not attempt detailed species classification as they argued that the input data were not spectrally discriminating enough to provide consistent species level classification (*Acer rubrum* versus *Quercus spp*.).

The literature review carried out as part of this study revealed that the study of Pignatti et al., 2009 is the only one that addresses the problem of forest species mapping of a Mediterranean site, using Hyperion imagery. Between other landcover classes, they classified three forest species, namely *Fagus sylvatica, Pinus nigra* and *Abies alba*, using techniques such as MLC, MD, SAM and MhDC. They found that classification accuracy varied according to species and from unacceptable to 100%, as well as that the best classification of each of the three species was not achieved by the same classifier. However, MD and SAM had the best performance. They also found that although a higher spatial resolution hyperspectral image (MIVIS) provided better accuracies, this was not the case for all combinations of species and classifiers, further strengthening the conclusion that mapping results depend on the species under investigation.

2.3 HYPERSPECTRAL IMAGE ANALYSIS TECHNIQUES IN FOREST SPECIES MAPPING

2.3.1 Hyperspectral data

Spectral resolution refers to the number and width of the portions of the electromagnetic spectrum measured by the sensor. A sensor may be sensitive to a large portion of the electromagnetic spectrum but have poor spectral resolution if it captures a small number of wide bands. This is the case with **multispectral** instruments, which usually collect data in three to six spectral bands in a single observation, from the visible and near-infrared region of the electromagnetic spectrum. A sensor that is sensitive to the same portion of the electromagnetic spectrum but captures many small bands within that portion would have greater spectral resolution, and referred to as **hyperspectral.** Ultraspectral is beyond hyperspectral, a lofty goal that has not yet been reached (Ball, 1995). Currently, hyperspectral data are the most advanced available spectral measurements and they are extensively investigated.

Hyperspectral systems is a relatively recent and novel technology; Jet Propulsion Lab produced Airborne Imaging Spectrometer 1 and 2 (AIS), operated between 1982 and 1987, and Airborne Visible/InfraRed Imaging Spectrometer (AVIRIS), operating since 1989. They have made it possible for the collection of several hundred spectral bands, typically throughout the visible, near infrared, mid-infrared, and thermal infrared portions of the electromagnetic spectrum, in a single acquisition, producing spectral data which provide a spatially and thematically rich description of the distribution of materials. These contiguous spectral bands allow for in-depth

examination of earth surface features that visually appear very similar and provide scientists the opportunity to investigate complex problems that were difficult if not impossible to approach through multispectral data.

There are several available operating systems as shown in table 2.5. These systems may be portable, mounted in aerial vehicles or satellites, operating from the ground, air or space respectively. Different advantages and disadvantages are attached to groundborne, airborne or spaceborne data.

Table 2.5 Major recent hyperspectral sensors and their related spectral properties (by Dalponte et al., 2009).

sensor name	manufacturer	platform	maximum number of bands	maximum spectral resolution	spectral range
Hyperion on EO-1	NASA Goddard Space Flight Center	Satellite	220	10 nm	0.4 – 2.5 µm
MODIS	NASA	Satellite	36	40 nm	0.4 – 14.3 µm
CHRIS Proba	ESA	Aerial	up to 63	1.25 nm	0.415 - 1.05 µm
AVIRIS	NASA Jet Propulsion Lab	Aerial	224	10 nm	0.4 - 2.5 µm
HYDICE	Naval Research Lab	Aerial	210	7.6 nm	0.4 - 2.5 µm
PROBE-1	Earth Search Sciences Inc.	Aerial	128	12 nm	0.4 - 2.45 µm
CASI 550	ITRES Research Limited	Aerial	288	1.9 nm	0.4 - 1.0 µm
CASI 1500	ITRES Research Limited	Aerial	288	2.5 nm	0.4 - 1.05 µm
SASI 600	ITRES Research Limited	Aerial	100	15 nm	0.95 - 2.45 µm
TASI 600	ITRES Research Limited	Aerial	64	250 nm	8 - 11.5 µm
HyMap	Integrated Spectronics	Aerial	125	17 nm	0.4 - 2.5 µm
ROSIS	DLR	Aerial	84	7.6 nm	0.43 - 0.85 µm
EPS-H (Environmental Protection System)	GER Corporation	Aerial	133	0.67 nm	0.43 - 12.5 µm
EPS-A (Environmental Protection System)	GER Corporation	Aerial	31	23 nm	0.43 - 12.5 µm
DAIS 7915 (Digital Airborne Imaging Spectrometer)	GER Corporation	Aerial	79	15 nm	0.43 - 12.3 µm
AISA Eagle	Spectral imaging	Aerial	244	2.3 nm	0.4 - 0.97 µm
AISA Eaglet	Spectral imaging	Aerial	200	-	0.4 - 1.0 µm
AISA Hawk	Spectral imaging	Aerial	320	8.5 nm	0.97 - 2.45 µm
AISA Dual	Spectral imaging	Aerial	500	2.9 nm	0.4 - 2.45 µm
MIVIS (Multispectral Infrared and Visible Imaging Spectrometer)	Daedalus	Aerial	102	20 nm	0.43 - 12.7 µm
AVNIR	OKSI	Aerial	60	10 nm	0.43 - 1.03 µm

Applications of hyperspectral data have been pursued in all areas of Earth science including land, water and atmospheric topics.

Achievements in hyperspectral vegetation studies are numerous and on-going research is very promising. Use of hyperspectral data for vegetation studies has been mostly focused on **forest**

biochemistry (Asner, 1998; Zarco-Tejada et al., 2004a, 2004b; Asner and Martin, 2008; Blackburn and Ferwerda, 2008; Kokaly et al., 2009), **leaf area and stand structure** (Broge and Leblanc, 2001; Gong et al., 2003; Lee et al., 2004; Pu and Gong, 2004; Pu et al., 2005; Schlerf et al., 2005; Darvishzadeh et al., 2008)

When species mapping is the focus, the need for exploring hyperspectral data is particularly important, considering the limitations of using traditionally available wavebands, where most of the landcover is grouped and identification of individual species is particularly difficult.

2.3.2 Analysis chain

Key features of hyperspectral data are their inherent high spectral dimensionality, redundancy and noise, which inevitably affect requirements in computational resources and analysis algorithms.

The spectral redundancy, exhibited by high correlation between adjacent bands, besides increasing computing complexity, degrades classification accuracy when not enough training data are available (Landgrebe, 2003); which is usually the case.

Conventional algorithms developed for multispectral data are usually unable to handle dimensionality of hyperspectral data and result in failure or unacceptable performance (Lee and Landgrebe, 1993). Boardman (2005), supported that algorithms and processing systems must grow exponentially in capability to match the information content of the present and future hyperspectral data. This challenge is approached by attempts either to minimize data dimensionality or to consider novel data analysis techniques properly adjusted to the nature of hyperspectral data.

Figure 2.7 Typical hyperspectral image analysis

A typical hyperspectral analysis chain includes data preprocessing, data analysis and accuracy assessment (Figure 2.7). **Data preprocessing** usually includes data dimensionality reduction and atmospheric correction, which are further discussed in sections 2.3.3 and 2.3.4. **Analysis techniques** used with hyperspectral data besides **classification,** which is discussed in section

2.3.5**,** include **regression models** (Lee et al., 2004), **partial least squares** (Hansen and Schjoerring, 2003; Townsend et al., 2003; Williams et al., 2009), **radiative transfer modeling** (Kötz et al., 2004; Meroni et al., 2004; Darvishzadeh et al., 2008), and **hyperspectral reflectance indices** (Thenkabail et al., 2000; Broge and Leblanc, 2001; Gong et al., 2003; Zarco-Tejada et al., 2004b; Oldeland et al., 2010). The aforementioned techniques are typically used in an attempt to establish quantitative linkages between biochemical and functional properties of vegetation and spectral properties. C**lassification**, as means of providing thematic maps, is the workhorse of remote sensing when it comes to characterize the cover of the earth's surface. Because of the great value that maps bring into both research and operational applications, new classification algorithms keep adding to the ones already in use. At the end of any classification exercise, the **accuracy** of the product needs to be estimated in order to provide an evaluation of the classifier's performance and the map's value.

The literature review revealed that that more advance and novel algorithms are tested in case studies from a technical (computational) point of view, while less sophisticated methodologies are implemented in larger scale projects, where characterizing the landcover of the study area is the main aim, and available resources are a regulatory factor. The first, focus on the performance of the methodology in terms of algorithmic design, and assess their accuracy accordingly. On the other hand, the later focus on the map product and assess their accuracy with reference to the actual distribution of the property under investigation.

2.3.3 Dimensionality reduction

Data dimensionality is barely a concern when analysis multispectral data, and thus dimensionality reduction is not considered typical in classical image processing. However, in the case of hyperspectral image analysis, data dimensionality reduction is more often than not considered a practical necessity in order to address data redundancy and noise.

To mitigate the problem of data dimensionality, **custom** feature selection (Serpico et al., 2001; Han et al., 2004; Moustakidis and Theocharis 2010) or extraction (Kumar et al. 2001 ; Jimenez-Rodriguez et al., 2007) techniques have been investigated for their performance in reducing it, while preserving useful information, as well as vegetation indices (Thenkabail et al., 2000; Broge and Leblanc, 2001; Gong et al., 2003; Zarco-Tejada et al., 2004b; Oldeland et al., 2010; Mitri and Gitas, 2010).

Among the proposed feature extraction techniques, Minimum Noise Fraction (MNF) and Principal Components Analysis (PCA) are commonly used, as they are available within commercial image analysis software. Further discussion of these techniques follows in section 4.6. Other transformations such as logarithmic or derivatives (Gong and Yu, 2001) have also been suggested as methods for enhancing spectral information. However, a comprehensive evaluation of techniques for selecting optimal waveband and transforms from hyperspectral images is lacking in the remote sensing literature (Hamada et al., 2007).

2.3.4 Atmospheric correction

The nature of remote sensing requires that solar radiation passes through the atmosphere before it is collected by the instrument. In the case of hyperspectral remote sensing particularly, atmospheric influences modify the reflected signal from the target to the sensor, in one sense decreasing relative spectral differences within the sensor record and in another sense adding fine atmospheric absorption features to the spectral record (Ramsey III et al., 2005). Atmospheric correction is used to minimize these atmospheric influences and serves a critical role in the processing of remotely sensed image data. Cooley et al. (2002), argue that this is particularly the case with respect to identification of pixel content.

To compensate for atmospheric effects, properties such as the amount of water vapor, distribution of aerosols, and scene visibility must be known. Because direct measurements of these atmospheric properties are rarely available, there are techniques that infer them from their imprint on hyperspectral radiance data. Atmospheric corrections of this type can be applied on a pixel by pixel basis because each pixel in a hyperspectral image contains an independent measurement of atmospheric water vapor absorption bands.

Atmospheric correction algorithms for retrieving surface reflectance from hyperspectral imaging data include, but are not limited to, the Atmosphere CORrection Now -ACRON (Miller, 2002), the ATmosphere REMoval - ATREM (Gao et al., 1993), the Fast Line-of-sight Atmospheric Analysis of Spectral Hypercubes - FLAASH (Matthew et al., 2000), the High-accuracy Atmospheric Correction for Hyperspectral Data - HATCH (Qu et al., 2003), and the Atmospheric and Topographic Correction - ATCOR (Richter, 1998).

Although atmospheric correction is not standard when working with a single scene (Datt et al., 2003), atmospheric correction of hyperspectral data is mandatory for conversion of radiance to reflectance (Goetz et al., 2002). Also, as reported by Datt et al. (2003) noise management such

as MNF transformation is best applied after atmospheric correction. Berk and Adler-Golden (2002), showed that atmospheric correction serves a critical role in the processing of remotely sensed image data, particularly with respect to identification of pixel content. Adding to that, several studies suggested that that atmospheric correction creates a more spatially and temporally extendable and comparable dataset that maximizes the spectral distinctiveness of the canopy reflectance spectra (Richards, 1999; Smith and Milton, 1999; Eckert and Kneubühler, 2004; Pignatti et al., 2009). In particular, Nagendra (2001) and Clark et al. (2005) argued that atmospheric effects have to be corrected or compressed before conducting a species recognition analysis.

2.3.5 Classification

Classification of remote sensing imagery has been extensively studied, because classification results are the basis for many environmental applications. Although scientists have made great efforts in developing advanced classification approaches and techniques, classifying remotely sensed data into a thematic map remains a challenge (Lu and Weng, 2007).

Factors, such as the complexity of the landscape in a study area, the selected remotely sensed data, the **number of classes** to be separated, **variability** of the property under investigation, image processing and **classification approaches**, determinately affect the result of a classification (Dalponte et al., 2009;). Further, a key issue in supervised classification is the adequacy of training data to characterize the properties of the selected class, as the training set has a remarkable influence on the accuracy of classification results (Campbell, 1996; Foody et al., 2006).

Image classification includes several components, as determination of the classification system, selection of training samples, image preprocessing, and selection of classifier. The accuracy is later assessed with the use of available reference data, in order to accompany the produced map.

A broad spectrum of classifiers has been tested on hyperspectral data. Traditionally, classifiers model the underlying density of the various classes and then find a separating surface. However, density estimation in high-dimensional spaces suffers from the Hughes effect; that is for a fixed amount of training data, the classification accuracy as a function of number of bands reaches a maximum and then declines, because there is limited amount of training data to estimate the large number of parameters needed (Hughes, 1968).

In the contrary, advance classifiers, such as SAM (Clark et al., 2005; Mundt et al., 2005), SCM (Pengra et al., 2007), SVM (Melgani and Bruzzone, 2004; Vyas et al., 2011), ANN (Foody, 2004; Vyas et al., 2011), FesLiC (Stavrakoudis et al., 2012a), DTC (Shafri et al., 2007) have proven very effective when combined with hyperspectral data.

Synergy between different sensors has also proved to be beneficial for species mapping. In particular, LiDAR data, which provide structural information, when used parallel to hyperspectral data add great value to the produced maps (Anderson et al., 2008; Asner et al., 2008; Dalponte et al., 2008).

Although **mixture** is inherent in remote sensed images, it decidedly depends on the relationship between the spatial resolution of the image and the scale of desired measurement. Techniques have been designed to detect this mixture in a subpixel level, which are particularly effective in hyperspectral space.

Spectral Mixture Modeling (SMM) analysis assumes that the spectral value of each pixel is a linear (Ustin and Xiao, 2001; Asner and Heidebrecht, 2003; Chen and Vierling, 2006; Miao et al., 2006; Walsh et al., 2008) or a non-linear (Chen and Vierling, 2006; Huang and Townsend, 2003) combination of defined pure materials. These pure endmembers assumed to have a proportional membership in each pixel. Therefore, SMM analysis maps cover types, based on their abundances and provides the respective outputs in a continuous scale.

To address cases where the spatial resolution of an image is finer than the 'object' of observation, object based classifications have been used in species mapping (Heumann, 2011b; Kamal and Phin, 2011; Feret and Asner, 2013). Object based techniques recognize that important semantic information is not always represented in single pixels, but in meaningful image objects and their contextual relations (Hay and Castilla, 2008; Jyothi et al., 2008). The expectation from object based techniques is that they will replicate and/or exceed experienced human interpretation of remotely sensed images, resulting in more accurate and repeatable information, less subjectivity and reduced labour and time costs (Hay and Castilla, 2008).

Classification techniques that were used in the proposed methodologies of this study are further disused in sections 2.36, 2.3.7 and 2.3.8, while discussion of the preprocessing methodology follows in the fourth chapter.

2.3.6 Spectral Angle Mapper

Spectral Angle Mapper (SAM) is a physically based classification algorithm that determines the spectral similarity between two spectra by calculating the angle between the two spectra, treating them as vectors in a space with dimensionality equal to the number of bands (Kruse et al., 1993). SAM is a complex non-linear classification algorithm, which when used on calibrated reflectance data is relatively insensitive to illumination and albedo effects (Kruse et al., 1993). However, it does not distinguish between positive and negative correlation (Lumme, 2004). SAM compares the angle between the training spectra vectors of each class to the candidate pixel vectors of unknown class in *n*-dimensional space. It assigns to teach candidate the class with the smallest angle.

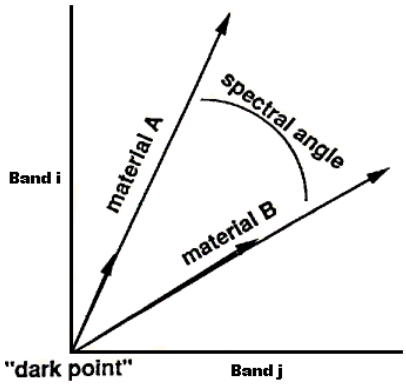

$$SAM(s_i, s_j) = \cos^{-1}\left(\frac{\sum_{l=1}^{L} s_{il} s_{jl}}{\left[\sum_{l=1}^{L} s_{il}^2\right]^{1/2} \left[\sum_{l=1}^{L} s_{jl}^2\right]^{1/2}} \right)$$

Figure 2.10 (a) Schematic representation of SAM consept, and (b) SAM similarity measure equation.

It is designed for use primarily with hyperspectral data, and has been repeatedly used in a broad range of vegetation applications (Piscini et al., 2001; Lumme, 2004; Buddenbaum et al., 2005; Shafri et al., 2007; Jollineau et al., 2008; Finley and Glenn, 2009; Pignatti et al., 2009; Mohd et al., 2010).

Finley and Glenn (2009) used SAM to map fire severity and oil water repellency achieving accuracies between 65% and 92%. Pignatti et al. (2009), used Hyperion to map landcover mapping in the fragmented ecosystem of Pollino National Park in Italy with SAM, achieving accuracies of 85%. Jollineau et al. (2008), when studying an inland wetland complex in southern Ontario in Canada found that SAM could distinguish between more classes than the Maximum likelihood classifier (MLC), achieving accuracies between 60% and 92%. Buddenbaum et al.

(2005), used SAM when investigated the value of geostatistical texture measures to find that application of pseudo-cross madograms increased accuracies.

In species level mapping, SAM has been used in several studies of invasive species (Mundt et al., 2005; Narumalani et al., 2006; Hestir et al., 2008; Cho et al., 2010; Miao et al., 2011). Hestir et al. (2008), used SAM together with SMM in a binary decision tree to map water hyacinth and submerged aquatic vegetation in Sacramento–San Joaquin River Delta. Narumalani et al. (2006), used SAM to detect saltcedar (*Tamarix sp*.) in Lake Meredith Recreational Ares in Texas and achieved accuracies of 83%. Cho et al. (2010), evaluated the performance of a traditional and a multiple-endmember SAM classification approach in discriminating ten common African savanna tree species, endorsing the later.

In studies that compared different classifiers SAM has been successful in (Narumalani et al., 2006; Pignatti et al., 2009) and less successful in others (Buddenbaum et al., 2005; Shafri et al., 2007).

2.3.7 Support Vector Machines

Support Vector Machines (SVM) is an effective, distribution free classifier that uses machine learning theory to maximize predictive accuracy while automatically avoiding over-fitting to the data. SVM derived from statistical learning theory, was introduced in the machine learning community in 1992 by Boser et al.

SVMs and related kernel methods have been one of the most popular and well-studied machine learning techniques of the past 15 years, with an amazing number of innovations and applications. They are used for many **pattern recognition** applications, such as **hand writing analysis** (Cortes and Vapnik, 1995; Stafylakis, 2008; Papavassiliou, 2010)**, face analysis** (Guo et al., 2001; Guo et al., 2008), **financial analysis** (Van Gestel, 2001), or **movie rating** (Lampropoulos et al., 2011). Although SVMs were initially developed to solve **classification** problems, they have been extended to solve **regression** and **distribution estimation** problems as well (Vapnik et al., 1997).

In the case of linear data, linear classifiers, which create separating hyper planes, can be used to divide the data. However it is often the case that the data is far from linear and as such inseparable by linear classifiers (see Figure 2.12).

Support vector machines (SVMs) are a set of related supervised learning methods, belonging to a family of generalized linear classifiers. Although SVM uses a linear separating hyperplane to create a classifier, for the problems that cannot be linearly separated in the original input space, SVM can non-linearly transform the original input space into a higher dimensional feature space (see Figure 2.11). In this feature space it is easier to find a linear optimal separating hyperplane, to separate classes with a decision surface which maximizes the margin between the classes, with respect to training data.

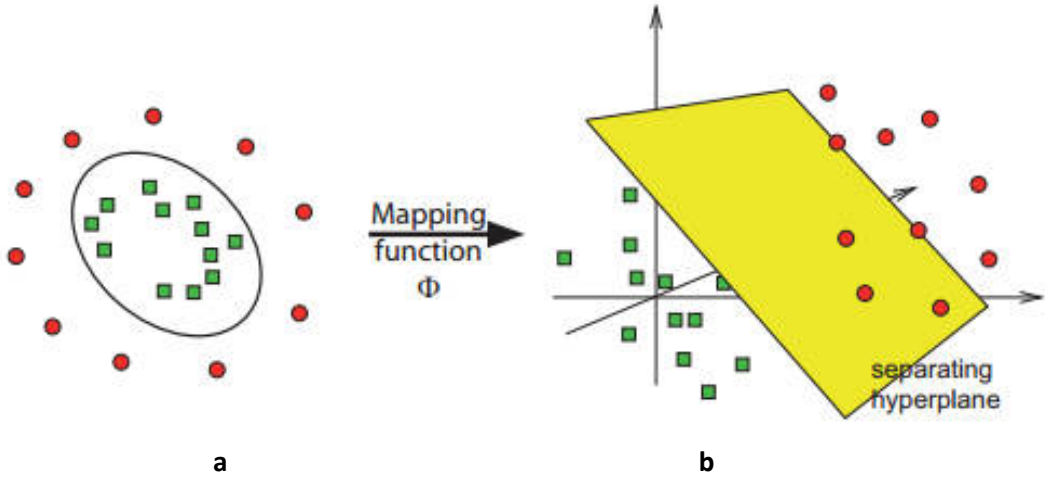

Figure 2.11 Non-linearly seperable training data (a) become seperable in higher dimention space (b) (by Huson, 2007).

The SVM based approach to classification seeks to find the optimal separating hyperplane between classes by focusing on the training cases that lie **at the edge** of the class distributions, the **support vectors**, with the other training cases effectively ignored (Brown et al., 2000; Belousov et al., 2002).

The goal in learning theory, and consequently SVM, is to maximize the generalization ability of the classifier, or, equivalently, to minimize the so-called **risk functional** (Vapnik, 1995)

According to Bruzzone and Carlin (2006), **structural risk minimization** instructs that a hyperplane is optimal, when it minimizes a **cost function** that expresses a combination of:

- maximizing the margin, i.e. the distance between the hyperplane and the closest training samples (Figure 2.13), and

- minimizing the error on training samples that can not be separated.

SVMs embody the structural **risk minimisation process (**Haykin, 1999**)** to reduce the risk of over-fitting the training set, when minimising the model's flexibility as part of the learning process (Figure 2.12).

A detailed description on the concept of SVM and the formulation of the problem is given in Burges (1998), and comprehensive introductions in a remote sensing context in Foody and Mathur, 2004, Melgani and Bruzzone, 2004, and Pal and Mather, 2006.

In essence, given a training set of instance-label pairs, the SVM (Boser et al., 1992; Cortes and Vapnik, 1995) requires the solution of the following optimization problem (equation 2.1) (Chang and Lin, 2011):

$$\min_{\boldsymbol{w},b,\boldsymbol{\xi}} \quad \frac{1}{2}\mathbf{w}^T\mathbf{w} + \mathrm{C}\sum_{i=1}^{l}\xi_i \qquad \text{eq. 2.1}$$

$$\text{subject to } y_i(\boldsymbol{w}^T\varphi(\boldsymbol{x}_i) + b) \geq 1 - \xi_i,$$

$$\xi_i \geq 0$$

Here, training vectors x_i are mapped into a higher (maybe infinite) dimensional space by the kernel function Φ. SVM finds a linear separating hyperplane with the maximal margin in this higher dimensional space. The concept of **maximal margin** hyperplanes was introduced by Vapnik and Lerner (1963), and Vapnik and Chervonenkis (1964) based on the intuition that the larger the margin, the better the generalization ability (Figure 2.13).

Margin parameter value *C*, is the penalty parameter of the error term and controls the trade-off between maximizing the margin and minimizing the training error, by shaping the discriminant function and consequently, the decision boundary when data are non-separable (Dalponte et al., 2008).

SVM uses the **kernel trick** to map indirectly to extremely high dimensional spaces (Aizerman et al., 1964; Boser et al., 1992). SVM builds on positive definite kernel methods, which are utilized to project the data into a high dimensional dot product space, in order to provide a measure of similarity between possibly complex objects. **Kernel** methods have a solid theoretical foundation

that has been studied by mathematics and statistics communities, additionally to their empirical success (Gehler and Schölkpf, 2009).

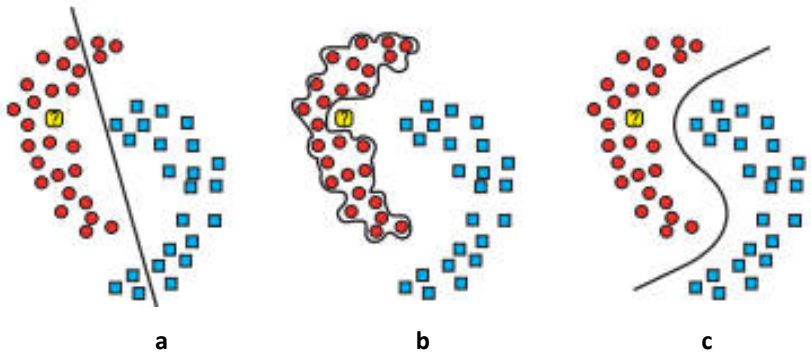

Figure 2.12 (a) A too simple model that would classify the yellow unknown datum correctly but mistake other training data, (b) a too complex model that quasi learns the training data and is intolerant of small acceptable deviations (overfitting), and (c) a model with good generalization ability that classifies the uknown datum correctly. (by Huson, 2007)

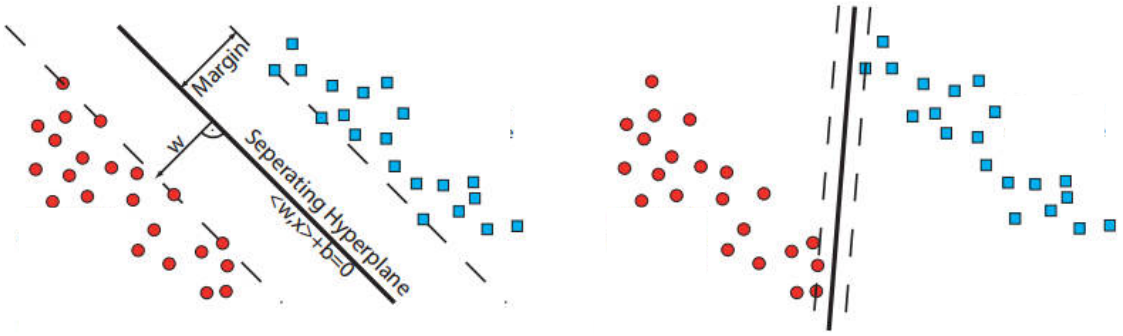

Figure 2.13 Optimal separating hyperplane that maximises margines (a). and a bad separating hyperplane with minimum margines (b). (by Huson, 2007)

Between the most utilized kernels there are:

- Linear $K(x_i,x_j) = x_i^T x_j$
- Polynomial $K(x_i,x_j) = (gx_i^T x_j + r)^d, g > 0$
- Radial basis function (RBF) $K(x_i,x_j) = \exp(-g||x_i - x_j||^2), g > 0$
- Sigmoid $K(x_i,x_j) = \tanh(gx_i^T x_j + r)$

Where, *γ, r*, and *d* are kernel parameters. In the case of RBF, *γ* is the parameter controlling the width of the Gaussian kernel. Choosing a small value for the kernel width parameter may lead to overfitting, while large kernel width values may lead to oversmoothing.

In SVM generalization ability is controlled by the choice of kernel (Abe, 2010), its parameters and the aforementioned margin parameter *C*. To select the optimal parameters to a given problem is called model selection. This is a **cross-validation** technique that estimates the generalization ability through repeatedly training support vector machines.

The SVM classifier was developed to solve **binary** classification problems, but it can be easily generalized to multiclass problems. There are roughly four types of SVM that handle multiclass problems (Abe, 2010): one-against-all (OAA) SVM, one-against-one (OAO) or pairwise SVM, error-correcting output code SVM and all-at-once SVM (Abe, 2010).

A common limitation to SVM methodologies is the selection of SVM key parameters such as the kernel functions and the *C* **parameter value**. There exist no established heuristics for selection of these SVM parameters, frequently leading to a trial-and-error approach (Mountrakis et al., 2011).

SVMs are particularly appealing in the **remote sensing** community due to their ability to generalize well even with limited training samples, a common limitation for remote sensing applications (Mountrakis et al., 2011). However, they suffer from parameter assignment issues, as mentioned above, which can significantly affect obtained results.

It was first applied in **hyperspectral** data by Gualtieri and Cromp in 1998. Recently SVMs attracted much attention and have been used in several hyperspectral remote sensing applications (Camps-Valls and Bruzzone, 2005; Bruzzone et al., 2006; Pal and Mather, 2006; Li et al., 2009; Dong and Liu, 2011; Petropoulos et al., 2011).

Comparative studies have shown that classification by a SVM can be more accurate than popular contemporary techniques such as neural networks and decision trees as well as conventional probabilistic classifiers such as the maximum likelihood classification (Melgani and Bruzzone, 2004; Pal and Mather, 2004, Dalponte et al., 2012; Feret and Asner, 2013).

The majority of the studies that used Hyperspectral imagery along with SVM were **algorithm oriented** (Pal and Mather, 2004; Pal and Mather, 2006; Dalponte et al., 2009), as opposed to actual **mapping** of a study area (Zhang and Xie, 2013; Petropoulos et al., 2011).

Melgani and Bruzzone (2004) found SVM effective in classifying **AVIRIS** hyperspectral data directly in the hyperspectral space, without the need of feature selection, and concluded that SVM is a valid and effective alternative to classify hyperspectral remote sensing data. **Vyas et al**. (2011), also achieved higher OA when classifying the entire data cube rather than the image produced after feature selection. In the contrary, several studies used SVM in datasets of reduced dimentionality (Campbell et al., 2004; Dalponte et al., 2008; Petropoulos et al., 2011; Petropoulos et al., 2012).

In the case of species mapping, Plaza et al. (2009) have successfully classified different tree species from urban area with the help of SVM classifier. Campbell et al., (2004) used SVM with HyMap data to classifiy 6 crop species and achieved accuracies between 90% and 99%. Dalponte et al. (2008), and Dalponte et al. (2008), successfully used SVMs to classify a complex forest environment with AISA data alone and fusion of AISA and LiDAR data, respectively. Karimi et al. (2006), used CASI data in conjunction with an SVM method in automatic field detection of weeds and nitrogen.

2.3.8 GEOBIA

It is commonly agreed that image pixels are cells of an arbitrarily imposed grid, whose boundaries lack any real counterpart, and exist solely for the purpose of measurement or representation (Atkinson, 2004). What is more, when a **human interpreter** views, a typically high-resolution image, she does not view a world composed of individual pixels, but a continuum of discrete objects, whose size, shape, spatial arrangement and context change depending upon the scale at which they are examined (Marceau, 1999; Marceau and Hay, 1999). She essentially sees the image filled with groups of pixels with meaning in the real world (Schneider and Steinwender, 1999).

This recognition that individual pixels are not true geographical objects, and the vision that simulation of visual interpretation through knowledge modeling is possible, were key promoters of the geographic object based image approach (GEOBIA). Hay and Castilla (2008) define GEOBIA as ‘a discipline that will primarily develop theory, methods and tools’.

GEOBIA is technically and theoretically different to pixel based image processing approach and allows for a shift from the pixel to the geographic object as a unit of analysis. The **conceptual framework** of the GEOBIA process focuses on the transformation of the image’s constituent

elements from the raw pixels to the final structures representing geographic objects (Lizarazo and Elsner, 2008).

GEOBIA commences with segmentation, the partition of an image into relatively homogeneous and semantically significant groups of pixels (Blaschke, 2010), in some way related to real world objects (Figure 2.14). These discrete, non-overlapping, space-exhausting image segments are generated by maximizing one or more criteria of **homogeneity** in one or more dimensions of a feature space, respectively (Hay et al., 2002; Hall and Hay, 2003). Homogeneity is based on a combination of **spectral similarity**, **contrast with neighboring** objects and **shape characteristics** of the resulting objects and is controlled by the analyst through **segmentation parameters.**

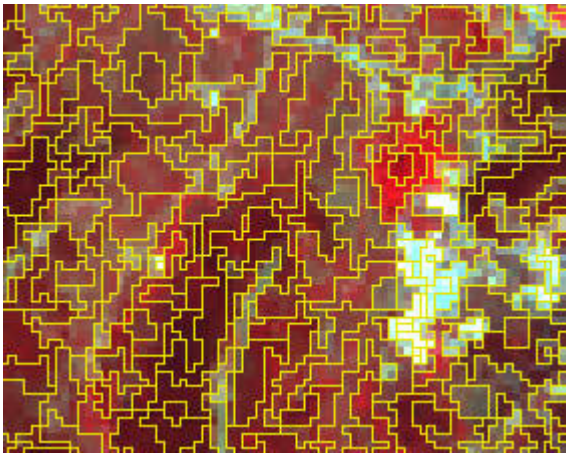

Figure 2.14 Segmentation result overlaid on a part of Thassos Hyperion image.

From an algorithmic perspective, i**mage segmentation**, is generally divided into four categories: (a) point-based, (b) edge-based, (c) region-based and (d) combined (Schiewe, 2002).

The challenge is to define appropriate **segmentation parameters** for the varying sized, shaped and spatially distributed image objects composing a scene, so that segments which satisfy user requirements can be generated.

Segments have additional spectral information compared to single pixels (mean, median, minimum and maximum values per band, mean ratios, variance etc.), but of even greater advantage is the generated **contextual information**, such as texture and compactness, and **topological relationships** between segments, such as adjacency (Blaschke and Strobl, 2001; Benz et al., 2004; Hay and Castilla, 2008; van der Werff and van der Meer, 2008;).

What is more, image objects can be produced at one single spatial scale or at several nested scales (Figure 2.15), thus providing a framework for **multiscale** analysis which is fundamental for ecological studies. GEOBIA allows the discretization and attribution of the multiple spatial dimensions at which entities, patterns and processes can be observed and measured (Hay et al., 2005).

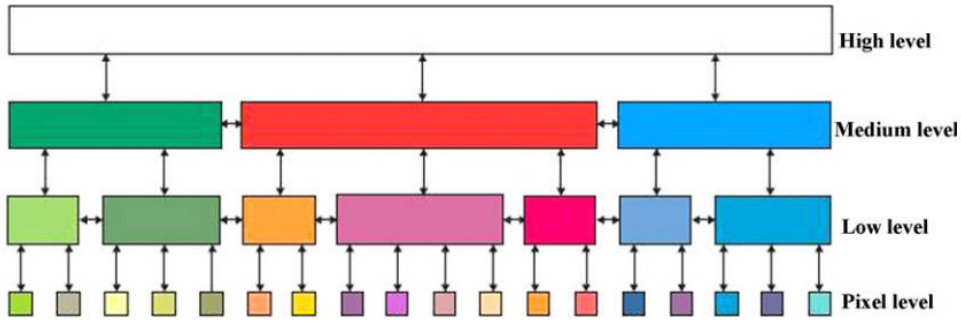

Figure 2.15 Object hierarchy.

Once the segmentation has provided image objects that satisfy user requirements, these serve as information carriers and building blocks for further classification analysis (Baatz and Schape, 1999; Hay and Castilla, 2008; Lang, 2008).

What is unique with GEOBIA is that it allows for the description of a class not only in spectral space, but also taking into consideration the integral contextual and topological information of image segments, which are the main discriminators of visually perceptible objects in the image. It allows for delineation of readily usable objects from imagery while at the same time combining image processing and **GIS functionalities** in order to utilize spectral and contextual information in an integrative way (Blaschke, 2010).

Adding to that, it also allows for soft classification which, instead of using 1 and 0 to declare whether an object belongs or not in a class respectively, uses values between 0 and 1 to assign a degree of membership of an object to a class.

This way, the analyst can build a process tree with rules that exploit both the spectral and spatial information of the image, not necessarily in a unidirectional flow, but also including feedback loops and knowledge inputs at any stage of the process.

Besides soft rule based classification, several other classifiers have been used within the GEOBIA framework such as LDA (Haest et al., 2010), SMM (Mücher et al., 2010; Nidamanuri and Zbell,

2011), data mining techniques (Formaggio, 2010), decision trees (Laliberte et al., 2007; Heumann, 2011b), and SVM (Heumann, 2011b).

Among others, the Nearest Neighbor (NN) classifier is a typical choice as it is built in the most commonly used GEOBIA software, namely eCognition Developer (Gao and Mas, 2008; Chmiel and Fijałkowska, 2010; Mitri and Gitas, 2010; Rafieyan et al, 2010; Aguirre-Gutiérrez et al., 2012). NN is a non-parametric classifier, widely used in the field of pattern recognition (Zammit et al., 2006), that labels an unclassified object according to its nearest neighboring training object in the feature space.

Although, GEOBIA developed along with the increase of VHR imagery availability and problems associated with the high spatial resolution domain (Blaschke and Hay, 2001; Hay et al., 2005; Laliberte et al., 2007; Wulde et al., 2008; Chmiel and Fijałkowska, 2010, Ke et al, 2010; Heumann, 2011b) it has also been employed in conjunction with medium resolution imagery.

In the case of **medium resolution** imagery, not all of the aforementioned advantages can be exploited because the features of observation in this scale are completely different than the ones observable by VHR imagery. In this case, one deals with geographic or landscape features as opposed to 'objects', such as trees, buildings etc. However, the delineation and manipulation of landscape features as opposed to pixels in this scale has many advantages, mainly focused around the GIS functionalities. Several studies used medium resolution imagery, (Eckert and Kneubühler, 2004; Gao and Mas, 2008; Formaggio, 2010; Aguirre-Gutiérrez et al., 2012; Petropoulos et al., 2012). GEOBIA has also been used with Landsat TM and ETM+, in two national scale studies of landcover change with focus on deforestation (Duveiller et al., 2008; Liarikos et al., 2012) and also in the United States National Coastal Wetlands Inventory (NCWI) (Stein eta al., 2012). Blaschke (2010), argues that **medium resolution imagery,** such as Landsat, does not support multi-level segmentation; however Eckert and Kneubühler (2004), Mitri and Gitas (2010), Polychronaki and Gitas (2010) and Petropoulos et al. (2012), have incorporated it in their methodologies, to improve classification results.

As an alternative to pixel based approaches, GEOBIA methodologies have also been evaluated in conjunction with hyperspectral imagery (Eckert and Kneubühler, 2004; Bunting and Lucas, 2006; Mücher et al., 2010; Petropoulos et al., 2012). However, the influence of high spectral dimensionality on the different GEOBIA components has not been yet evaluated and remains to be assessed how the **segmentation** algorithms manage this high dimensionality.

In GEOBIA, a comprehensive trial and error investigation of the numerous spectral bands provided by hyperspectral imagery does not appeal feasible. To account for this, spectral transformations such as vegetation indices have been used prior to rule based model development (Bunting and Lucas, 2006; Vanhuysse et al., 2010; Kamal and Phin, 2011), as well as the NN classifier in the original spectral space (Eckert and Kneubühler, 2004, Kamal and Phin, 2011; Skoupý et al., 2012). Nidamanuri and Zbell (2011), used object information to train a SAM classifier.

Aguirre-Gutiérrez et al. (2012), used NN and Landsat ETM+ to map forest changes due to illegal logging, in a combination of pixel and objet based classification system. Bunting and Lucas (2006), used CASI-2 data for tree crown delineation and classification. Duveiller et al. (2008), used GEOBIA to estimate deforestation rate in Central Africa with Landsat imagery, which is considered of high spatial resolution in the sub Continental scale of the study. Eckert and Kneubühler (2004), used Hyperion and GEOBIA and SAM to classify agricultural land and vegetation properties. Formaggio (2010), used Landsat with GEOBIA and data mining techniques to map sugarcane achieving OA of 94%. Gao and Mas (2008), compared pixel and object based classification (NN) on different resolution images (10 to 250m) and found that the advantages of GEOBIA are more evident in high spatial resolutions.

In the case of forest species mapping few studies have been reported. Kamal and Phin (2011), used CASI-2 to compare pixel and object based approaches in differentiating three mangrove species and found that GEOBIA gave the most accurate results (76%), followed by SAM (69%) and LSU 56%). Feret et al. (2011), also compared pixel (LDA and RDA) and object based classification of 13 species using CAO-Alpha system. Ke et al. (2010), investigated several segmentation schemes and employed machine learning decision trees to map 5 forest species, using multispectral Quickbird imagery combined with LiDAR measurements. Rafieyan et al. (2010), mapped disturbed natural broadleaved and mixed forest in Iran, with NN in a GEOBIA and reported KIA between 0.61 and 0.79. Heumann (2011b), used Worldview-2 in a GEOBIA classification, which combined decision-trees with SVM, to map fringe against true mangrove species and reported overall accuracy greater than 94%.

Concluding, GEOBIA methods are making considerable progress towards a spatially explicit information extraction workflow (Blaschke, 2010), such as is required for environmental research and management, as well as other spatial planning applications. This progress, which may be attributed to the documented limitations in the use of pixel based image approaches,

regarding **relative scale**, incorporation of **spatial context**, and **fuzzy or smooth transitions** (Blaschke and Strobl, 2001), motivates research for operational regional forest species mapping.

2.3.9 Accuracy assessment

Overall quality evaluation of the image analysis is usually conducted at the end of the process. Several statistical methods for **accuracy assessment** have been discussed in the remote sensing literature (Congalton, 1991; Foody, 2002; Smith et al., 2002, 2003a; Stehman et al., 2003).

The standard method for **validation of image** output uses a confusion matrix (Congalton and Green, 1999). This cross-tabulates labels assigned to pixels by the classifier with labels assigned to the sampling points during field survey, using geographic location as the key to cross-tabulation. The resulting matrix is analyzed with one or more measures of agreement, usually the Kappa Index of Agreement (KIA) (Cohen, 1960), overall (OA), user's and producer's accuracy (Story and Congalton, 1986). The OA is the percentage of cases that are correctly classified, calculated along the confusion matrix diagonal, while the KIA shows how each classification differs from a random classification of landcover types (equation 2.1). The producer's accuracy refers to the probability that a certain land-cover of an area on the ground is classified as such, while the user's accuracy refers to the probability that a pixel labeled as a certain land-cover class in the map is really this class. The user's accuracy details errors of commission resulting when a pixel is committed to an incorrect class, while the producer's accuracy details the errors of omission resulting when a pixel is incorrectly classified into another category and omitted from its correct class. The KIA statistic (equation 2.1) is a suitable measure of the accuracy in thematic classification procedures because it takes into account the entire error matrix instead of simply the diagonal elements, like the overall accuracy does.

$$K = \frac{N\sum_{i=1}^{r} X_{ii} - \sum_{i=1}^{r}(X_{i+} * X_{+i})}{N^2 - \sum_{i=1}^{r}(X_{i+} * X_{+i})} \qquad \text{eq. 2.1}$$

x_{ii} is the number of combinations along the diagonal

x_{i+} is the total observations in row i

x_{+i} is the total observations in column i

N is the total number of matrix cells

r is the number of row in cross classification table

These statistics provide a measure of how well a classification performed with respect to ground-truth data (Michelson et al., 2000), thus spatially explicit reference data are regarded as an important aspect, especially when employing classification results for decision making (McIver and Friedl, 2001; Liu et al., 2004). A per se 100% OA would not imply that a map correctly describes the exact extent of the class examined, but would indicate that all the reference data were correctly classified. It then remains to the validity of the sampling methodology, which produced the reference data, to determine the value of the map.

An absolute boundary of what is considered acceptable accuracy can not be set, as it is inextricably related to the nature of every study. However, Thomilnson et al. (1999) set a target of an overall accuracy of 85% with no class less than 70%, Foody (2002) also argues that a target of 85% OA should be considered, while Goodenough et al. (2003), suggest that discrimination accuracies of species over 80% correct would be considered operational and exceed that found in most forest inventory systems. Although this limit can be considered arbitrary, it provides a useful qualitative benchmark.

In the case of GEOBIA, classical point-based sampling strategies using systematic, probabilistic or stratified probabilistic sampling may prove to be less appropriate as they do not rely on the concept of objects (Radoux et al., 2011). There is currently an open discussion on the accuracy assessment methodologies that best apply to GEOBIA (Albrecht et al., 2010; Lang et al., 2010; Hernando et al., 2012).

2.4 CHAPTER CONCLUSIONS

The key points discussed in this chapter are summarized below.

- Although Mediterranean forests represent a **small fraction of the world's forest** cover, they are of great importance mostly because of their high biodiversity and support of human population growth. They have been under the influence of men for more than 10,000 years; however, modern anthropogenic pressures seem to threaten the dynamic equilibrium of the past.

- Greek forest are of typical Mediterranean type and despite their great value, they face many threats, such as wildfires and encroachment, resulting from urban expansion and uncontrolled human activity. What is interesting and unfortunate is the lack of spatial data to support policy making and sustainable management.

- Remote sensing has been used successfully over the past decades in the collection of essential spatial information for the monitoring and management of the Mediterranean forests, and continues to offer grounds for novel applications.

- Advances in hyperspectral technology, which is capable of resolving the spectrum in continuous narrow bands and allow detection of subtle spectral changes of various targets, provide means for in depth analysis of forest species level mapping, which was not successful until the emergence of hyperspectral technologies.

- Conventional algorithms developed for multispectral data are usually unable to handle dimensionality of hyperspectral data and result in failure or unacceptable performance. This challenge is approached by attempts either to minimize data dimensionality or to consider novel data analysis techniques properly adjusted to the nature of hyperspectral data.

- As data dimensionality reduction is often considered a practical necessity in hyperspectral data analysis, custom feature selection or extraction techniques have been investigated, along with traditional MNF and PCA transformations, for their performance in reducing it, while preserving useful information.

- Several atmospheric correction algorithms have been used to retrieve surface reflectance from hyperspectral imaging data and create a more spatially and temporally extendable and comparable dataset, which maximizes the spectral distinctiveness of target features.

- Classification of remote sensing imagery is the basis of many environmental applications, as it provides valuable thematic maps. It is controlled by factors such as the number of classes to be separated, the quality of training data, variability of the property under investigation, and image-processing and classification approaches.

- SAM is a physically based classification algorithm traditionally used with hyperspectral imagery in a broad range of applications. It determines the spectral similarity between two spectra by calculating the angle between them, treating them as vectors in a space with dimensionality equal to the number of bands.

- SVMs are derived from **statistical learning theory,** and are particularly appealing in the remote sensing community due to their ability to generalize well, even with limited

training samples; a common limitation for remote sensing applications. They are increasingly used over the past few years as they usually outperform other classifiers.

- GEOBIA includes processes that transform image data from the remotely sensed physical reality to the human conceptualization of the geographic objects, through a segmentation stage. The classification of the objects can be implemented in a soft way, either by the development of a rule model or by using other classifiers such as NN.

- Overall quality evaluation of the image analysis is usually conducted at the end of the process. The standard method for validation of image output uses a confusion matrix and cross-tabulation of labels assigned to pixels by the classifier with labels assigned to the sampling points during field survey, using geographic location as the key to cross-tabulation. As suggested in the literature, overall accuracy of grater than 80% or 85% could be considered operational and exceed that found in most forest inventory systems.

- In the case of mapping an ecological asset, such as forest, a complete methodology, which makes use of available data and processing techniques and has an associated estimation of accuracy, is necessary in order to deliver a useful product for understanding, planning and managing.

3

STUDY AREAS AND DATASET DESCRIPTION

Chapter 2 discussed the importance of Mediterranean forest, forest mapping with the use of remote sensing and the value of hyperspectral data in species level mapping. This chapter describes the two study areas, which were chosen to examine the use of EO1 Hyperion satellite hyperspectral imagery in species level mapping. These two areas, namely Thassos and Taxiarchis, differ both in species composition and distribution pattern complexity, allowing for in depth investigation of the problem. In sections 3.1 and 3.2 their geomorphology, climate, landcover and management history is described. The data used in this study, coming from satellite and airborne sensors, as well as from thematic imagery photointerpretation and extensive field surveys, are also described in sections 3.3.

3.1 THASSOS

3.1.1 Phisiography

The first study area is a part of the island of Thassos, Greece's most northerly island that extends from 24°30' to 24°48' East and 40°33' to 40°49' North. The island's surface is 400 km^2, however, Hyperion imagery after the exclusion of the area heavily affected by clouds, covers 110km^2 in the northern middle part of the island.

From a geological point of view Thassos belongs to the crystalline schistose Rhodopi Massif and is formed by alternating marbles, gneisses and schists, with numerous minerals and dense accumulation of lead, zinc, iron and magnase (Moundrakis, 1985). Thassos is characterized by an abundance of natural mineral resources, which have been mined since ancient times. In particular the mining gallery located at Tzines is a unique testimony of what could possibly be the most ancient mining gallery in Europe.

The terrain of the island is diverse and in places very rough, forming streams with deep slopes and ridges with small to large gradients. Altitude ranges from sea level to 1204m, in the highest peak Ipsario.

The soil depth varies widely depending on surface geology, relief and vegetation density (Spanos, 1992). Shallow soils (5-10 cm) prevail due to steep slopes, grazing and repeated forest fires. Shallow soils constitute almost the half of the islands soils, while deep soils constitute 35%, with the remaining 15% classified as bare soil (Nakos, 1995). As a result, the mean height of the forest stands in Thassos is lower than the average for this type of forest (Spanos, 1994). The soil is mostly clay. The small degree of soil genesis, due to unfavorable conditions, justifies its moderate mechanical composition and the presence of abundant inert material. The porous structure, the permeability, the consistency, the water storing capacity and the color of the ground material depends on the texture and the content of organic matter which varies across the island.

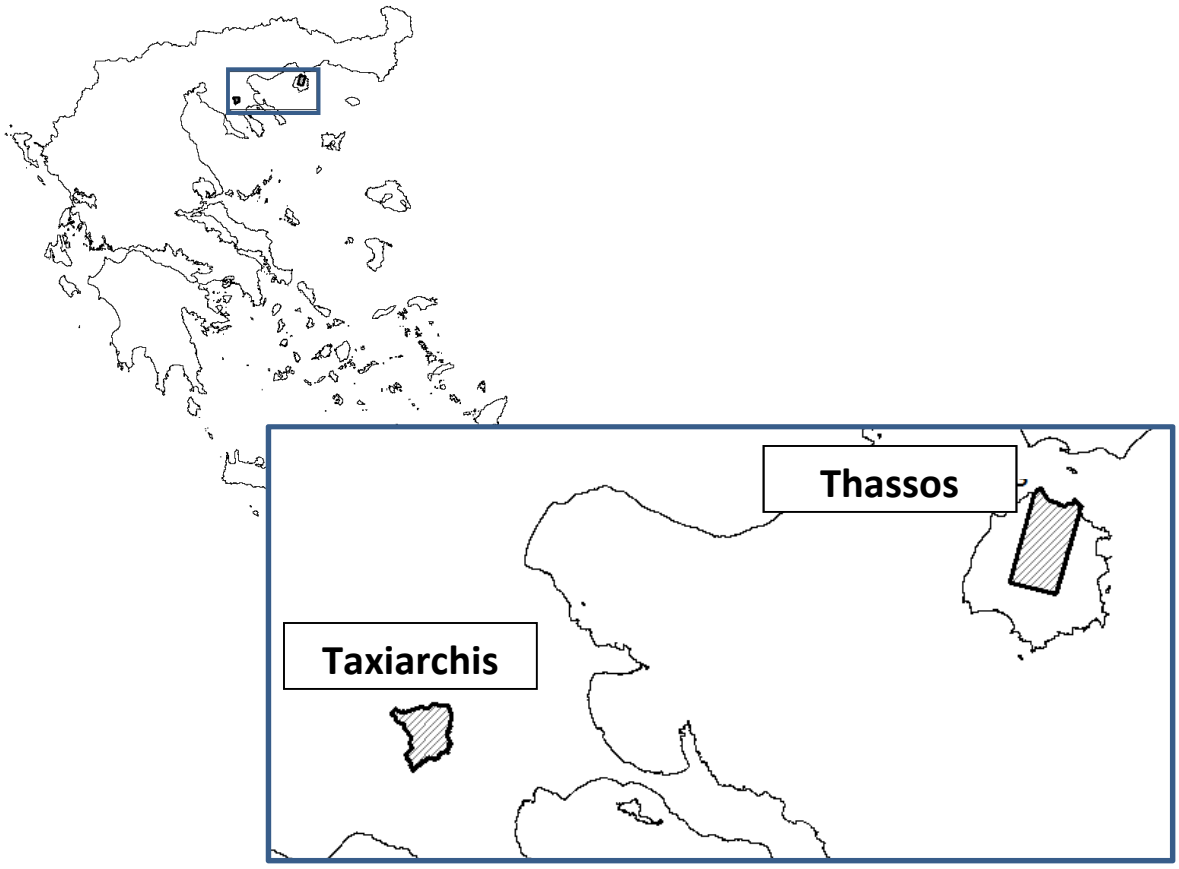

Figure 3.1 Location map of the two study areas.

Figure 3.2 shows the Bagnouls-Gaussen's index of aridity of the island, from observations between 1976 and 1999.

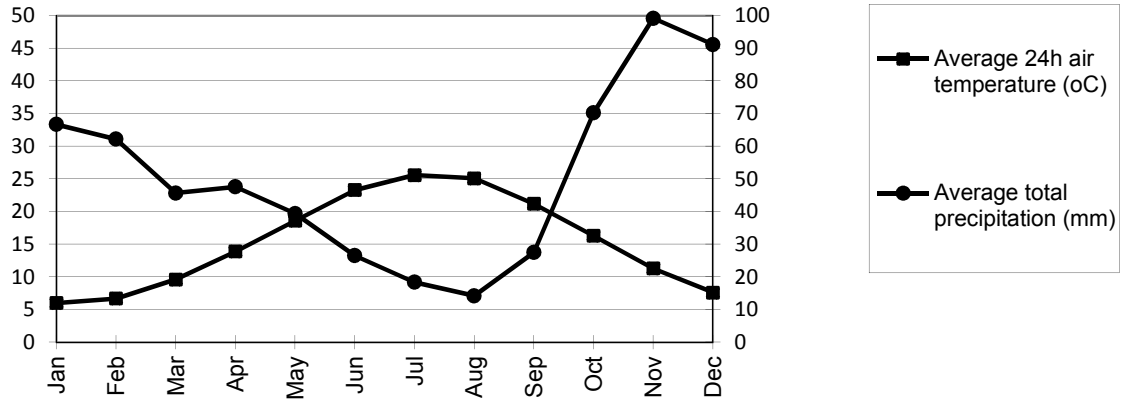

Figure 3.2 Bagnouls-Gaussen's index of aridity of the island.

3.1.2 Vegetation

Thassos belongs to three of the Greek vegetation zones, as described by Dafis (1976), namely Quercetalia ilicis, Quercetalia pubescentis and Fagetalia:

1. ***Quercetalia ilicis***. It is found in altitudes ranging from sea level to 300m, close to the coastline of the island and is typical for the dry and warm climate of the island. The dominant forest species of this zone is *Pinus brutia*. It is represented by its both sub zones:

- *Oleo-Ceratonion*, and in particular growth space Oleo-Lentiscetum is found in the southern part of the island. *P. brutia* stands belonging to this formation were burnt in the 1984 and 1985 forest fires. The representative maquis species are *Pistacia lentiscus, Erica manipuliflora, Myrtus communis, Olea europea, Quercus coccifera, Lonicera etrusca, Rosa sempervirens, Phillyrea latifolia and Rubia peregrina*;
- *Quercion ilicis*, and in particular growth space Orno-Quercetum ilicis is found in the Northern part of the island. *P. brutia* stands that belong to this subzone were burnt in the 1989 forest fire. In Northern aspects where the soils are deeper, more fertile and moister *Quercus ilex, Arbutus unedo, Phillyrea latifolea and Fraxinus ornus* dominate the understorey, while in Southern aspects with low site quality *Erica arborea* and *Erica manipuliflora* are mostly found;

2. ***Quercetalia pubescentis***. It is found in altitudes ranging from a 300 to 800m in both Southern and Northern parts of the island. It is represented by the sub zone *Ostryo-Carpinion*, which is dominated again by *P. brutia*. There is a very dense understory that consists of *Quercus coccifera* which is very resistant to fire, grazing and other anthropogenic influence

3. ***Fagetalia***, is represented by the sub-zone Abietion cephalonicae and in particular growth space Abietum borisii regis. It is found in mountainous areas of the island and is dominated by *P. nigra* stands, while small *Abies borisii regis* and *Quercus-Castanea* stands can also be found at the highest altitudes.

Although, fauna of the island lacks large mammals such as wolf, jackal, fox and boar, it exhibits populations of small mammals such as hares and ferrets, which occasionally show excessive growth, leading to ecological imbalances. The avifauna of the island is quite interesting (with endemic and migratory species) having partridges, quails, turtle dove, and eagles as main representatives.

The two dominant forest species of the island are *P. brutia* and *P. nigra*, growing quite separately as also noted in the description of the vegetation zones above. Following the pine-species functional classification of Keeley and Zedler (1998), *P. brutia* belongs to the ‘‘R’’ functional type of pines and presents traits such as seed serotiny, short juvenile period, short lifespan and enhanced wind seeddispersal ability that enables it to deal with ‘‘predictable standreplacing fires’’. On the other hand, *P. nigra* belongs to the ‘‘U’’ functional group, which contains species found in productive sites with ‘‘unpredictable stand-replacing fires’’.

Figure 3.3 shows some typical landscapes of Thassos.

In Thassos the existing *Pinus brutia* forest consists of 30% even-age stands and 40% uneven-age stands while the remaining 30% is a mosaic of even-age and uneven-age stands (Gitas et al., 2000). The shrub understory of brutia pine forests of Thassos island varies from site to site and in many cases, it is floristically rich, comprising various evergreen sclerophyllous (maquis) species (e.g. *Quercus coccifera, Phillyrea latifolia, Pistacia terebinthus, P. lentiscus, Arbutus unedo, A. andrachne, Myrtus communis*) as well as phryganic subshrubs (e.g. *Erica arborea, E.*

manipuliflora, Cistus creticus, C. salviifolius, Paliurus spina-christi, Calicotome villosa) (Spanos et al., 2001).

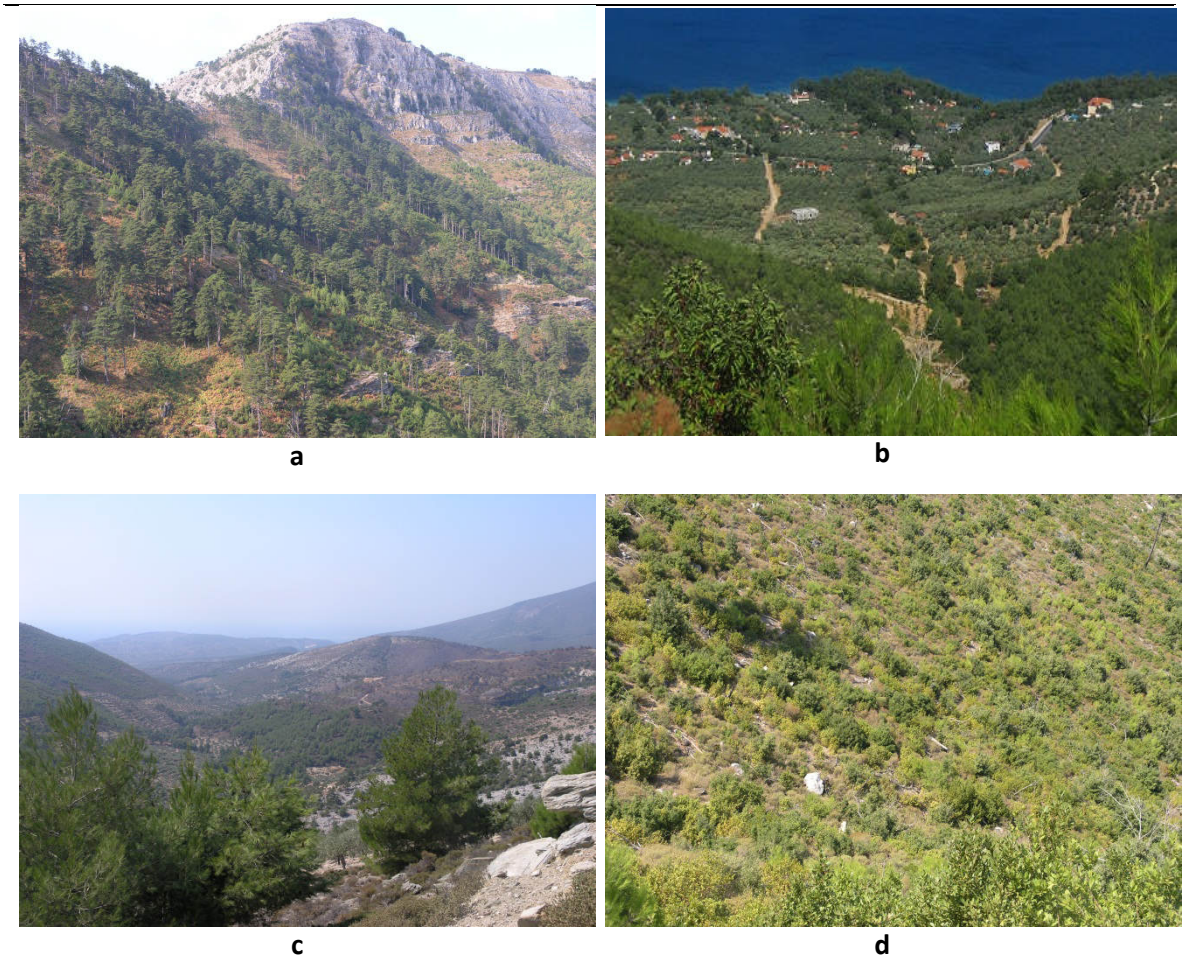

Figure 3.3 Typical landscapes of Thassos. (a) Open *P. nigra* stands close to the mountain top, (b) mix of *P. brutia* stands and olive orchards at the lowland, (c) young *P. brutia* trees mixed with maquis, (d) phrygana.

P. nigra is found in the higher altidudes of Thassos at the middle part of the island. It forms both closed stands but also mixed in a variety of patterns with grasslands and bare rocks, mostly limestone pavements. In places, the pines are ancient and resemble the 'granny' pines of the Caledonian forests in the Scottish Highlands.

Phrygana and maquis are widely distributed around the island and are currently extending their range as they colonize lowland slopes cleared of conifers in the past devastating wildfires (Karteris et al., 1992).

Olea europaea, in olive groves, is the most abundant broadleaf tree, close to 21% of the island. Olive groves, widely distributed around the coast, are the main part of the local agriculture, but also support a rich variety of wildlife. Most of them are grazed to a greater or lesser extent.

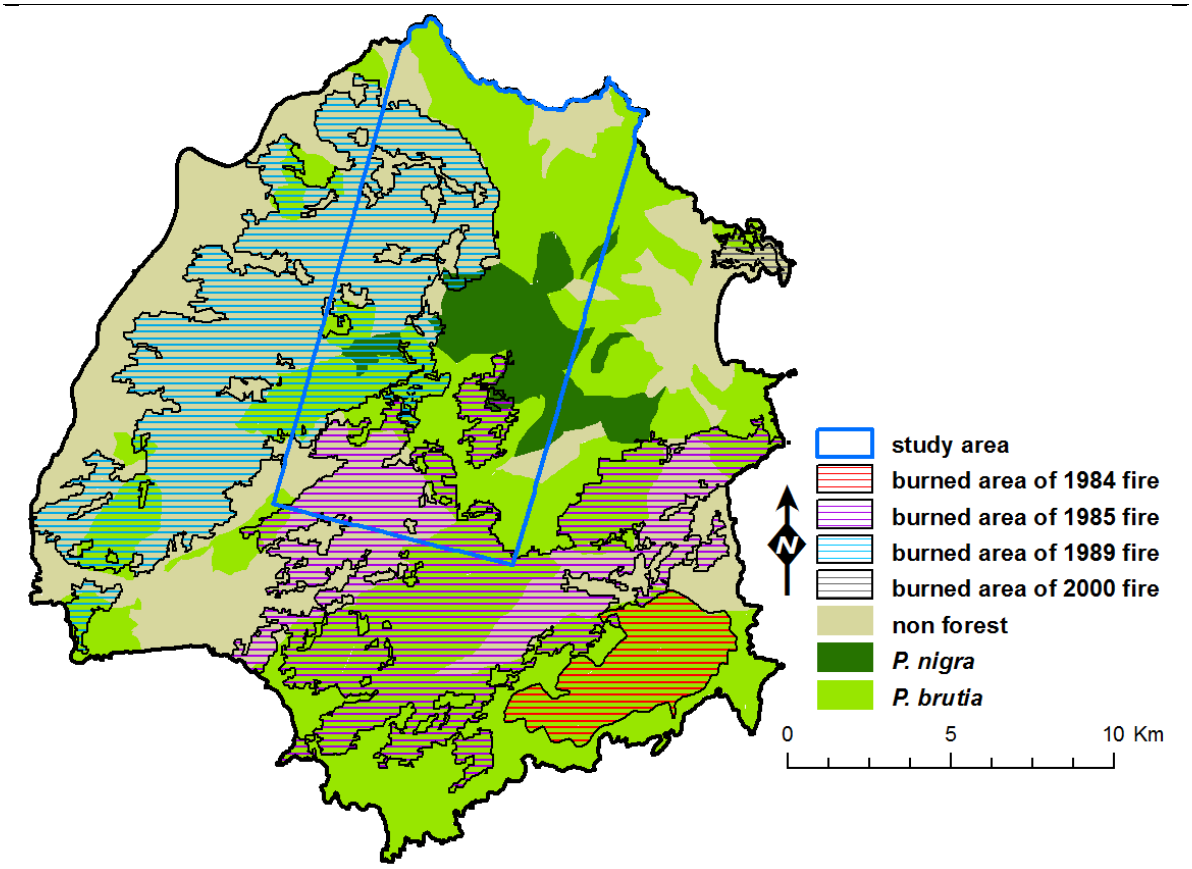

Figure 3.4 Overview map of the island according to data provided by Thassos forest service. Spatial distribution of forests dates prior to the devastating fires.

3.1.3 History and Management regime

Forest in Thassos is divided in Municipal authorities and State forest. Municipal owned forest is administrated and managed by Thassos Association of Municipalities and Communities while State forest, falls under the administration and management of the Greek State (Makedos, 1987). Because of this division, each forest is managed based on a different Management Plan. The last plan for the municipal owned forest was conducted in 1997 while the last one for the State forest in 1986.

Thassos has very 'rich 'fire history. The island is known as the *island of thunder* due to the large amount of fires caused by lightning. However, it is the anthropogenically caused fires that mostly affect the island, as the ones caused by lightning are of much lesser extent (Makedos 1987). In the last 30 years, four major fires (1984, 1985, 1989, 2000) occurred in Thassos (Figure 3.4). The wildfires of 1984, 1985 and 1989 have destroyed more than 80 % of the total forest area of Thassos (Spanos, 1992, 1994). However, most burned sites have been restored by post-fire natural regeneration, with a rich vegetation cover and high species abundance (Gitas et al., 2000; Spanos et al 2001)

Before the two fires of 1984, forest and forested lands covered 47.5% of the island (Gitas, 1999); making forests the dominant landcover type at the time. After the fire of 1985, forest covered 38% of the island (Makedos, 1987) and nowadays the remaining forest is 11% of the island according to Thassos Forest Service.

Since after these fires, the main effort of the administrative authorities is the protection of the remaining forest from fires as well as the rehabilitation of the degraded forest. Only limited production of technical timber and firewood is undertaken. The Forest Service has adopted a multiple-purpose forest management strategy including recreation, grazing, resin-collection and apiculture, together with silvicultural rotation of 100 years.

3.2 TAXIARCHIS

3.2.1 Phisiography

The University Forest in Taxiarchis is located on the southern and southwestern slopes of mount Cholomontas in Chalkidiki, in Central Macedonia region. It extends from 40° 23' to 40° 28' East and 23° 28' to 23° 34' North and covers an area of 58 km^2.

The terrain of the study area is diverse and very rough at places as a result of high difference in altitude, namely between 320 and 1200m. The dense river network in conjunction with the sudden and intense rainfall during the winter period has formed gullies and has a wide affect in the region.

Geologically the study area belongs to the Perirodopiki zone, under Melissohoriou - Holomonta. However, the northeast part belongs to Serbomacedonian mass range Vertiskos. Hence the geological substrate is not uniform but varies. Rocks, mainly metamorphic, can be roughly

divided into: marbles, crystalline limestones, schists, gneisses, amphibolites, splintery, Arnaia type granites, chalazitikoi sandstone etc.

Taxiarchis's soil is derived from the weathering of rocks present in the area and belongs to acidic orfnon forest soils. In general, the soil of the area can be considered immature with prior intense erosion. According to soil depth, there are three classes found in the study area:

1. shallow soil (0.15 – 0.30m): present in NE part of the area, at the mountain ridges
2. medium depth soils (0.30 – 0.60m): present in pits and moderate slopes.
3. deep soil (0.60 – 1.20m): present in the NW part of the study area.

The existing litter decomposes each year to humus with depth that does not exceed 5cm. In general, the soil is considered adequate for the growth of two main forest species, namely *Quercus frainetto* and *Fagus sylvatica*.

As a result of weathering of different kinds of rocks, a variety of land types is found in the area, which depending on their characteristics host different vegetation.

There is a meteorological station which operates in this area since 1974 in altitude of 860m under the supervision of Aristotle University of Thessaloniki, School of Forestry and Natural Environment. All following data come from observations of this station between 1974 and 2006.

The climate is terrestrial mediterranean with short periods of drought, hot summers and mild winters. Main characteristic of the climate is the large fluctuations of rainfall during summer as well as the double dry season (July and September) with limited duration and intensity.

Figure 3.5 shows the Bagnouls-Gaussen's (1993) index of aridity of the area, from observations between 1974 and 2006for the 1976-1999 period.

According to the Emberger (1995) taxonomic system, which has been used to set the bioclimatic floors for the Mediterranean climate, the bioclimate of the study area is classified as wet with harsh winters.

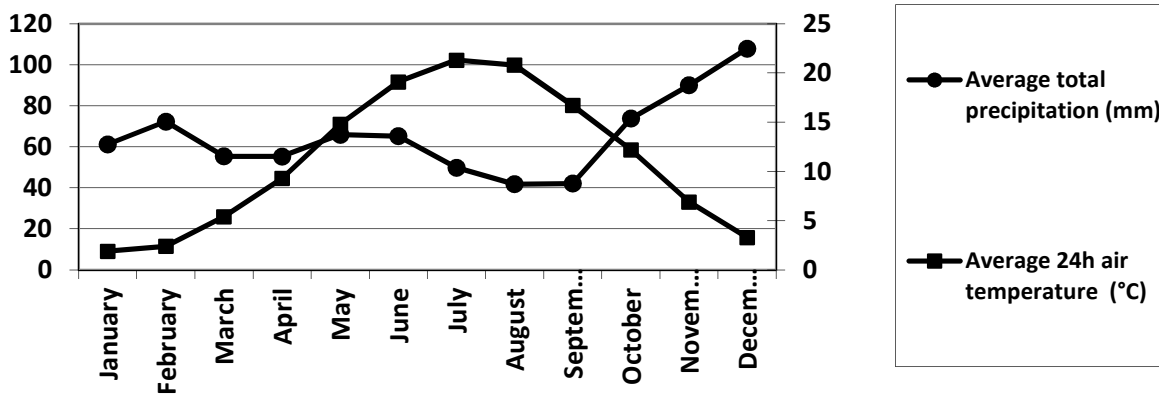

Figure 3.5 Bagnouls-Gaussen's index of aridity of the area.

3.2.2 Vegetation

Three out of the five Greek vegetation zones are present in the area of Taxiarchis, according to Dafis (1976).

1. **Quercetalia ilicis**, and in particular subzone Quercion ilicis and growth space Orno-Quercetum ilicis, is found in altitudes ranging from sea level to 600m in the Southern and South Eastern parts of the study area. It is dominated by Quercus frainetto. Other woody species found there are Quercus ilex, Fraxinus ornus, Arbutus unedo, Erica arborea, Phillyrea latifolia, Lonicera etrusca, and Pistacia terebinthus. In this subzone there are also large reforestation plantations of *P. brutia* (age between 50 and 65 years).

2. **Quercetalia pubescentis**. It is found in altitudes ranging from 320 to 1000m. It is the zone that covers the largest part of the study area and it is represented by its both sub-zones, namely Ostryo -Carpinion orientalis and Quercion frainetto.

- Ostryo - Carpinion orientalis, and in particular growth spaces Coccifero - Carpinetum and Cocciferetum. The main species that dominate these areas is *Quercus coccifera*. Other woody species found there are *Juniperus oxycedrus, Phillyrea latifolia, Arbutus unedo*, *Arbutus andrachne, Quercus pubescens, Carpinus orientalis, Fraxinus ornus* and *Erica manipuliflora.*

- Quercion frainetto. It is represented by all three growth spaces, namely Quercetum frainetto, Quercetum montanum and Tilio-Castanetum. It covers areas with altitude

ranging from 400 to 1000m and it is dominated by *Q. frainetto*. Other species found in this subzone include *Acer campestre, Carpinus orientalis, Cornus mas, Crataegus monogyna, Fraxinus ornus, Hedera helix, Juniperus oxycedrusQuercus coccifera, Rubus canescens* and *Ostrya carpinifolia.*

1. **Fagetalia**, and in particular sub-zone Fagion moesiacae (hellenicum) which is represented by the growth space Fagetum moesiacae (hellenicum), is found in altitudes ranging from 600 to 1165m. Although this area is dominated by *Fagus sylvatica*, there are also large areas of productive *P. nigra* forests, which resulted from reforestation (age between 50 and 65 years).

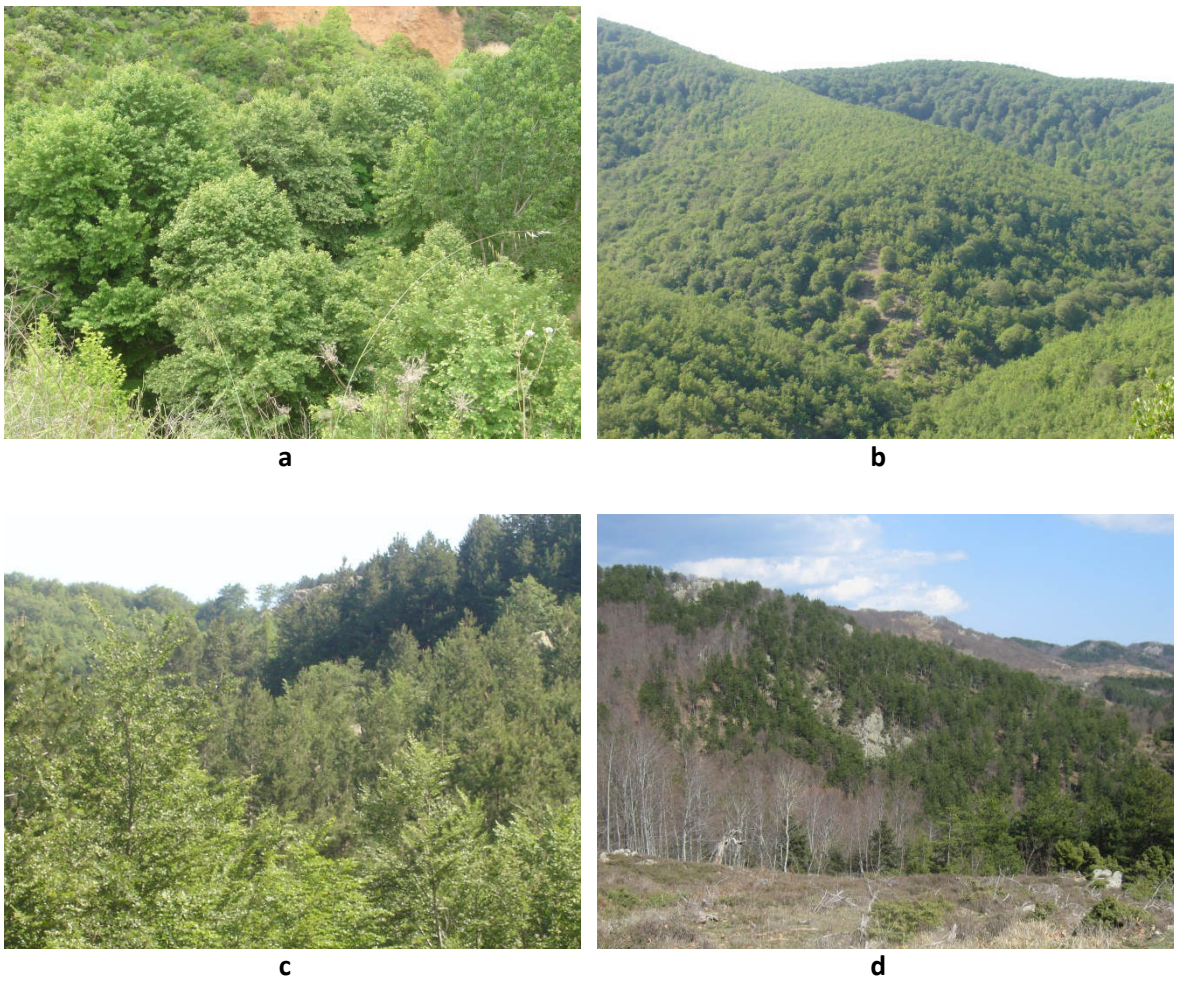

Figure 3.6 Typical landscapes of Taxiarchis. (a) *Q. frainetto* stands, (b) maquis, (c) mixture of *P. nigra* and *F. sylvatica* in summer time, (d) mixture of *P. nigra* and *F. sylvatica* in winter time.

Taxiarchis flora consists of more than 1000 taxa, among these 63 are of great importance; 2 are endemic in Greece and 18 are endemic in Balkans. The vegetation of the study area consists mainly of deciduous forests and coniferous reforestation plantations, maquis and bare land.

The forest is also home to rich fauna, including large populations of wild boars, roe deers, hares and partridges. In particular, Mount Cholomontas was granted protection under an EU order, mainly with regards to the predator birds living in the forest.

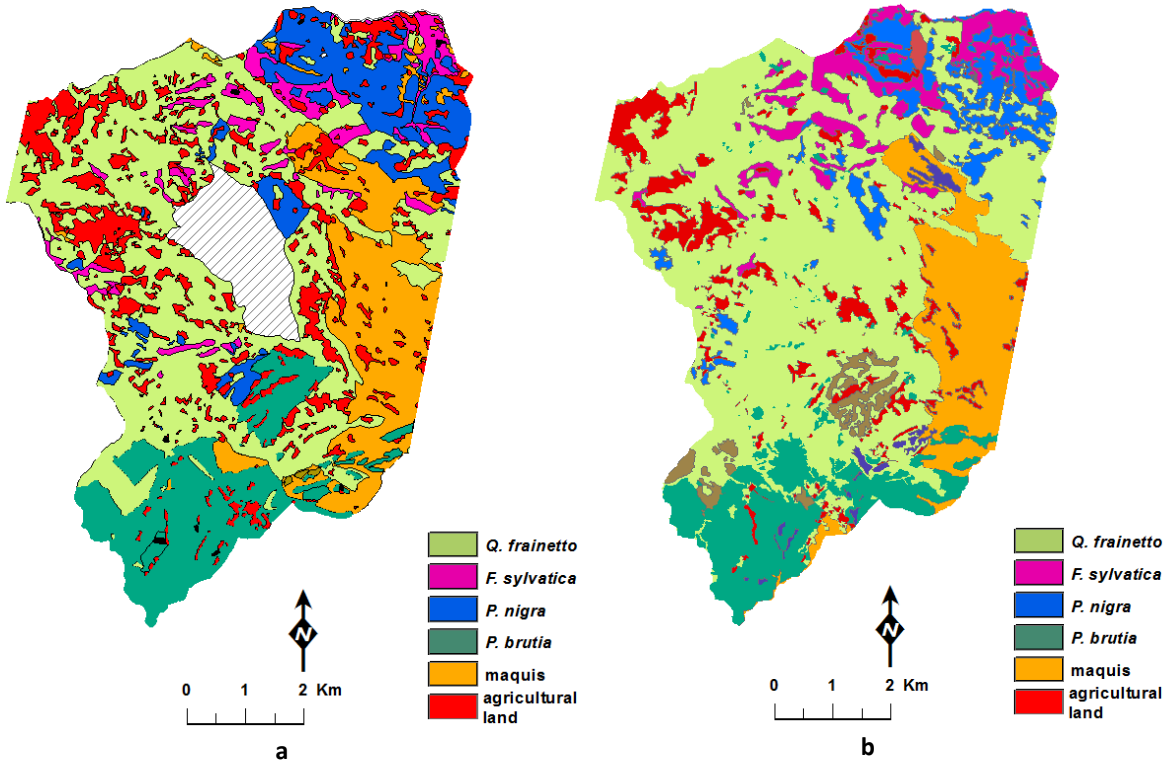

Figure 3.7 Vegetation map of Taxiarchis from the Management Plan (a) and the Fire Management Plan (b).

3.2.3 History and Management regime

The University Forest in Taxiarchis is a publicly owned forest estate that has been granted to the Aristotle University of Thessaloniki for purposes of training, research and exemplary management, since 1934. The forest also bears rights for sheep and cattle grazing as well as logging to cover the needs of villagers for fuel wood and timber to construct stables.

The systematic and sustainable management of the forest over the last decades has encouraged local populations to continue to reside in their villages. The main forest products include oak, beech, pine firewood and charcoal. Since the forest is not mature enough, little timber is produced (wooden beams, planks, parquet elements, etc.). Agricultural fields of the area are mostly covered by fir trees that are traded as Christmas trees since 1969. There are more than 2 million fir trees in the area, offering income opportunities to villagers, protecting the land and providing shelter to wildlife. The area is also of great apicultural interest. The main threats of the forest are illegal grazing, illegal logging and forest fires.

Taxiarchis forest has a rich history of forest fires. Between 1977 and 2007 there have been 18 documented fire events that burned 96 ha of mostly forest land. However, the percentage of infertile or bare land is insignificant due to the great effort made by the management of the forest for the rehabilitation and return to the production process of these surfaces.

Since 1971, a 10 year Management Plan is formed and used for the forest management. Currently, the forest is divided into 6 forest systems and managed accordingly:

1. maquis system - silvicultural rotation 30-35 years
2. *Quercus* high forest passage system - silvicultural rotation 100-120 years
3. *Quercus* coppice system
4. *Fagus* high forest passage system- silvicultural rotation 100-120 years
5. Pine forest after underplanted in *Quercus* stands system
6. Pine forest after underplanted in maquis system

3.3 DATASET DESCRIPTION

The data used in this study come from satellite and airborne sensors, as well as from thematic imagery photointerpretation and extensive field surveys, and are further described in the following sections.

3.3.1 Imagery

Hyperion was designed as a technology demonstration to build and maintain a “science” grade instrument to validate pushbroom performance and support evaluation of hyperspectral technology applications on a global scale.

Hyperion is a high resolution hyperspectral pushbroom, imaging spectrometer capable of resolving 242 spectral bands (from 0.4 to 2.5 μm) with a 30-meter resolution and provides radiometrically calibrated spectral data. Since Hyperion is a pushbroom system, the entire 7.65 km wide swath is obtained in a single frame. It has a single telescope and two spectrometers, one visible/near infrared (VNIR) and one short-wave infrared (SWIR).

Since 2001 USGS distributes Hyperion data in processing Level 1R, which have been processed for: smear and echo artifacts correction, background removal, radiometric calibration, DN rescale, bad pixel mask generation, VNIR/SWIR alignment and output data preparation.

Hyperion data products are provided in 16-bit radiance values, in Hierarchical Data Format (HDF) version 4.1r5, and are delivered tarred and gzip-compressed. The data files are organized in band-interval-by-line (BIL) format, and the byte order is Network (IEEE) integer. Values represent absolute radiance values with a scaling factor of 40 for VNIR bands and80 for SWIR bands. Level 1R product is radiometrically corrected with no geometric correction applied while the later Level 1Gst product is radiometrically corrected and resampled for geometric correction and registration to a geographic map projection. The data image is ortho-corrected using digital elevation models (DEM) to correct parallax error due to local topographic relief. The source of DEM used varies according to local availability of elevation information.

Two images were acquired for this study. Their characteristics are shown in table 3.1.

Table 3.1 Characteristics of the two Hyperion images used in this study.

	Thassos	**Taxiarxis**
scene name	EO1H1830322003213110PZ.L1R	EO1H1830322008287110PY_L1T
date of acquisition	01-08-03	13-10-08
spatial resolution	30 m	30 m
spectral resolution	10 nm	10 nm
VNIR calibrated bands	8-55 (426 - 895 nm)	8-55 (426 - 895 nm)
SWIR calibrated bands	77-224 (912 - 2396 nm)	77-224 (912 - 2396 nm)
NW Corner	41°01'49"N, 24°43'28"E	40°40'41"N, 23°33'18"E
NE Corner	41°00'47"N, 24°48'47"E	40°39'42"N, 23°38'31"E
SW Corner	40°15'17"N, 24°28'10"E	39°50'23"N, 23°17'14"E
SE Corner	40°14'17"N, 24°33'26"E	39°49'25"N, 23°22'23"E
Look Angle	3.8431	1.8361
Sun Azimuth	131.153506	155.116086
Sun Elevation	59.701685	38.561229
Processing level	1R	1Gst

3.3.2 Field data

The major components of a sampling strategy include sampling unit (pixels or polygons), sampling design, and sample size (Muller et al., 1998).

A stratified random sampling scheme was chosen to assess the accuracy of the maps produced throughout this study. ENVI software was used to create 265 random points in the case of Thassos and 172 in the case of Taxiarchis, stratified according to preliminary classification result. The number of points was indicated by Fitzpatrick-Lins (1981) formula (euation 3.1), for Z=1.96, p= 85% and E= 5%.

$$N = \frac{Z^2 pq}{E^2} \qquad \text{eq. 3.1}$$

where:

p is the expected percent accuracy,

$q = 100 - p$,

E is the allowable error, and

Z = 1.96 from the standard normal deviant for the 95% 2-sided confidence level.

These points were visited and sampled by a team of 2 experienced foresters, with the use of a Garmin 550t GPS.

The sampling coordinates were located on the ground. Taking into account the 30 meter resolution of the image and the locational accuracy of the GPS device, homogenous areas of 90m by 90m were necessary to provide a valid sample unit. In the case of a sampling point not meeting this criterion, a homogeneous area at the nearest proximity of the indicated sampling point was sampled and assigned a label. The coordinates of the sampling point were readjusted when processing.

Thassos is a typical case of Mediterranean landscape where maquis, phrygana, olive trees, bare land and pines mix in various patterns and scales. In Hyperion's 30 meter pixel or 900 square meters on the surface, it is apparent that more than one of these covers coexists resulting in mixed spectra reaching the satellite sensor.

Key features of the ground truth sampling are listed below:

- Each sampling point was assigned a class label.
- Sampling units with over 30% forest tree cover were considered forest and a species label was assigned.
- To bridge the time gap between imagery acquisition and field survey, expert knowledge of the processes of the ecosystem and local history were combined and evaluated before assigning the label.
- While most of the points were visited, there were some clearly viewed from other locations, and assigned a label remotely. Some of the points were impossible to approach and they were assigned a label by photo interpretation.

Tables 3.2and 3.3 show the number of sampling points per landcover class, after processing, for Thassos and Taxiarchis. Figure3.8 shows the geographic location of sample points collected in the study areas.

Table 3.2 Sampling points in Thassos

Thassos landcover classes	number of points sampled in the field
Pinus brutia	62
Pinus nigra	61
broadleaved	14
agricultural land	25
maquis	28
phrygana	42
bare land	33
TOTAL	265

Table 3.3 Sampling points in Taxiarchis

Taxiarchis landcover classes	number of points sampled in the field
Querqus frainetto	62
Fagus sylvatica	10
Pinus nigra	20
Pinus brutia	21
agricultural land	12
maquis	31
bare land	16
TOTAL	172

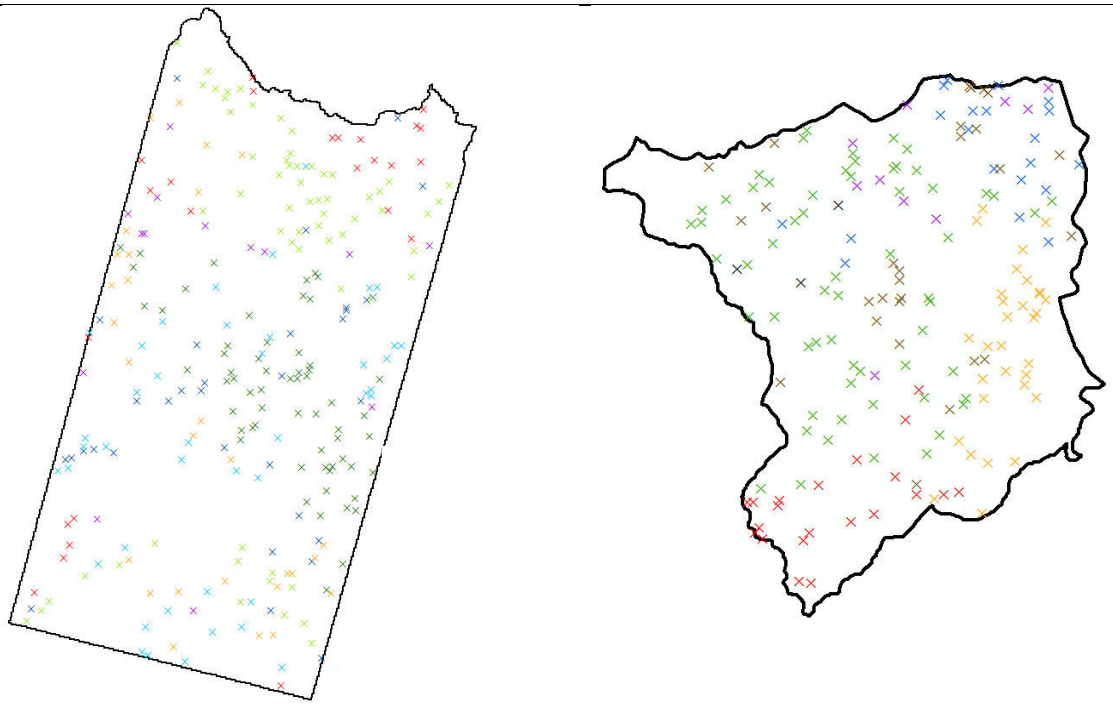

Figure 3.8 Sampling locations in (a) Thassos ans (b) Taxiarchis.

3.3.3 Reference data

Several reference datasets were used in the course of this study such as digital land use/cover maps, digital aerial ortho-photographs, digital elevation models and orthorectified Landsat 5TM imagery.

Datasets used in the preliminary phase as reference data:

In the case of Thassos:

1. Digital map of the local Forest Service based on the digitizing of aerial ortho-photographs of 1975 and field visits (MMU = forest stand, 2 ha). It was used to locate the conifer species found in the island. It is safe to assume that where major disturbance has not occurred (file, logging) mature forest inhabits the same locations.

2. Digital map of the fires that occurred in the study area in 1985 (size: 8.130 ha) and 1989 (size: 8.540 ha). There was no reference of the areas affected by fire prior to the field visit.

3. Digital landcover map based on digitizing on ortho-photographs of 1986. The general shapes of the main landcover types were used as guidance in the training and evaluation exercise.

4. Digital landcover map of the island produced by OPEKEPE. In this map there was no information regarding forest species. All forest species were grouped in the class "forest". It was used to give insights for the rest of the classes as well as the general distribution pattern.

5. Cadastre map server with aerial ortho-photographs of 2009 (spatial resolution 1m). Knowledge of the study area in such spatial detail was valuable in several cases, even though the time gap between datasets acquisition dates and the lack in information on forest species.

6. Digital Elevation Model (DEM) of the area with 30m spatial resolution.

In the case of Taxiarchis:

1. Digital landcover map based on the digitizing of aerial ortho-photographs of 2006. This map depicting landcover information at species level was produced within a Fire Management Plan framework.

2. Digital landcover map based on the digitizing of aerial ortho-photographs of 2000. This map also depicts landcover information at species level and was produced as a component of the Forest service Management Plan. It is interesting to note that although the production method and date of this and the above mentioned dataset are very similar these maps show substantial differences. This is a typical shortcoming of manual digitizing as it heavily depends on analyst's personal interpretation.

3. Cadastre map server with aerial ortho-photographs of 2009 (spatial resolution 1m). Imagery of the study area, though highly unusual for this product, was of winter time so deciduous species were captured without foliage making them indistinguishable.

3.3.4 Computing environment

All data used in this study, besides the field collected data, were acquired in digital form. Their analysis was done in a Windows 2007 environment, using commercial remote sensing and GIS software, such as ENVI, Definience, ERDAS, and ArcMap. Also, a Graphical User Interface (GUI)

which uses the LIBSVM software (Chang and Lin, 2011) was developed in MATLAB, for a function that was not available commercially.

3.4 CHAPTER CONCLUSIONS

The key points discussed in this chapter are summarized below.

- Both study areas are typical landscapes of the Mediterranean region.
- Thassos study area forms a simple pattern of forest landscape with two pine species, namely *P. brutia* and *P. nigra*, growing in quite separate zones. Other landcover, phrygana, maquis, agricultural and bare land are also key components of the landscape.
- Taxiarchis study area forms a more complex mosaic. *Q. frainetto* dominates the largest part of the forest; while fewer stands of *F. sylvatica* as well as reforestation plantations of *P. brutia* and *P. nigra* are also present together with an extended maquis area.
- Mapping four forest species is under investigation. Two of them, namely *P. brutia* and *P. nigra* are present in both study areas. They belong to the same genus; fact that gives them plethora of common characteristic and spectral responses with subtle differences. The other two species *Q. frainetto* and *F. sylvatica* are deciduous species often found in adjacent stands.
- Two summer Hyperion images were used for this investigation. Their 30 meter spatial resolution is assumed to provide maps in scale 1:60,000 or less, with minimum mapping unit of approximately 1ha.
- Field data were collected using a stratified random sampling scheme. 265 and 172 points were sampled in Thassos and Taxiarchis respectively in order to be used for the accuracy assessment of the produced maps.

4

DATA PREPROCESSING

Chapter 3 described the geomorphology, climate, landcover and management history of the two study areas, as well as the various data used in this study. This chapter outlines the importance of preprocessing Hyperion imagery and thoroughly describes the techniques used to enhance the images prior to subsequent image analysis.

Imagery preprocessing is a key component of hyperspectral analysis, particularly with images from an experimental satellite sensor such as EO1 Hyperion and especially in studies where the outcome is potentially a product to be used for resource management. Most remotely sensed data are processed through a set of preprocessing or clean-up routines that remove or correct unwanted artifacts (both geometric and radiometric) (Chavez, 1988).

Since Hyperion operates from a space platform with consequently modest surface signal levels between 50 and 150 des (Pearlman et al., 2003) and full-column atmospheric effects, its data demand careful processing to manage sensor and processing noise (Datt et al., 2003). As found during this study, failure to address any of the various integral artifacts, leads to characteristically flawed results. Hyperion has a low signal to noise ratio in comparison to airborne hyperspectral sensors, the result of signal lost to atmospheric absorption and the reduced energy available from surface reflectance at orbital altitude. In addition, detector arrays used in the Hyperion sensor were “spares” originally designed for another purpose, which further decreases the signal to noise ratio (Jupp and Datt, 2004). As a result, Hyperion data require preprocessing to address problems of miscalibration and noise before use (Goodenough et al., 2002; Han et al., 2002; Datt et al., 2003).

Hyperion imagery has many shortcomings that need to be addressed before it gets into analysis. The two images were obtained in different processing level by the provider, so the preprocessing steps varied accordingly (Figures 3 and 4). Many have proposed custom algorithms and techniques to correct and process Hyperion data (Staenz et al., 2002;

Goodenough et al., 2003; Liang, 2004; Khurshid et al., 2006). however this is out of the scope of this study. Tools and techniques readily available in commercial software packages are used throughout this study so that any useful result can be straightforwardly replicated.

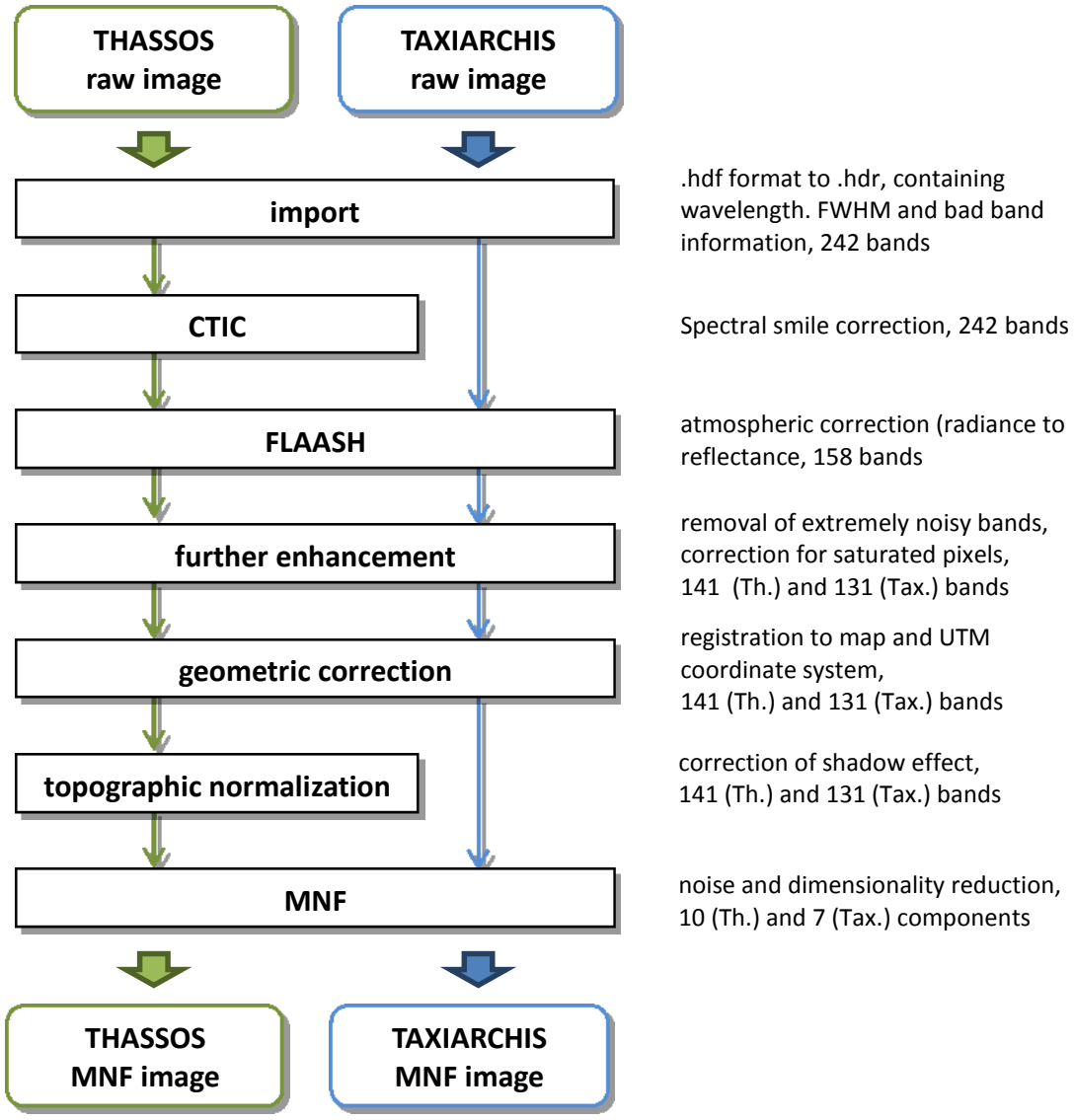

Figure 4.1 Preprocessing steps of this study.

4.1 Import

Hyperion Tools plug-in of ENVI v5 suite was used to convert the .LR1 and 1Gst files to ENVI compatible format, which contains wavelength, FWHM and bad band information. The new file format is fully functional and allows for accurate manipulation of data. This import function also

provided the scale factors necessary to the FLAASH model, which was used for the atmospheric correction as discussed in section 4.3.

4.2 Smile

Spectral Smile is an identified effect of the Hyperion imaging spectrometer (Neville at al., 2003) and there has been an effort for prelaunch smile estimates. However, Hyperion prelaunch smile estimates are inapplicable, as the smile appearance varies from scene to scene (Neville at al., 2008). Smile is a cross track wavelength shift between 2.5 – 4.2 nm in the VNIR bands, caused by the change of dispersion angle with target position (Goodenough et al., 2003). Some suggest that the smile effect should be considered an inherent part of the data, thus they do not include its correction in the preprocessing steps (Vyas et al., 2011; Petropoulos et al., 2012). However, during this study it was noted that smile led to inadequate atmospheric correction, noisy reflectance product and low thematic accuracy, thus correction was considered necessary. No standard correction method is available (Dadon et al., 2010; San and Süzen, 2011). Kennedy et al., (1997), suggested that an intelligent use of empirical models for a description of the bidirectional reflectance from vegetated surfaces can be used for the correction of brightness gradients in airborne line scanner imagery. Such an approach is implemented by the Cross Track Illumination Correction module (CTIC) in ENVI software, which is the only commercially available tool for this purpose.

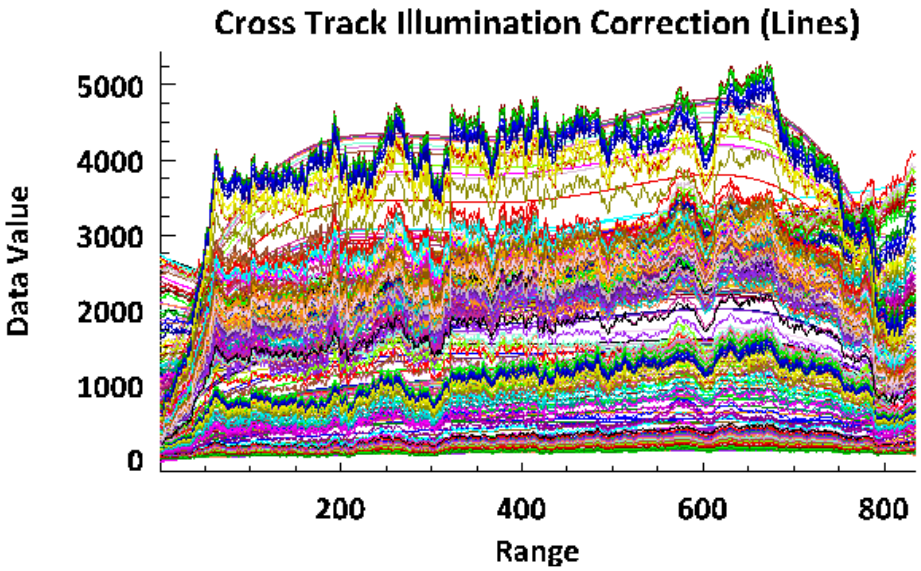

Figure 4.2 Plot of row average DNs and the fitted polynomials

In the case of Thassos, where the image was acquired in processing level 1R, CTIC was used to minimize this effect (Figure 4.3).

The routine calculates the overall row average digital numbers (DNs) within an image and then fits a polynomial to the averages, for each band, to remove variation and potentially correct the reflectance data in the cross-track direction.

Although smile is not observable in spectral space, it becomes obvious once the data are transformed to MNF space. Figure 4.2a shows the Smile effect in 1st MNF component and Figure 4.2b shows the same component after the CTIC. CTIC was implemented on a masked image, where sea and clouds were removed in order for the column means used during the correction to be more representative of the area under investigation.

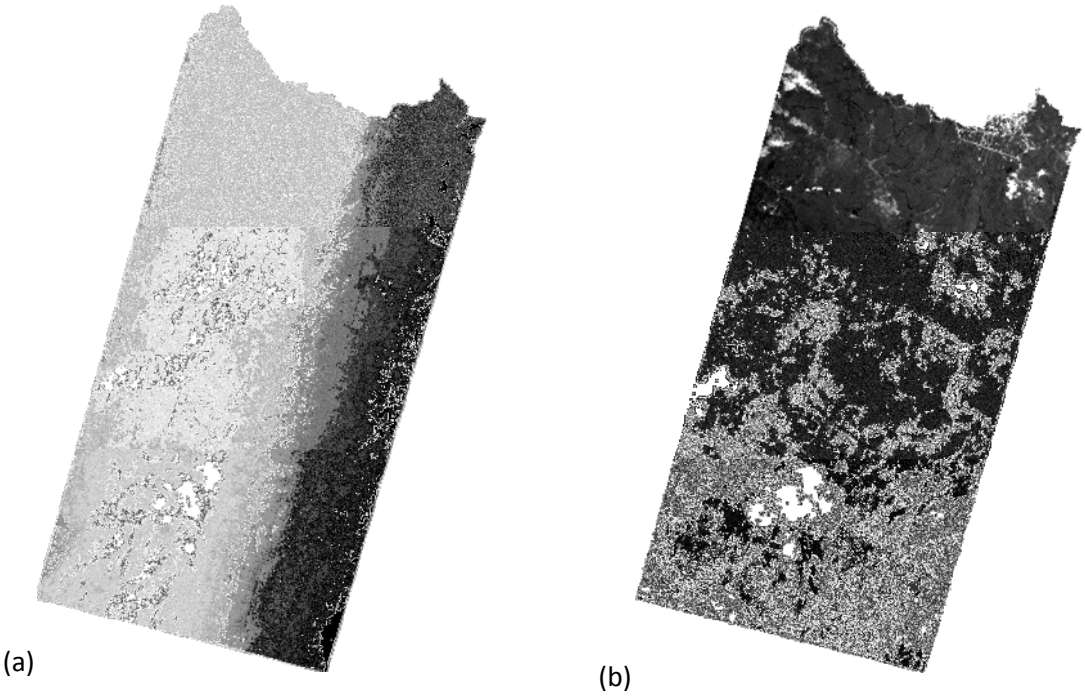

(a) (b)

Figure 4.3 Smile effect, apparent in 1st MNF component prior to the CTIC (a), and minimized after CTIC (b)

In the case of Taxiarchis, where the image was acquired in processing level 1Gst, this module could not be used; smile was not corrected and was carried into subsequent analysis.

4.3 Atmospheric correction

FLAASH is a model-based atmospheric correction tool that corrects wavelengths in the visible through near-infrared and shortwave infrared regions, up to 3 µm (RSI, 2001). Unlike many other atmospheric correction programs that interpolate radiation transfer properties from a pre-calculated database of modeling results, FLAASH incorporates the MODTRAN4 radiation transfer code (Berk et al., 1998). FLAASH derives atmospheric properties such as surface pressure, water vapor column, aerosol and cloud overburdens, and incorporates them into a correction matrix to finally invert 'radiance-at-detector' measurements into 'reflectance-at-surface' values. It also offers an additional option of correcting light scattered from adjacent pixels. Spatially averaged reflectance is used to account for the "adjacency effect'' - radiance contributions that, because of atmospheric scattering, originate from parts of the surface not in the direct line of sight of the sensor (AdlerGolden et al., 1999; Mathew et al., 2000).

FLAASH starts from a standard equation for spectral radiance at a sensor pixel, L, that applies to the solar wavelength range (thermal emission is neglected) and flat, Lambertian materials or their equivalents. The equation is as follows (equation 4.1):

$$L = \left(\frac{\mathrm{A}\rho}{1-\rho_{\mathrm{e}}\mathrm{S}}\right) + \left(\frac{\mathrm{B}\rho_{\mathrm{e}}}{1-\rho_{\mathrm{e}}\mathrm{S}}\right) + L_a \qquad \text{eq. 4.1}$$

where:

ρ is the pixel surface reflectance

ρ_e is an average surface reflectance for the pixel and the surrounding region

S is the spherical albedo of the atmosphere

L_a is the radiance back scattered by the atmosphere

A and **B** are coefficients that depend on atmospheric and geometric conditions but not on the surface.

FLAASH allows several parameters to be set by the analyst (Figure 4.4). It also incorporates options such:

- water retrieval

In order to solve the radiative transfer equations, FLAASH includes a method for retrieving the water amount for each pixel instead of using a constant water amount for the entire scene. This

way produces a more accurate correction than in the first case. This option was used in the study.

- spectral polishing

Polishing is a term used by Boardman (1998) for a linear renormalization method that reduces spectral artifacts in hyperspectral data using only the data itself. This option was used in the study.

- wavelength recalibration

An accurate wavelength calibration is critical for atmospherically correcting hyperspectral data. Even slight errors in the locations of the band center wavelengths can introduce significant errors into the water retrieval process, and reduce the overall accuracy of the modeled surface reflectance results. To minimize such errors, FLAASH includes a method for identifying and correcting wavelength miscalibrations. It was found that this option provided no further improvements in the atmospheric correction, thus it was not used in this study.

Examination of vegetation spectral signatures in the output reflectance image showed that they follow the typical vegetation spectral curve (Figure 4.6.b).

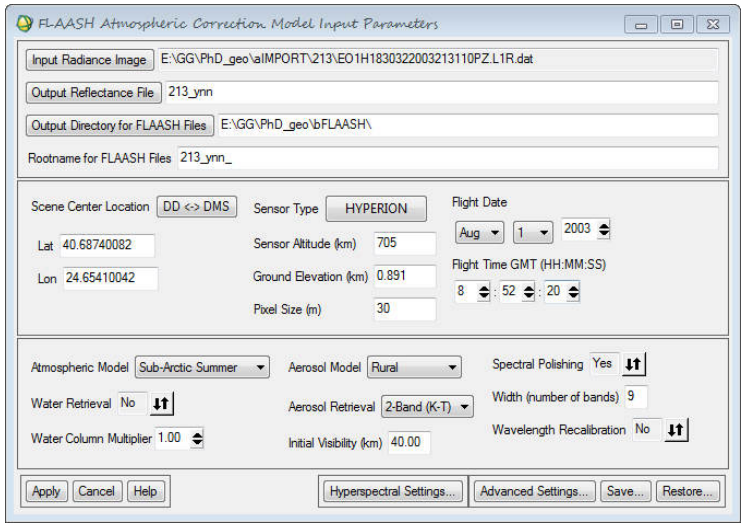

Figure 4.4 Parameters used in the atmospheric correction of Thassos image.

4.4 Further enhancement

After the atmospheric correction, some of the Hyperion bands recorded no data or were too noisy, so they were removed from the image cube, resulting in a 141 band image in the case of Thassos and 131 in the case of Taxiarchis. The selection complied with the band selection principles presented by Datt et al. (2003), who proposed a 155-band 'stable' subset to further avoid residual atmospheric noise for the application of agricultural indexes. Tsai et al. (2007) on the same basis retained 95 bands and, Pengra et al. (2007) 147.

In the case of Thassos it was also observed that some of the pixels of the 141 band image had reflectance values beyond the point of what is physically acceptable. After visual inspection it was noted that those pixels depicted parts of the marble quarries and that these unacceptable values were due to sensor saturation. These values were removed and replaced with neighboring 'quarry' pixel values.

Masks were also created to exclude cloud, cloud-shadow and sea pixels from analysis.

4.5 Geometric correction

Geometric correction is aimed to avoid image geometric distortions, typically contained in digital images collected from airborne or spaceborne sensors. Some of these distortions can be corrected by matching image coordinates of physical features recorded by the image to the geographic coordinates of the same features collected from a map or global positioning system (GPS). This is referred to as ground control point (GCP) registration.

Jensen (2005) described geometric correction as a four step process which includes:

- Identification of Ground Control Points (GCPs) in the original imagery and the reference map

- mathematical modeling of the geometric distortion, by fitting the GCPs into a polynomial equation using least-square criteria

- relocation of every pixel in the original input image (x', y') to its proper position in the rectified output image (x, y)

- extraction of the brightness value for every pixel from its (x', y') location in the original image and its relocation to the appropriate (x, y) coordinate location in the rectified output image (image resampling).

The fitness of the mathematical model, which is built using the GCPs, is calculated by the Root Mean Square Error (RMSE) between the predicted and known image location (equation 4.2). RMSE is generally reported in units of image pixels and according to Luque (2000) it should be 0 ≥RMSE≤ 0.6.

$$RMS = \sqrt{\left(x_{prec} - x_{known}\right)^2 + \left(y_{prec} - y_{known}\right)^2} \quad \text{(eq 4.2)}$$

The images were geometrically corrected using Landsat 5TM orthorectified images in UTM (zone35 for Thassos, zone34 for Taxiarchis) coordinate system. Ground control points pairs (19 for Thassos, 17 for Taxiarchis) evenly distributed in the whole extend of the image were located and 1st order polynomial models and a nearest neighbor resampling method were chosen. RMSE was 0.481 in the case of Thassos and 0.387 in the case of Taxiarchis.

4.6 Topographic correction

Imagery from mountainous regions often contains a radiometric distortion known as topographic effect. Topographic effect results from the differences in illumination due to the angle of the sun and the angle of the terrain. This results in pixels which although represent the same landcover, have particularly different reflectance values because of the different orientation to the sun's position. Several studies have shown the advantages of correcting the topographic effect (Tokola et al., 2001; Gitas and Devereux, 2006).

Satellite images are often normalized according to the cosine of the effective illumination angle (Smith et al., 1980) assuming Lambertian reflectance characteristics. The cosine correction is a statistic-empirical method described by equation 4.3, where:

$$L = \left(\frac{\mathrm{A}\rho}{1 - \rho_{\mathrm{e}}\mathrm{S}}\right) + \left(\frac{\mathrm{B}\rho_{\mathrm{e}}}{1 - \rho_{\mathrm{e}}\mathrm{S}}\right) + L_a \quad \text{(eq 4.3)}$$

LH is the radiance observed for horizontal surface;

LT is the radiance observed over sloped terrain;

sz is the sun's zenith angle;

i is the sun's incidence angle in relation to the normal on a pixel.

In the case of Thassos a Digital elevation model (DEM) was used as well as solar elevation and azimuth at time of image acquisition, to topographically correct the image, using ERDAS Imagine 2011 (Figure 4.5). In the case of Taxiarchis an adequate DEM was not available, thus topographic correction was not applied.

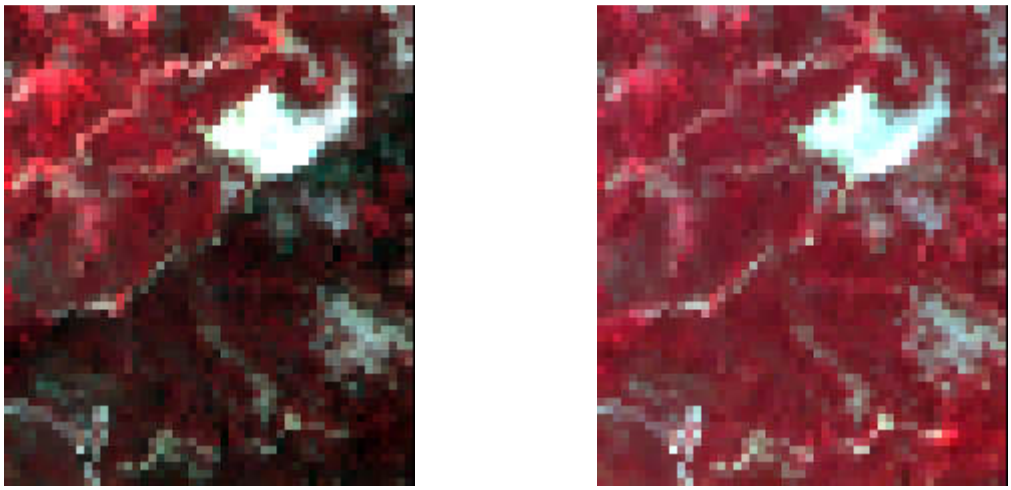

(a) (b)

Figure 4.5 *P. nigra* stands with different orientation, prior (a) and post (b) topographic correction.

4.7 MNF transformation

The MNF transformation has been used in a number of studies with aerial imagery (Aspinall, 2002; Zhang and Xie, 2013) and Hyperion imagery (Goodenough et al. 2003; Galvao et al., 2005; Mundt et al., 2005; Pengra et al., 2007; Pignatti et al., 2009) for data dimensionality reduction.

The MNF transformation determines the inherent dimensionality of image data, segregates noise in the data, and reduces the computational requirements for subsequent processing (Boardman and Kruse, 1994). The MNF transformation as modified from Green et al. (1988) is essentially two cascaded Principal Component's transformations. The first transformation, based on an estimated noise covariance matrix, decorrelates and rescales the noise in the data, resulting in transformed data in which the noise has unit variance and no band-to-band correlations. The second step is a standard Principal Components transformation of the noise-whitened data. Chen (2000), studied the performance of Princilpal Components Analysis (PCA), an alternative commercially available dimensionality reduction method, and MNF in AVIRIS data and reaffirmed the findings of Lee et al. (1990) and Green et al. (1998), that the MNF transformation is more reliable that PCA when the image quality is the primary concern.

Moreover, Mundt et al. (2005) compared PCA and MNF preprocessing in a classification exercise and reported better results with the MNF transformed data.

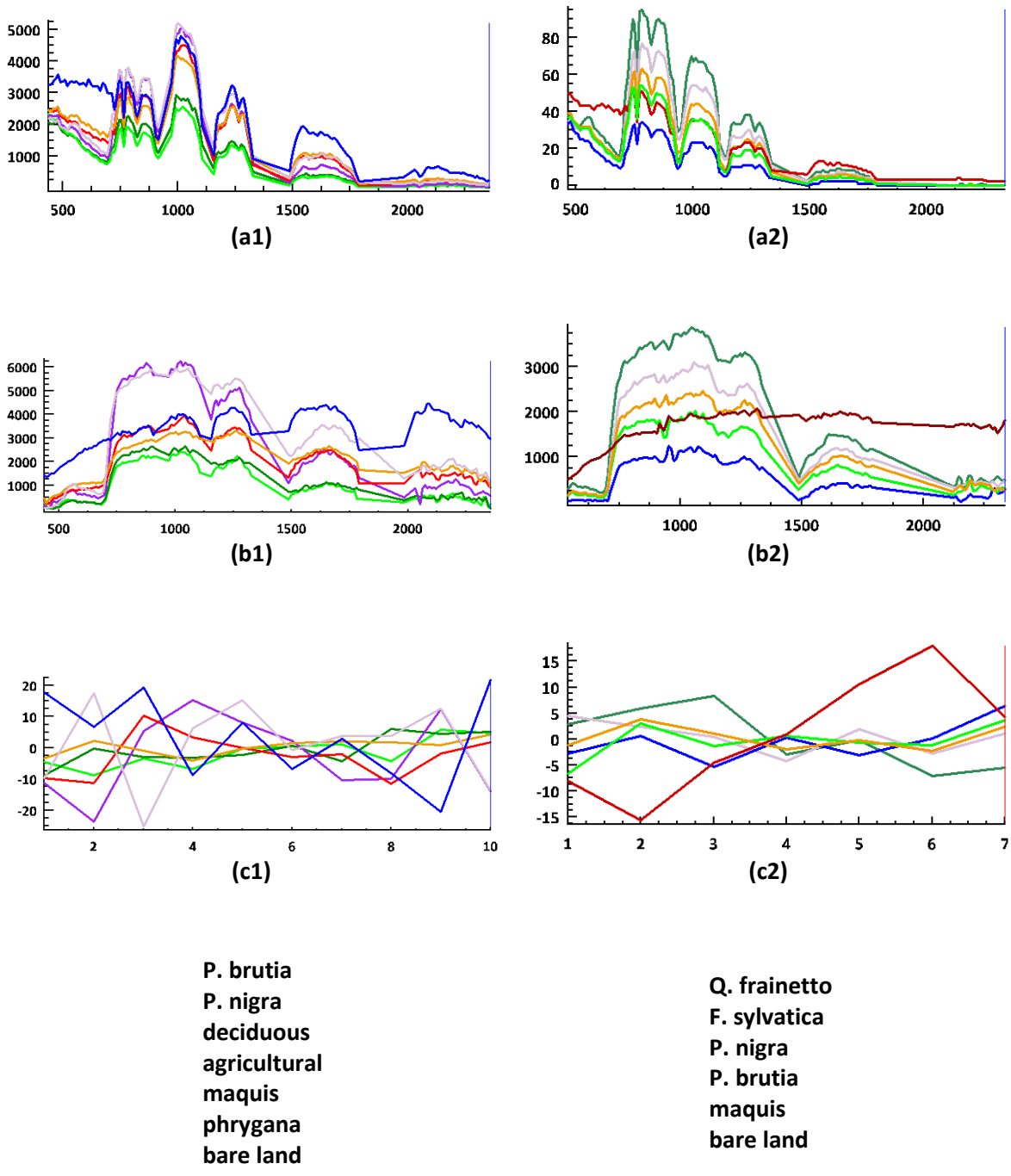

Figure 4.6 Spectral signatures of the classes of the classifiacation schemes of the two study areas (1 - Thassos, 2 – Taxiarchis) in (a) radiance space (prior to atmospheric correction), (b) reflectance space (after atmospheric correction) and, (c) MNF space.

Datt et al. (2003) showed that handling the VNIR and SWIR data separately provides greater capacity to manage the noise in Hyperion images, due to its different structure in the two arrays. Additionally, Tsai et al. (2007) developed a spectrally segmented PCA based on the established knowledge that biological factors of plant leaves affect the spectral reflectance of vegetation over different ranges of wavelength (Chelle et al., 1998; Bell and Baranoski, 2004) and improved classification results compared to the ones obtained with the use of traditional PCA. Miao et al. (2011) also used a spectrally segmented MNF approach.

Based on the above mentioned research findings, the MNF transformation was used in this study. The data cube was divided in two parts, namely VIS (436.9 to 905.0nm) and SWIR (915.2 to 2355.2nm) before taken into the MNF transformation.

After the spectral segmentation, MNF was applied independently to each spectral part. The statistics of the data noise content are often calculated from a homogenous subset of the image assuming that noise is the same for the whole image. This approach was adopted in this study. Based on the eigen analysis and visual inspection, the first few MNF bands of each segmented group were collected and stacked to form a new MNF component image to be taken into the classification exercise (Figure 4.6c).

4.8 CHAPTER CONCLUSIONS

The key points discussed in this chapter are summarized below.

- Tools and techniques readily available in commercial software packages are used throughout this study so that any useful result can be straightforwardly replicated.
- Hyperion Tools plug-in within the ENVI v5 suite was used to convert the .LR1 and 1Gst files to ENVI compatible format that allows for accurate manipulation of data.
- The CTIC tool was used to correct smile, an integral cross track wavelength shift present in Hyperion imagery. This correction was only possible for the case of Thassos, as in the case of Taxiarchis the 1Gst level of acquisition prohibited its use.
- The FLAASH model was use to convert at sensor radiance of the raw images to apparent surface reflectance and minimize the influence of the atmosphere as well as accommodate for the ‘adjacency effect’.

- Hyperion bands which after the atmospheric correction recorded no data or were too noisy, were removed from the image cube.

- Geometric correction using GCPs, 1st polynomial models and the nearest neighbor resampling method was implemented for both images, to obtain images registered to maps. After this registration the images could be used in conjunction with other available data, also registered to the same coordinate system.

- Topographic correction was implemented on the Thassos image, where a DEM was available, in order to account for the differences illumination of areas due to the angle of the sun and the angle of the terrain.

- The MNF transformation was used to determine the inherent dimensionality of data, segregate noise, and reduce the computational requirements for subsequent processing. The VNIR and WSIR bands of the image were treated separately and the statistics used to parameterize the transformation were calculated from a homogenous subset of the image rather than the whole image.

5

SPECTRAL ANGLE MAPPER IN MEDITERRANEAN FOREST SPECIES MAPPING

Chapter 4 discussed the preprocessing methodology that was followed, in order to enhance the images to be carried into further image analysis. Chapter 5 describes the investigation of the methodology developed employing the SAM classifier. Along with the presentation of the methodology and the acquired results, this chapter also discusses the various aspects that influence the efficiency of the methodology, and the value of the produced maps.

5.1 METHODOLOGY

5.1.1 Classification schemes

Guided by:

- the spectral and spatial resolution of the images,
- the landscape of the study areas, and
- the aim of this study

the classification schemes shown in table 5.1 were designed.

Table 5.1 Classification schemes of the two study areas.

Thassos	Taxiarchis
1. *Pinus brutia*	1. *Quercus frainetto*
2. *Pinus nigra*	2. *Fagus sylvatica*
3. Deciduous species (*Platanus sp., Quercus sp., Ficus sp*.)	3. *Pinus nigra*
4. Agricultural land (vast majority *Olea sp*.)	4. *Pinus brutia*
5. Maquis	5. Maquis
6. Phrygana	6. Bare land
7. Bare land	

It was decided to approach the classification of the area as a landcover mapping exercise, in the sense that the entire image would be classified, as opposed to only the forest species. However, in both study areas, all efforts were directed to the forest species mapping, treating the rest of the classes as of complementary importance.

The nomenclatures formed for this study are the following:

- *Pinus brutia* class includes *Pinus brutia* forest stands of trees over 15 years old, with various understory and estimated cover over 30%.
- *Pinus nigra* class includes *Pinus nigra* forest stands of trees over 15 years old, with various understory and estimated cover over 30%.
- Broadleaves class includes various broadleaved trees, mostly *Platanus sp., Quercus sp., Castanea sp*., *Ficus sp.* and other riverain vegetation.
- Agricultural land class includes mostly orchards of *Olea sp*. and other fruit trees.
- Maquis class includes maquis as well as shrublands with scattered trees. This class may include areas with mix of maquis and *Pinus sp.* under 15 years old or forest cover lower than 30%.
- Phrygana class includes typical phryganic vegetation or other scattered or herbaceous vegetation with high degree of soil exposure.
- Bare land class includes residential areas, quarries and other non vegetated areas.
- *Quercus frainetto* includes *Quercus frainetto* coppice or high stands of all ages, with estimated cover over 30%.
- *Fagus sylvatica* includes *Fagus sylvatica* high stands of all ages, with estimated cover over 30%.

5.1.2 Training samples

SAM is a supervised classification method, which requires from the analyst to provide description of the classes to be distinguished, by providing typical representatives as training samples for each class. SAM compares the angle between the training spectra vectors of each

class to the candidate pixel vector of unknown class, in n-dimensional space. It assigns to each candidate the label of the class of which the angle between the candidate and training sample is the smallest.

Table 5.2. Training point used per class in Thassos and Taxiarchis

class	number of training points
Thassos	
1. *Pinus brutia*	48
2. *Pinus nigra*	41
3. Deciduous (*Platanus sp., Quercus sp., Ficus sp*.)	18
4. Agricultural land (mostly Olive orchards)	23
5. Maquis	16
6. Phrygana	20
7. Bare land	56
Taxiarchis	
1. *Querqus frainetto*	210+100
2. *Fagus sylvatica*	30
3. *Pinus nigra*	30
4. *Pinus brutia*	30
5. Maquis	50+30
6. Bare land	60

Spectra from spectral libraries (collected either in the field or in the laboratory) or image spectra may be used to train the classifier. In this study, image spectra were used. Several studies that used field collected spectra reported low compatibility when used to classify remote sensed images Lee et al. (2007) found that canopy-level spectral characteristics of forest stands did not quite correspond with the leaf-level reflectance spectra. Rao (2006) used two sets of reference spectra, the first one from in situ measurements and the second one derived from the Hyperion image itself. A higher OA accuracy (88.8%) was obtained at the second case.

Cingolani et al. (2004), identified the selection representative training sites as one between the major problems when employing medium spatial resolution imagery. However, selection of training samples must consider the spatial resolution of the remote-sensing data being used, availability of ground reference data, and the complexity of landscapes in the study area (Lu and Weng, 2007).

An arbitrary number of image pixels, intentionally kept to the minimum, were chosen from what was considered typical pixel of each class, referencing knowledge of the region, use of available thematic maps and visual interpretation of VHR images of the scenes. These pixels were used to train the SAM classifier (table 5.2).

5.1.3 SAM Parameters

As implemented by ENVI, SAM allows the choice of a maximum angle threshold per class, for the assignment of a class label to a pixel. The maximum allowed value 1 was used for all classes, as lowering this threshold several pixels remained unclassified.

5.2 RESULTS

5.2.1 Thassos

The implementation of SAM on the Hyperion image of Thassos as described above resulted in the map shown in Figure 5.1. However, as the objective of the study is to map the two forest species, the rest of the cover classes were grouped to one other class, namely 'other'. Figure 5.2 is the map of the resulting three classes, namely '*P. brutia*', 'P. *nigra*' and 'other', excluding the area covered by clouds and their shadow. According to these maps 1,700 ha of the study area are covered by *P. brutia*, and 1,740 ha are covered by *P. nigra*.

To estimate the accuracy of the map and refer the value of the product, reference data collected during field surveys were used.

A confusion matrix (table 5.3) was populated by labels assigned to pixels by the classifier, and labels assigned to the respective reference data; cross-tabulated, using geographic location as key.

The matrix was analyzed with four measures of agreement, namely KIA, OA, user's and producer's accuracy (Cohen, 1960; Story and Congalton, 1986).

Table 5.3 Confusion matrix of the implementation of SVM in Thassos.

Reference / Classification	*P. brutia*	*P. nigra*	deciduous	agricultural	maquis	phrygana	bare land	producer's accuracy %	user's accuracy %
P. brutia	55	0	0	1	1	0	0	**88.7**	**96.5**
P. nigra	0	59	0	0	0	4	1	**96.7**	**92.2**
deciduous	2	0	14	0	1	0	0	100	82.4
agricultural land	0	0	0	22	2	2	0	88.0	84.6
maquis	4	1	0	2	17	0	1	60.7	68.0
phrygana	0	1	0	0	3	36	0	85.7	90.0
bare land	1	0	0	0	4	0	31	93.9	86.1
TOTAL	62	61	14	25	28	42	33		

The OA of the complete classification scheme map was **88.4%**, and the KIA was **0.859**. However, as the objective of the study is to map the two forest species, the rest of the cover classes were grouped to one other class, namely 'other'. In this case, the OA of the map was **94%**, and the KIA was **0.9**, respectively.

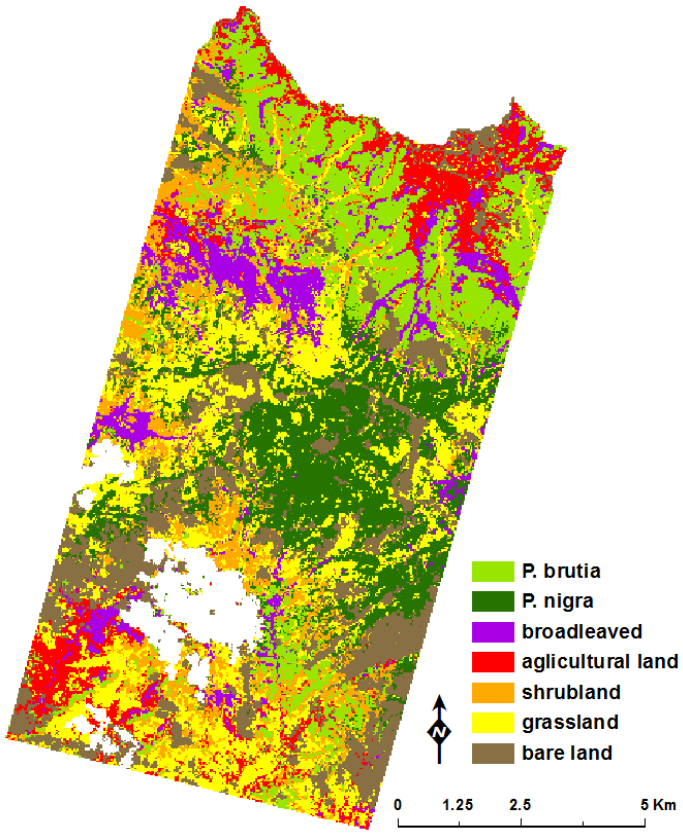

Figure 5.1 Thassos map of the seven landcover classes produced by SAM.

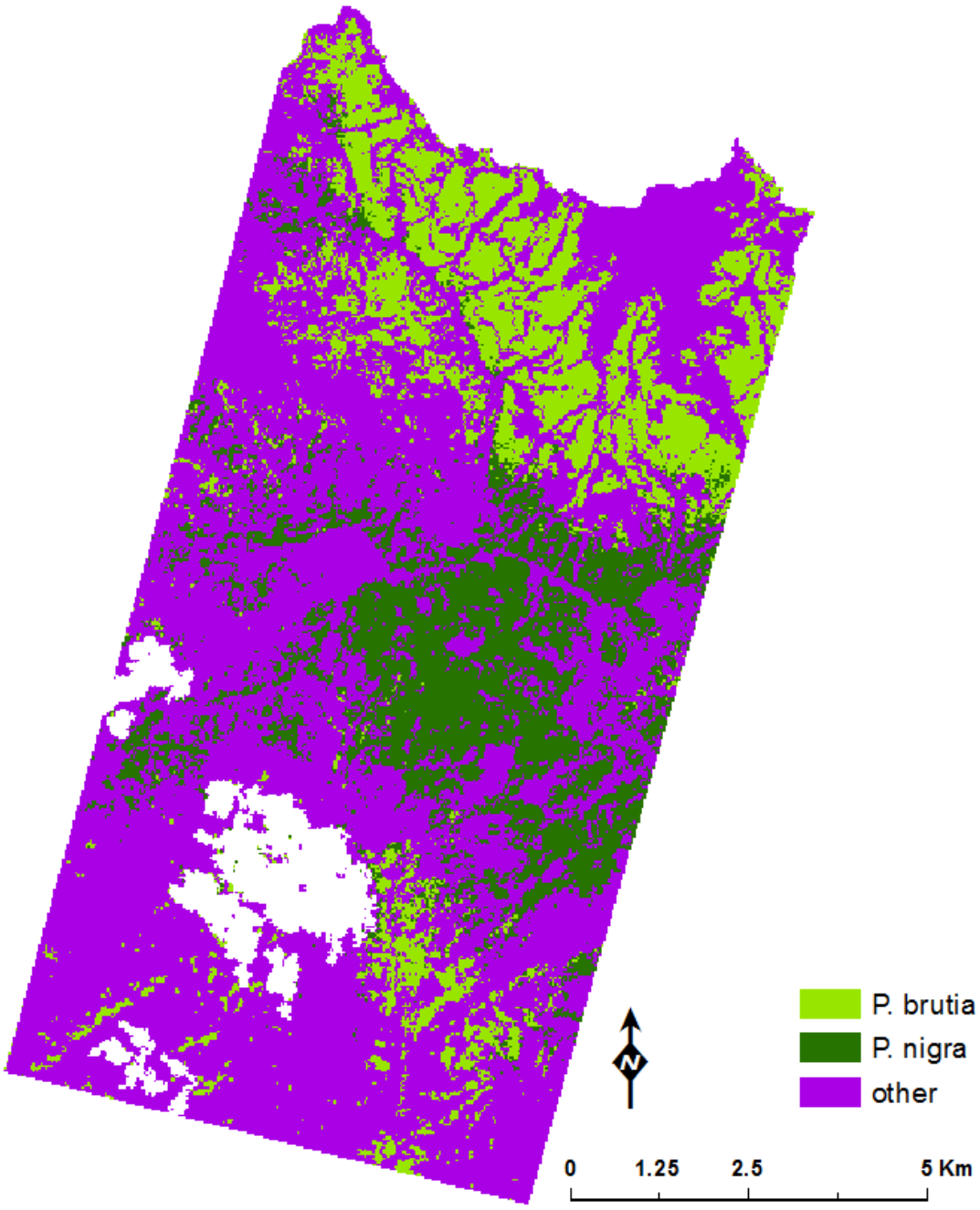

Figure 5.2 Thassos species map produced by SAM (other classes grouped).

5.2.2 Taxiarchis

The implementation of SAM on the Hyperion image of Taxiarchis as described above resulted in the map shown in Figure 5.3, excluding the area covered by clouds and their shadow. As in Thassos, the secondary landcover was grouped into a new class, namely 'other'. Figure 5.4 is the map of the resulting five classes, namely '*Q. frainetto'*, '*F. sylvatica',* 'P. *nigra',* '*P. brutia'* and 'other'.

The confusion matrix is shown in table 5.4, together with the user's and producer's accuracy. The OA of the complete classification scheme map was 80%, and the KIA was 0.751. When the rest of the cover classes are grouped to one 'other' class the OA of the map does not change as there is no confusion between maquis and bare land.

According to this map, 1,690 ha of the study area are covered *Q. frainetto*, 480 ha are covered *F. sylvatica*, 600 ha are covered by *P. nigra* and 780 ha are covered by *P. brutia*.

Table 5.4 Confusion matrix of the implementation of SAM in Taxiarchis.

Reference / Classification	*Q. frainetto*	*F. sylvatica*	*P. nigra*	*P. brutia*	maquis	bare land	producer's accuracy %	user's accuracy %
Q. frainneto	45	6	0	1	1	1	**73.7**	**83.3**
F. sylvatica	6	5	1	0	1	0	**45.4**	**38.5**
P. nigra	1	0	18	0	1	0	**90.0**	**90.0**
P. brutia	1	0	0	19	4	0	**90.5**	79.2
maquis	8	0	0	1	24	0	77.4	72.7
bare land	0	0	1	0	0	27	96.4	96.4
TOTAL	61	11	20	21	31	28		

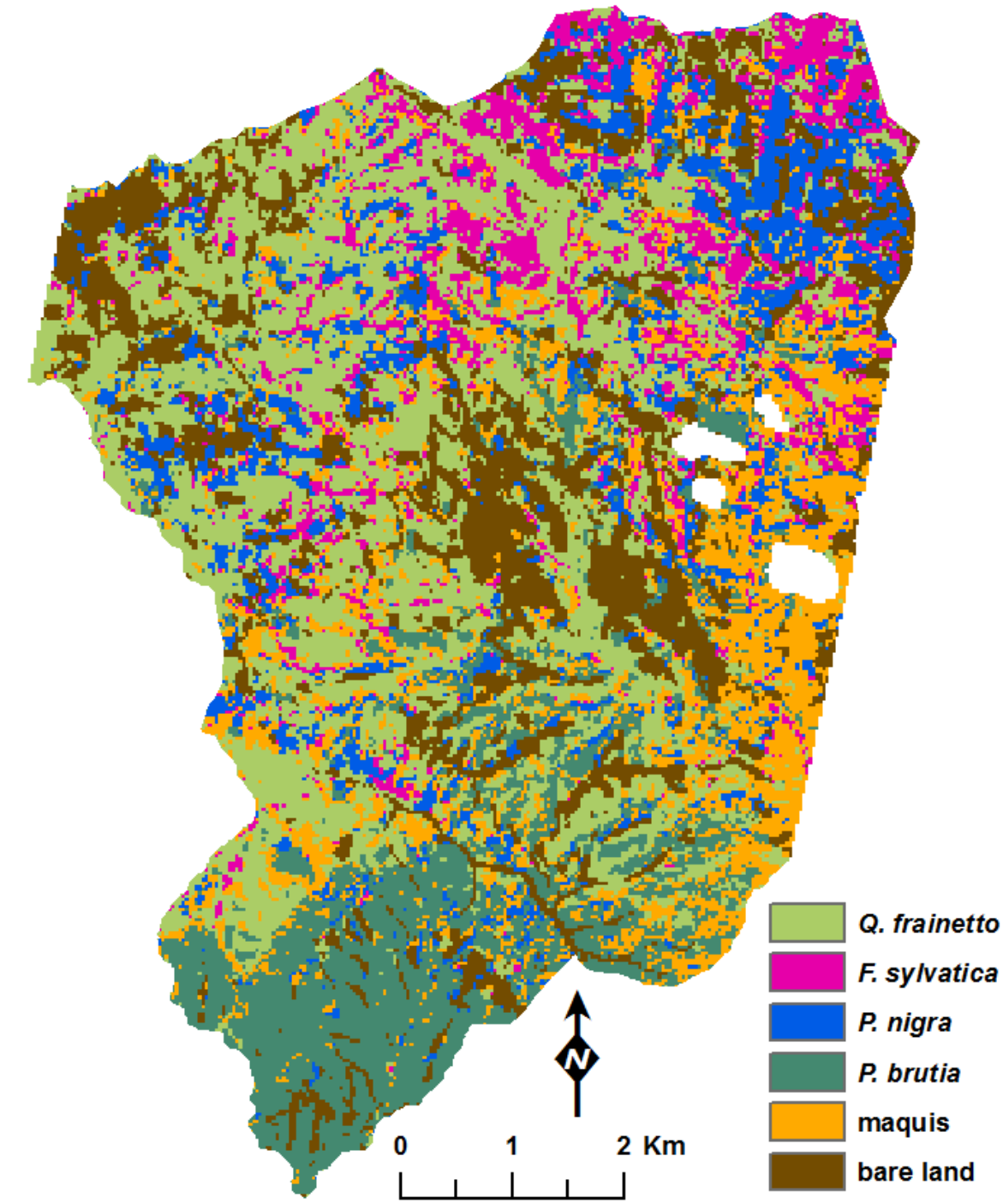

Figure 5.3 Taxiarchis map of all the landcover classes produced by SAM.

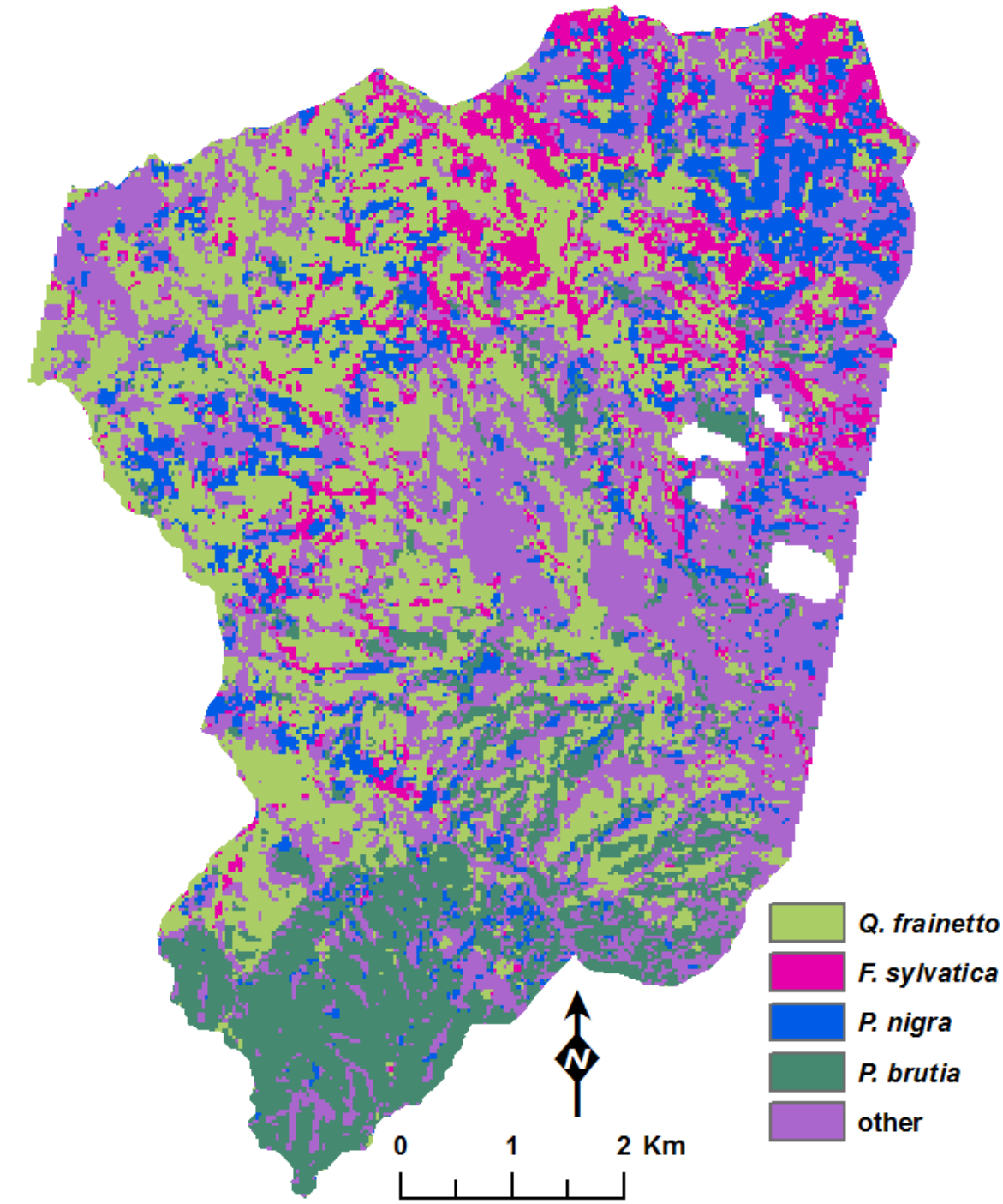

Figure 5.4 Taxiarchis species map produced by SAM (other classes grouped).

5.3 DISCUSSION

A methodology based on SAM was designed to map Mediterranean forest species in two typical Greek forests, with varying species and distribution pattern complexity. This methodology was the first one to be implemented, as SAM is the most straightforward between the techniques investigated.

The classification schemes were designed based on the spatial resolution of the images, the landscape of the study areas, and the aim of the study. The exercise was approached as a landcover mapping, to investigate the detection of the forest species both against each other, and against other landcover that coexist in the landscape.

The 30 by 30 meter spatial resolution introduces mixture in two fashions. First, there is a landcover mixture in the arbitrary imposed pixel grid; particularly prominent in the versatile Mediterranean region. Further, there is spectral mixture between adjacent pixels, due to the scattering of light from neighbors into the target pixel. This 'adjacency effect' is documented for satellite sensors and it is allegedly accounted for by the atmospheric correction performed during preprocessing.

The firm description of the classes is vital for a classification exercise, thus solid class nomenclatures were formed to denote the measurement of landcover that is anticipated.

The training of the classifier was implemented in an iterative manner. Single samples, considered 'pure', were chosen for each class; however, this did not prove efficient as the resulted map barely depicted the study areas. With the intention to keep them to minimum, more training samples were added, up to the point that the accuracy of the maps increased to a sill.

The training samples were chosen based on available thematic maps and VHR imagery, but were later adjusted based on observations made during the field surveys.

Individual angle thresholding of classes was considered, however did not added any value to the maps, thus a single threshold was chosen.

Most of the misclassification occurred due to landcover mixture in the image pixels. This was evident as the misclassification was minimal in large areas with the same cover, while it was increased in transition zones and areas where forest was of lower density; where trees, shrubs and bare land are in a continuous mix.

5.3.1 Thassos

Thassos study area was the first to be investigated because of image availability. However, this was ideal, as the examination of a simple species distribution pattern was a rational choice for the study launch.

In the case of Thassos, the two species under investigation belong to the same genus; fact that gives them plethora of common characteristic and spectral responses with subtle differences, making their mapping a very challenging task. It is interesting to note that *P. brutia* stands tend to be denser, with often impenetrable understory. On the other hand, *P. nigra* often forms open stands, with less understory and more obvious bare land.

Preparatory investigation showed that preprocessing of the image allowed for superior classification results, with dimensionality reduction playing the decisive role.

A visual comparison between the maps produced using the 10 MNF component image (Figure 5.1.a) and the 141 spectral bands (Figure 5.1.b), is enough to illustrate the critical role of dimensionality reduction. It is apparent that in the second case, the distribution pattern of the species is nonexistent.

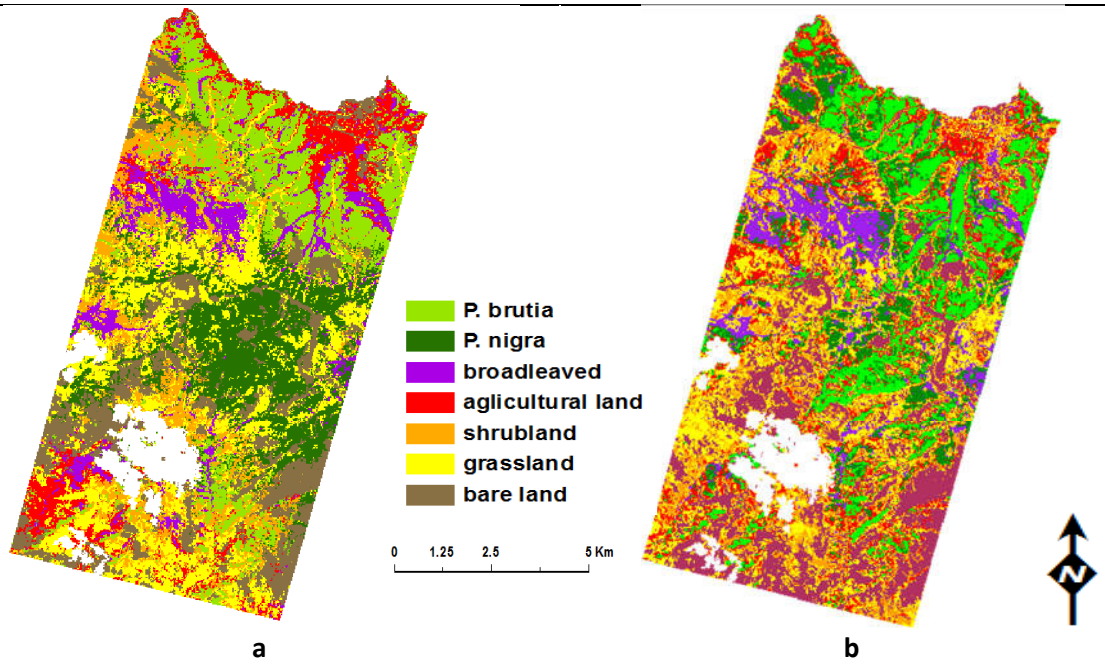

Figure 5.5 (a) Thassos map of the seven landcover classes produced by SAM and MNF component image, (b) the respective map, produced by SVM and original spectral bands.

Field reference data, collected in 265 locations, were used to assess the accuracy of the map and the efficacy of the methodology. SAM proved to be very efficient in mapping the two *Pinus* species, achieving OA of 94% and KIA equal to 0.9. This level of accuracy is considered operational according to literature.

A closer look of the confusion matrix reveals that there was no confusion between the two species. However, visual examination regarding knowledge of the area and available reference data indicated that there was some limited confusion in a North East mountainous area. Despite that, the identification of the two forest species was very successful.

P. brutia was mostly confused with maquis, which can be mostly attributed to their proximity as they both extend in the lowland vegetation zone. The user's accuracy was higher than the producer's, 96.5 % and 88.7% respectively, which implies that it was overestimated rather than underestimated.

P. nigra was mostly confused with phrygana and bare land, the two landcover with the less vegetation cover. This can be attributed to the lower density stands that this species form, condition that increases the contribution of soil spectra in the canopy spectra of these stands. In this case the producer's accuracy (96.7%) was higher than the user's (92.2%) indicating that there were more errors of commission the errors of omission (figure 5.6).

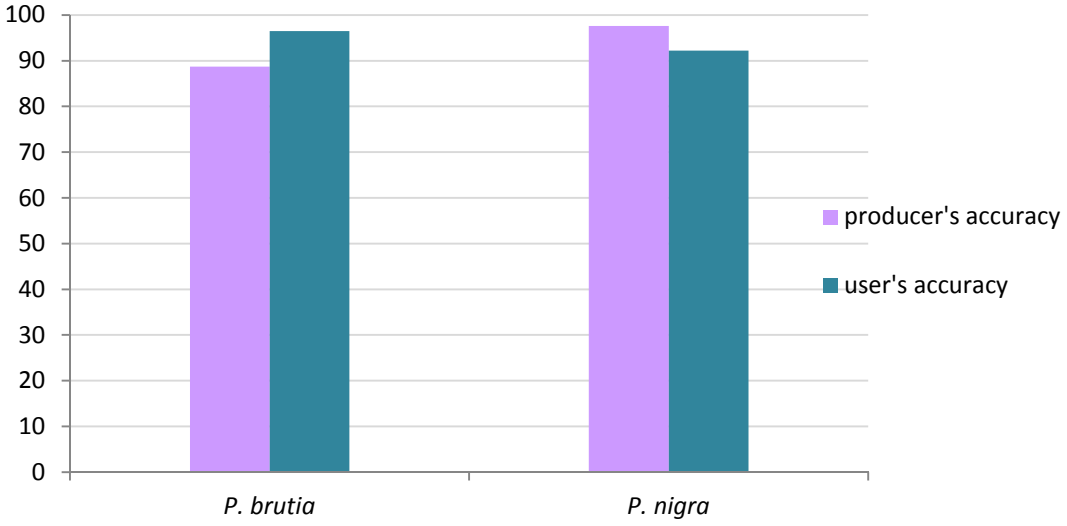

Figure 5.6 Producer's and user's accuracy of SAM classification map for the two *Pinus* species of Thassos.

As indicated by the class statistics (see Figure 5.6), *P. nigra* was more accurately mapped than *P. brutia*.

In any case, overestimation of bare land over what would be considered bare by a photointerpreter is given. This is because although small areas of bare land within a forested area would be considered insignificant by the photointerpreter and would be contained in a forest stand polygon, this is not the case in image classification, which only takes spectral attributes into consideration, and label these areas as bare land.

5.3.2 Taxiarchis

Taxiarchis study area forms a more complex mosaic. *Q. frainetto* dominates the largest part of the forest; while fewer stands of *F. sylvatica* as well as reforestation plantations of *P. brutia* and *P. nigra* are also present together with an extended maquis area.

It should be noted that in the case of Taxiarchis, although agricultural land is present as described in section 3.2.2, fields were either with no vegetation cover at the time of the image acquisition, or covered with fir trees. In the first case they were regarded as bare land. In the second case, fields with fir trees were ignored because of their relative size to the spatial resolution of the image, which rendered them 'undetectable'.

The increased difficulty of mapping this more complex area was evident from the beginning of the exercise, as training the classifier was more challenging. Shadows due to the rough terrain were identified as the main obstacle, as the Taxiarchis image was not corrected for topography effects. In order to overcome this problem, training samples were separately collected for shadowed and non-shadowed areas of the same landcover classes. These classes were later merged during a post classification phase.

Beside the shadow effect, another constraining factor was the small extend of *F. sylvatica* and *P. nigra*, which made it difficult to locate adequate training samples. It is interesting to note that narrow stands of these species mix in the North West of the area, which combined with the rugged terrain made this area the most problematic.

Field reference data, collected in 172 locations, were used to assess the accuracy of the map and the efficacy of the methodology. SAM proved to be efficient in mapping the four forest species, achieving OA of 80% and KIA equal to 0.751. This level of accuracy is very close to be considered operational according to literature.

The lower producer's accuracy (73%) indicates that *Q. frainetto* class was underestimated against maquis and *F. sylvatica* classes, also losing some areas to *P. nigra* and *P. brutia* classes. The user's accuracy was higher (83%), indicating that fewer areas were erroneously assigned the *Q. frainetto* label, with *F. sylvatica* the most common between them.

At the same time, *F. Sylvatica* class was mapped with unacceptable user's and producer's accuracy, 45% and 38% respectively. It was somewhat confused with *Q. frainetto* as mentioned above, with both commission and omission errors between these two classes. This result could be attributed to several reasons. First, the small extent of the *F. sylvatica* did not allow for optimal training sample collection. Adding to that, the spatial distribution pattern of narrow stands mixing with *Q. frainetto* and *P. nigra* gives this class lengthy borders, which as explained above are more prone to misclassification errors. In order to account for this weakness it would be rational to examine the phenology of the two deciduous species, to find whether imagery of different season allows for better discrimination between them.

Another source of error was the confusion between *P. brutia* and maquis, which had already been noticed in the case of Thassos. Maquis were erroneously mapped as *P. brutia*, rather than *P. brutia* being erroneously mapped as maquis. Besides the aforementioned reasons, this could also be attributed to the fact that *P. brutia* and maquis often form mixed stands to which is difficult to draw a crisp nomenclature line and assign a single label.

As apparent in Figure 5.7, SAM more accurately classified *P. nigra*, with *P. brutia,* Q*. frainetto*, and *F. sylvatica* following in the mentioned order. It was notable that the two pines were again mapped with very high accuracies between 79% and 90%, as in the case of Thassos, while *F. sylvatica* classification was unacceptable. However, the 90% producer's accuracy of *P. nigra* is somehow misleading as the P. nigra label has also been assigned to several pixels that are covered with small fields with fir trees. As already discussed, it was decided to overpass Abies sp. classification because of the small extent relatively to the spatial resolution of the imagery.

As explained in section 5.3.1 bare land overestimation is given, affecting the overall appearance of the map.

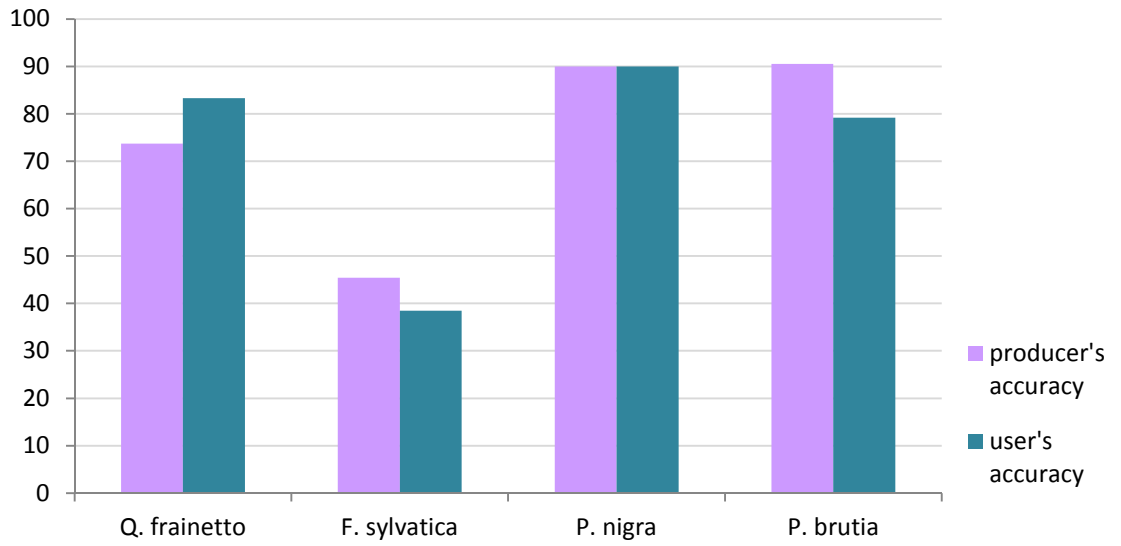

Figure 5.7 Producer's and user's accuracy of SAM classification map for the species of Taxiarchis.

5.4 CHAPTER CONCLUSIONS

The key points discussed in this chapter are summarized below.

- SAM is the straightest forward of the techniques that were investigated in his study, and as such, it was the first one to be implemented. Thassos Island, where the spatial distribution of the forest species is simpler, was the first study area to be analyzed, while image analysis of the more complex Taxiarchis study area followed.

- For both study areas, the classification schemes were designed based on the spatial resolution of the images, the landscape, and the aim of the study. The exercise was approached as a landcover mapping, in order to investigate the detection of the forest species both against each other, and against other landcover that coexist in the landscape.

- Solid nomenclatures were formed to denote the measurement of landcover that is anticipated, and facilitate the robust implementation of the classification.

- Image spectra, as opposed to library spectra, were used to train the classifier and effort was put to keep their number to the minimum.

- In the case of Thassos the OA achieved was 94% and the respective KIA was 0.9. Both species, namely *P. brutia* and *P. nigra*, were mapped with very high user's and

producer's accuracy (>88%) and no confusion was noted between them. This was almost certainly facilitated by the simple distribution pattern of the two species. This conclusion is drawn, as it was revealed that most misclassification occurs in mixed pixels, where landcover meets within the boundaries of the 30 by 30 meters pixel boundaries. In this sense, the fact that in Thassos landscape the two *Pinus* species meet in limited areas allowed for very accurate mapping.

- In the case of Taxiarchis the resulting map was of lower OA (80%) and KIA (0.751). This could be attributed to several factors. The first factor is that Taxiarchis image was not corrected for the spectral smile or the topographic effect, and thus it was of poorer quality at the point of getting into the main image analysis. Another reason is that more species were under investigation which multiplies the importance of misclassification. Also, the mix of the stands was continuous, lengthening the susceptible to misclassification borders between classes.

- The investigation of SAM in two study areas revealed that the proposed methodology is efficient in mapping forest species in a regional level; however there is ground for improvement, especially for the more accurate classification of the two deciduous species, namely *Q. frainetto* and *F. sylvatica*.

- It is interesting to note, that although Taxiarchis forest is a well spatially documented forest area , in the case of Thassos available maps date back to the 80's, thus the map produced in this study is of increased value.

6

SUPPORT VECTOR MASCHINES IN MEDITERRANEAN FOREST SPECIES MAPPING

Chapter 5 discussed the investigation of a SAM based methodology to map Mediterranean forest species. Chapter 6 describes the investigation of the methodology developed employing SVM for the species level classification of the study areas. Along with the presentation of the methodology and the acquired results, this chapter also discusses the various aspects that influence the efficiency of the methodology, and the value of the produced maps.

6.1 METHODOLOGY

6.1.1 Classification scheme

The classification schemes developed for the investigation of SAM were also used in this investigation (see section 5.1.1).

6.1.2 Training samples

As SVM is a supervised classification technique, a training set of vectors, each with a label class that attaches meaning to the vector, needs to be chosen in order to train SVM to provide correct class labels to the testing set of feature vectors with unknown labels.

Due to reasons discussed in the section 5.1.2, image spectra were used for training the SVM classifier. The training samples collected for the investigation of SAM did not prove efficient for this classification technique, so new training samples were collected as shown in table 6.1.

Table 6.1. Training point used per class in Thassos

class	number of training points
Thassos	
1. *Pinus brutia*	100
2. *Pinus nigra*	100
3. Deciduouss (*Platanus sp., Quercus sp., Ficus sp*.)	60
4. Agricultural land (mostly Olive orchards)	60
5. Maquis	100
6. Phrygana	100
7. Bare land	100
Taxiarchis	
1. *Querqus frainetto*	300+140
2. *Fagus sylvatica*	60
3. *Pinus nigra*	60
4. *Pinus brutia*	120
5. Maquis	90+80
6. Bare land	100

6.1.3 Binary to multiclass SVM

As discussed in section 2.3.7, SVM is essentially a binary classification technique, which needs to be modified in order to handle the multiclass problems which are very common in remote sensing applications.

In this study, a 'one against one' (OAO) approach (Knerr et al. 1990) was used, in which all possible two-class classifiers are evaluated from the training set of n classes, each classifier being trained on only two out of the n classes, giving a total of n(n-1)/2 classifiers. Applying each classifier to the test data vectors gives one vote to the winning class. The pixel is given the label of the class with most votes.

6.1.4 SVM and Kernel Parameters

Again as discussed in section 2.3.7, SVMs use kernel functions to project the data from input space to a higher dimensional feature space, where it is easier to find a linear optimal hyperplane to separate training data. The RBF Kernel (equation 6.1) was used in this study, as it has been demonstrated that it produces higher classification accuracies in remote sensing applications (Vyas et al., 2011; Pal and Mather, 2004; Nidamanuri and Zbell, 2011).

$$\textbf{(RBF): } K(x_i,x_j) = \exp(-g||x_i - x_j||^2),\ g > 0 \qquad \text{eq.6.1}$$

Along with margin parameter *C*, RBF kernel makes use of parameter *γ*. *C* is a penalty value for misclassification errors and *γ* is a parameter controlling the width of the Gaussian kernel. It is not known beforehand which *C* and *γ* are optimal for a given problem; consequently some kind of model selection (parameter search) must be done to identify optimal *C* and *γ* so that the classifier can accurately predict unknown data.

In order to test the performance of classifiers with different pairs of *C* and *γ,* a common strategy is to separate the data set into two parts, of which one is considered unknown. *N*-cross-validation is a procedure in which the training set is divided into *n* subsets of equal size and sequentially assess the accuracy of each classified subset using the classifier trained on the remaining *n − 1* subsets.

Cross-validation for the selection of optimal kernel parameters is not available in any of the leading commercial remote sensing software. To overcome this absence, a Graphical User Interface (GUI) which uses the LIBSVM software (Chang and Lin, 2011) was developed in MATLAB, to implement a 5-fold cross validation. In this application, exponentially growing sequences of *C* and *γ* values are tested in a "grid-search" and the pair with the best cross-validation accuracy is considered for optimal for kernel parameterization.

This custom cross-validation tool operates on polygon shapefile data, thus the raster format training samples were imported into a geographic information system (GIS), where they were converted to separate polygons, each of them having its MNF components values attached.

The necessary normalization of data is an integral part of the ENVI implementation of SVM and thus was not performed separately.

6.2 RESULTS

6.2.1 Thassos

The implementation of the cross-validation routine indicated that the best parameter pair was *C*=8 and *γ*=2; thus these values were used to parameterize SVM.

The implementation of SVM on the Hyperion image of Thassos, excluding the area covered by clouds and their shadow, resulted in the map shown in Figure 6.1. However, as the objective of

the study is to map the two forest species, the rest of the cover classes were grouped to one other class, namely 'other'. Figure 6.2 is the map of the resulting three classes, namely '*P. brutia'*, '*P. nigra'* and 'other'. According to these maps 1,890ha of the study area is covered by *P. brutia*, and 1,690 ha is covered by *P. nigra*.

A confusion matrix (table 6.2) was populated by labels assigned to pixels by the classifier, and labels assigned to the respective reference data; cross-tabulated, using geographic location as key, and was analyzed with four measures of agreement, namely KIA, OA, user's and producer's accuracy.

The OA of the complete classification scheme map was 80%, and the KIA was 0.762. However, as the objective of the study is to map the two forest species, the rest of the cover classes were grouped to one other class, namely 'other'. In this case the OA of the map was 89%, and the KIA was 0.821, respectively.

Table 6.2 Confusion matrix of the implementation of SVM in Thassos.

Reference / Classification	*P. brutia*	*P. nigra*	deciduous	agricultural	maquis	phrygana	bare land	producer's accuracy %	user's accuracy %
P. brutia	52	1	2	2	1	0	0	**83.9**	**89.7**
P. nigra	0	58	0	0	0	8	3	**95.1**	**84.1**
deciduous	0	0	12	0	0	0	0	85.7	100
agricultural land	3	0	0	22	1	0	1	88.0	81.5
maquis	6	0	0	0	14	2	3	50.0	56.0
phrygana	1	2	0	1	10	32	3	76.2	65.3
bare land	0	0	0	0	2	0	23	69.7	92.0
TOTAL	62	61	14	25	28	42	33		

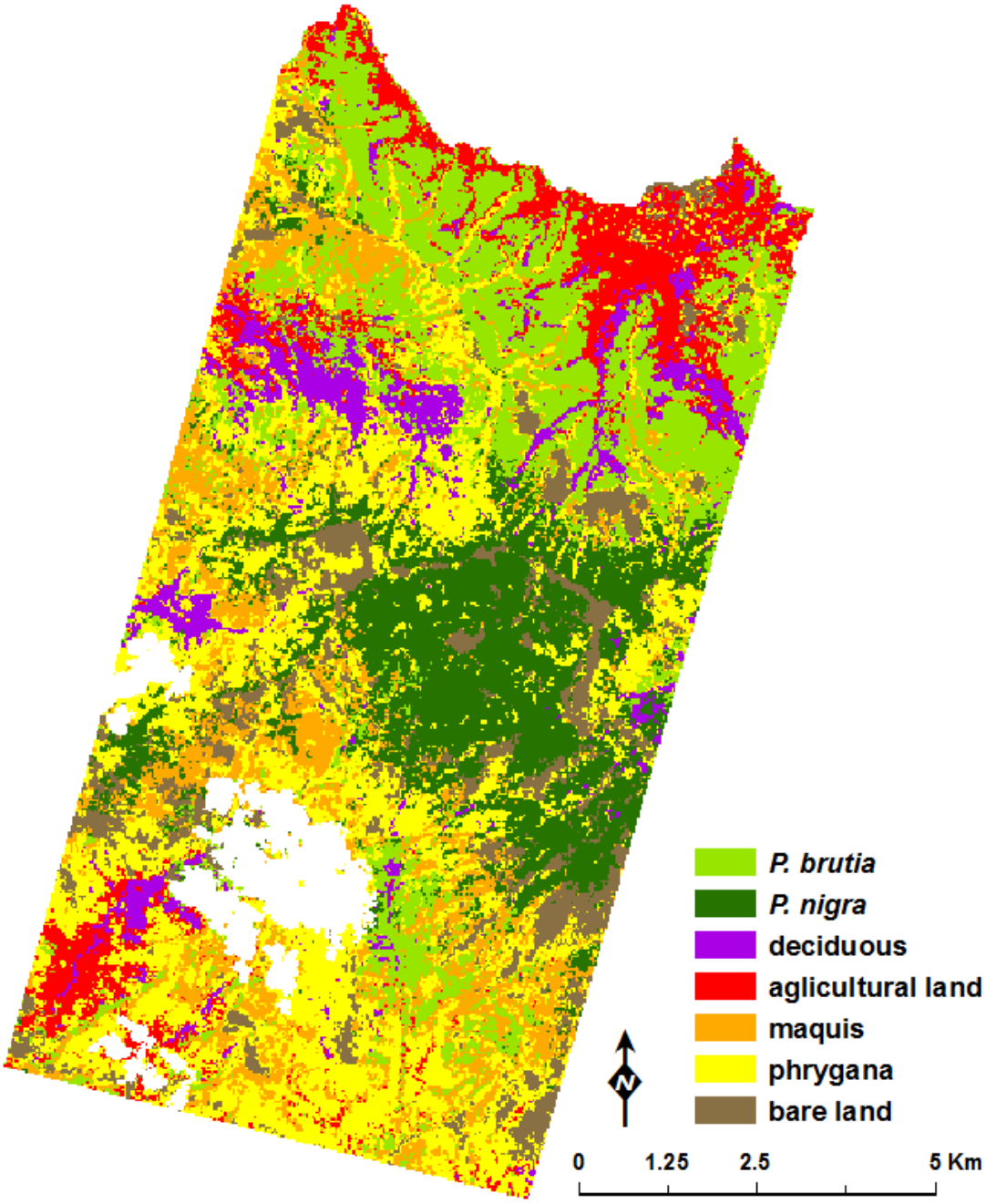

Figure 6.1 Thassos map of the seven landcover classes produced by SVM.

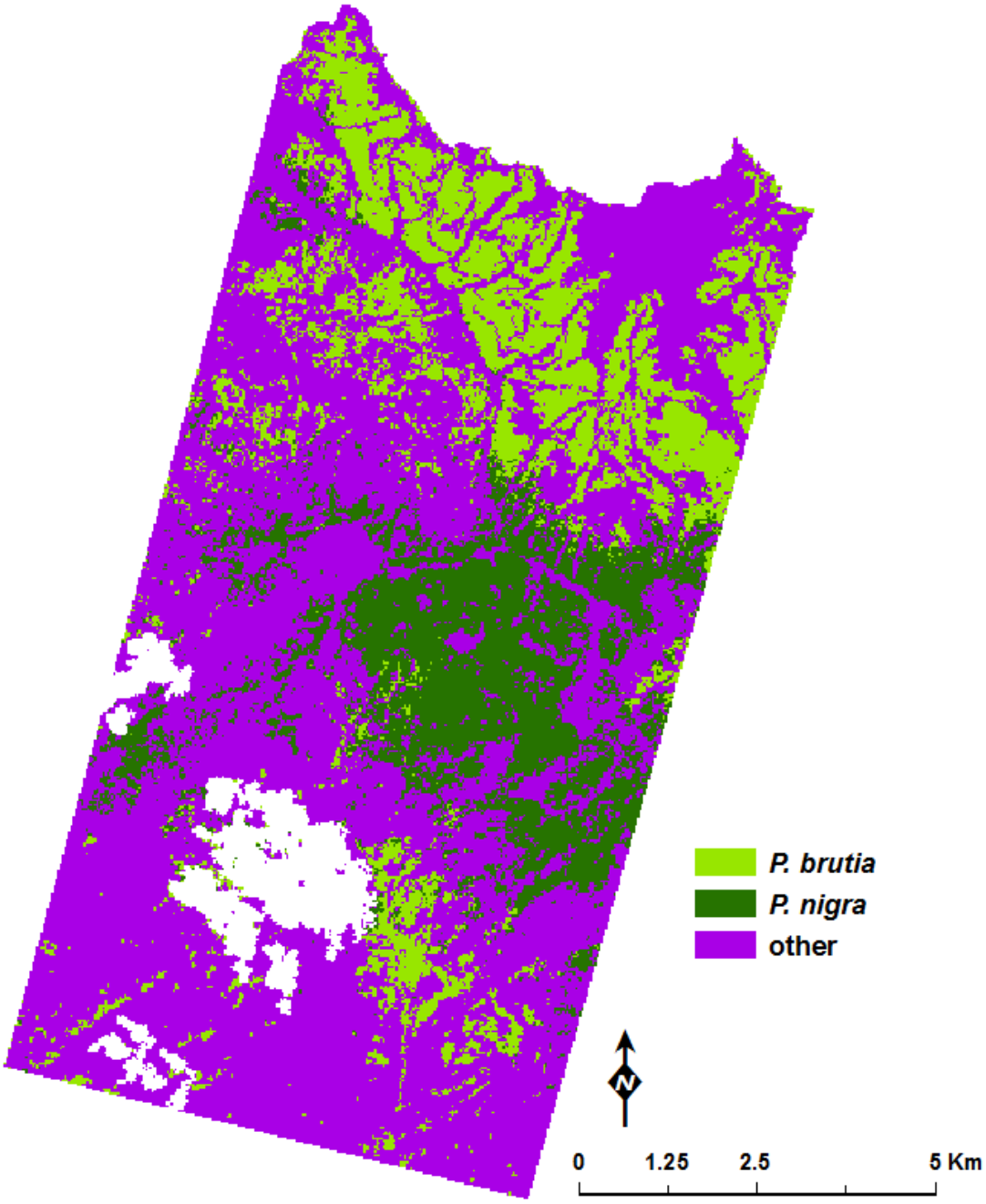

Figure 6.2 Thassos species map produced by SVM (other classes grouped).

6.2.2 Taxiarchis

The implementation of the cross-validation routine indicated that the best parameter pair was *C*=32 and *γ*=8; thus these values were used to parameterize SVM.

The implementation of SVM on the Hyperion image of Taxiarchis as described above resulted in the map shown in Figure 6.3, excluding the area covered by clouds and their shadow. As in Thassos, the secondary landcover was grouped into a new class, namely 'other'. Figure 6.4 is the map of the resulting five classes, namely *Q. frainetto*, *F. sylvatica,* '*P. nigra',* '*P. brutia'* and 'other'.

The confusion matrix is shown in table 6.3, together with the user's and producer's accuracy of each class. The OA of the complete classification scheme map was 81%, and the KIA was 0.750. When the rest of the cover classes are grouped to one 'other' class the OA of the map increased to 82.6% and KIA to 0.757.

According to this map, 1,590 ha of the study area are covered *Q. frainetto*, 600 ha are covered *F. sylvatica*, 700 ha are covered by *P. nigra* and 600 ha are covered by *P. brutia*.

Table 6.3 Confusion matrix of the implementation of SVM in Taxiarchis.

Reference / Classification	*Q. frainetto*	*F. sylvatica*	*P. nigra*	*P. brutia*	maquis	bare land	producer's accuracy %	user's accuracy %
Q. frainneto	49	2	0	1	2	3	**80.3**	**86.0**
F. sylvatica	5	8	0	0	0	0	**72.7**	**61.5**
P. nigra	0	1	19	0	1	0	**95.0**	**90.5**
P. brutia	1	0	0	18	5	0	**85.7**	**75.0**
maquis	6	0	1	2	23	3	74.2	65.7
bare land	0	0	0	0	0	22	78.6	100
TOTAL	61	11	20	21	31	28		

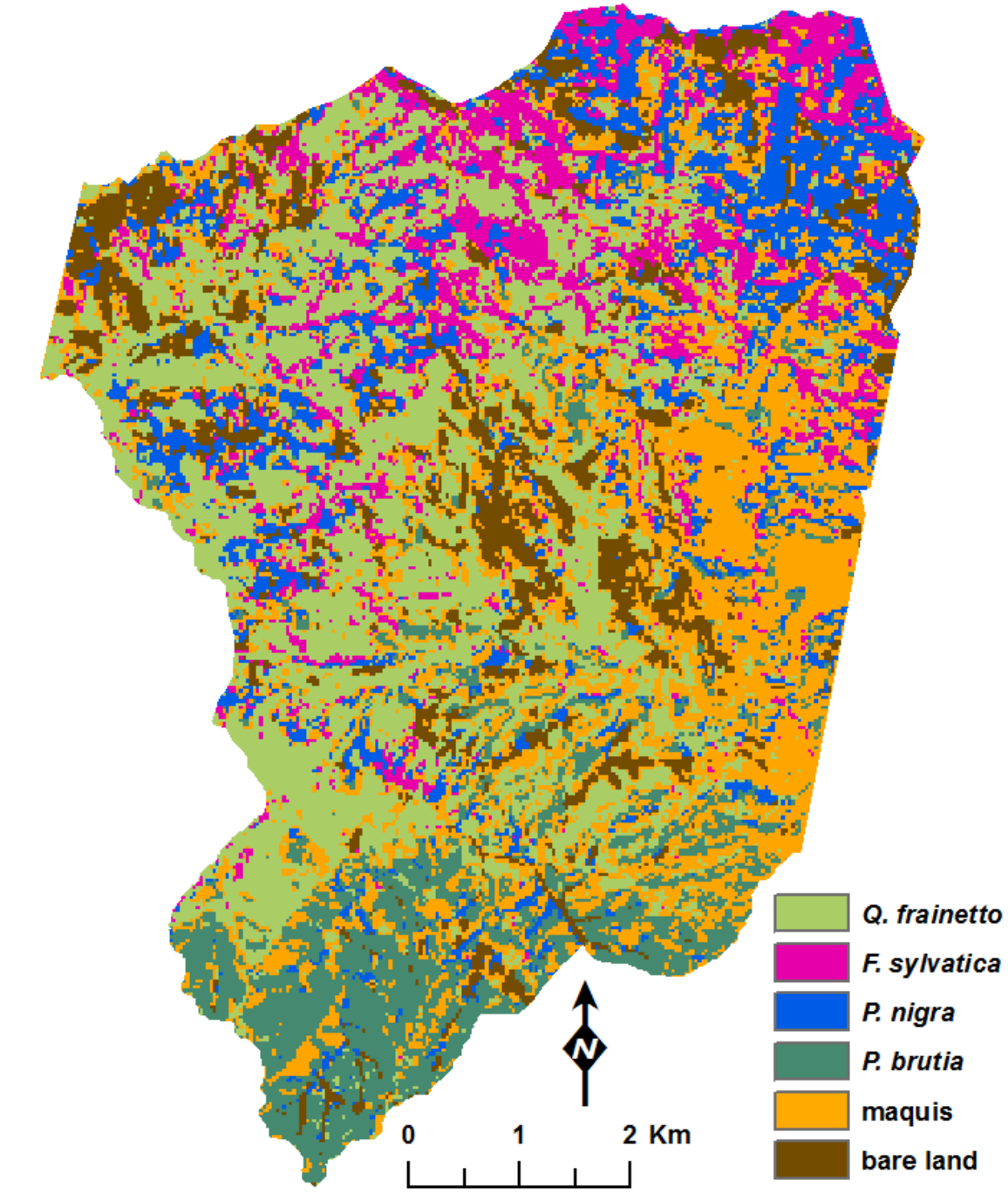

Figure 6.3 Taxiarchis map of all the landcover classes produced by SVM.

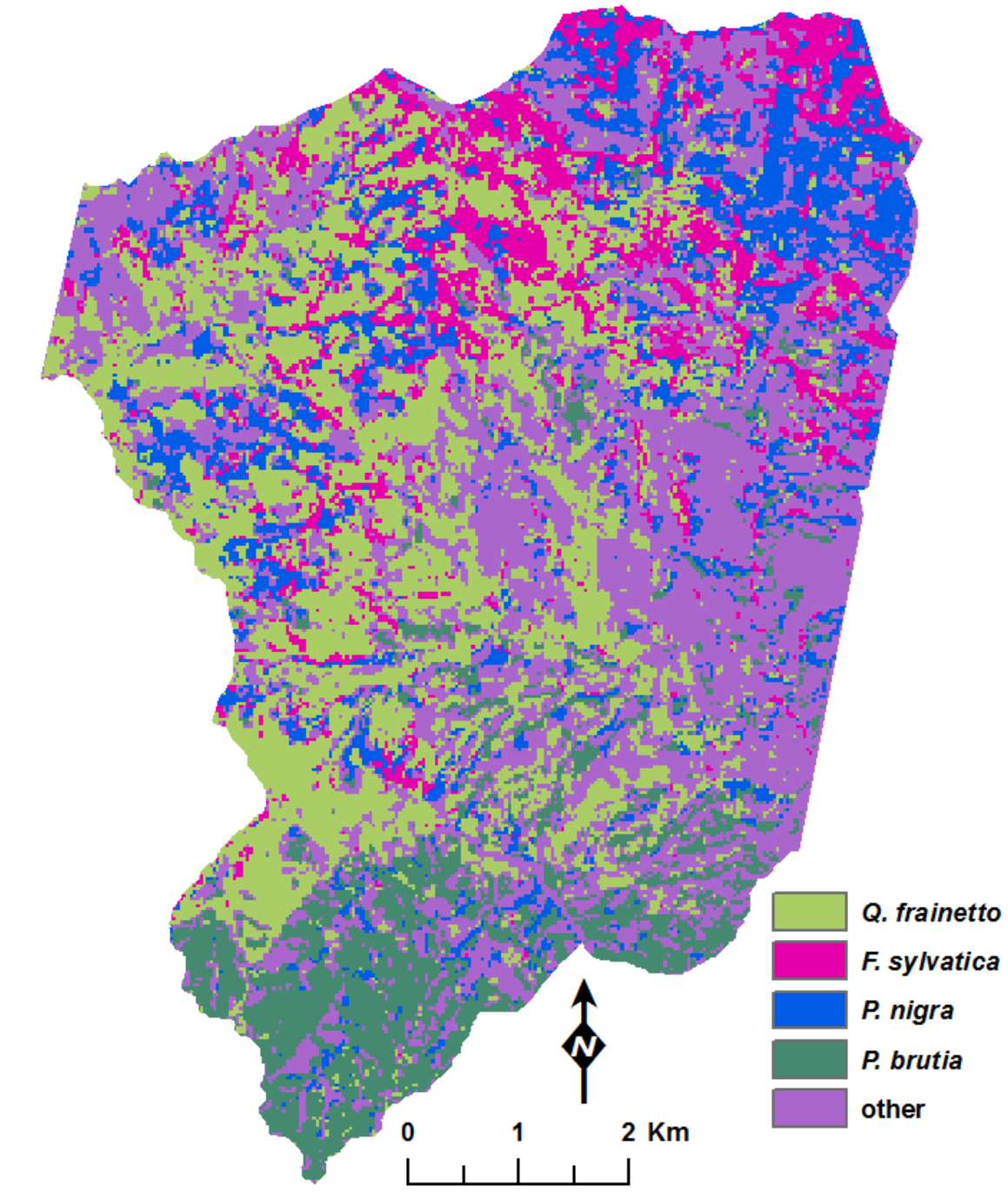

Figure 6.4 Taxiarchis species map produced by SVM (other classes grouped).

6.3 DISCUSSION

A methodology based on SVM was developed to map Mediterranean forest species in two typical Greek forests, with varying species and distribution pattern complexity. This methodology **followed** the investigation of a SAM based methodology, to examine whether the use of a novel technique allows for advanced mapping results.

The **classification scheme** as described in section 5.1.1 was also used in this methodology, in order to investigate the detection of the forest species both against each other, and against other landcover that coexist in the landscape.

At first the **training samples** already collected for the SAM classifier were used for cross-validation and classification. However, the maps produced were of very low accuracy, thus new training samples were collected following the rational described in 5.3. Although SVM has the advantage of generalizing well even with limited training samples, this was not the case in this study. More training samples were used in order to achieve accurate maps. This could be the case because landcover is a continuous mixture of numerous components in various scales, rendering difficult to locate marginal samples on which SVM is based to separate classes.

An OAO approach was used to address the multiclass scheme, and an RBF kernel was chosen to project the data from input space to a higher dimensional feature space. A custom 5-fold cross-validation application was used to indicate the optimal combination of margin parameter C and kernel parameter γ, after training samples were converted to vector (as opposed to raster) format. However, other values resulted from experimentation provided more accurate maps and were therefore used.

Published studies have reported that SVM usually outperforms SAM (Piscini et al. 2001; Vyas et al., 2011), which is not the case for both study areas of this study. This could be attributed to the way SVM is implemented by remote sensing software. The ENVI software used in this study does not allow for interference at various steps of the classification progress and fine-tuning the system with the aid of analytical and visual tools, as software for numerical computation and programming (i.e. MATLAB) allow. This lack of in depth manipulation possibly decreases the performance of this otherwise sophisticated technique. However, the more complex problem of Taxiarchis was better addressed by SVM than SAM.

6.3.1 Thassos

Thassos study area was again the first to be investigated because of the simple species distribution pattern that presents; setting however the challenge of mapping species that belong to the same genus.

As in the case of SAM, in preparatory analysis, SVM was applied to the original 141 spectral bands as well as the 10 MNF components. Contrary to SAM, in the first case the distribution pattern of the forest species was preserved, however the accuracy was considerably lower that when the MNF components were used, demonstrating again the value of data dimensionality reduction. This is in agreement with studies that tested the performance of SVM in datasets with varying dimensionality and showed that the accuracy of the classification is in fact affected by the increasing number of features (bands) used as input (72%) (Figure 6.5).

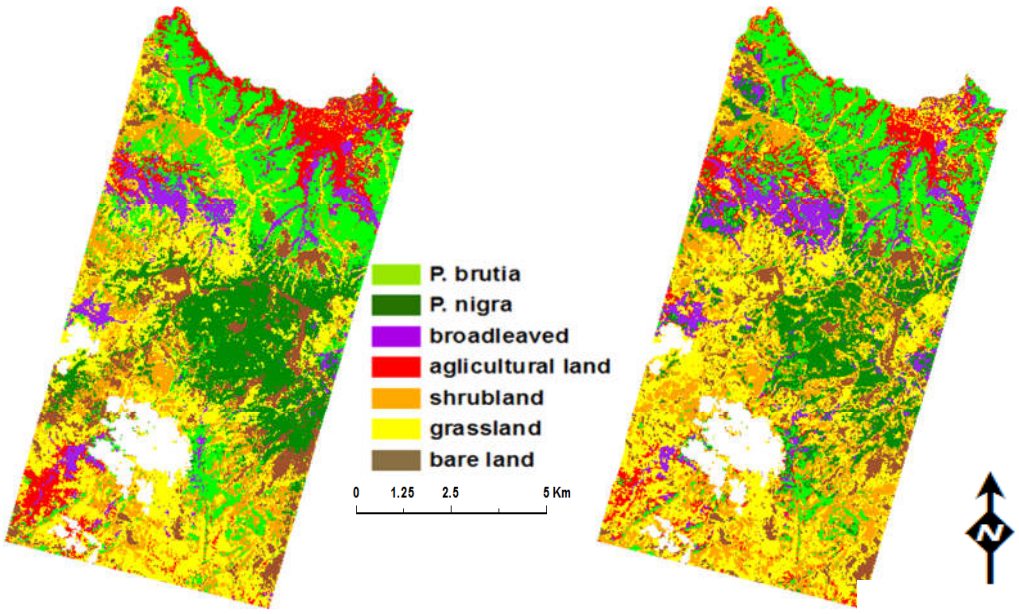

Figure 6.5 (a) Map of the seven landcover classes produced by SVM and MNF component image, (b) the respective map, produced by SVM and original spectral bands.

Field reference data, collected in 265 locations, were used to assess the accuracy of the map and the efficacy of the methodology. SVM proved to be very efficient in mapping the two *Pinus* species, achieving OA of 89% and KIA equal to 0.821. This level of accuracy is considered operational according to literature.

A closer look of the confusion matrix reveals that between the 123 reference points belonging to the two forest species classes, only one *P. nigra* point was erroneously classified as *P. brutia*. This shows that SVM is very efficient in distinguishing between the two forest species. The lower OA of the map was caused by misclassifications between forest species and other landcover.

In particular, *P. brutia* was rather underestimated, as omission errors were more than commission errors. As in the case of SAM the landcover that was more often confused with *P. brutia* was the maquis. As explained in section 5.3.1 this is probably because of to their neighboring as they both extend in the lowland vegetation zone. For the *P. brutia* class the producer's accuracy was 83.9% while the user's accuracy was 89.7%.

In the case of *P. nigra*, commission errors were much higher than omission errors. The majority of erroneously classified as *P. nigra* reference points were identified as phrygana in the field. As discussed in section 5.3.1 this could be attributed to the fact that the contribution of soil spectra in both these classes is increased due to the denser cover. For the *P. nigra* class the producer's accuracy was 95.1% while the user's accuracy was 84.1%.

As explained in section 5.3.1 bare land overestimation is given, affecting the overall appearance of the map.

As indicated by the class statistics, *P. nigra* was more accurately mapped by *P. brutia* (Figure 6.6).

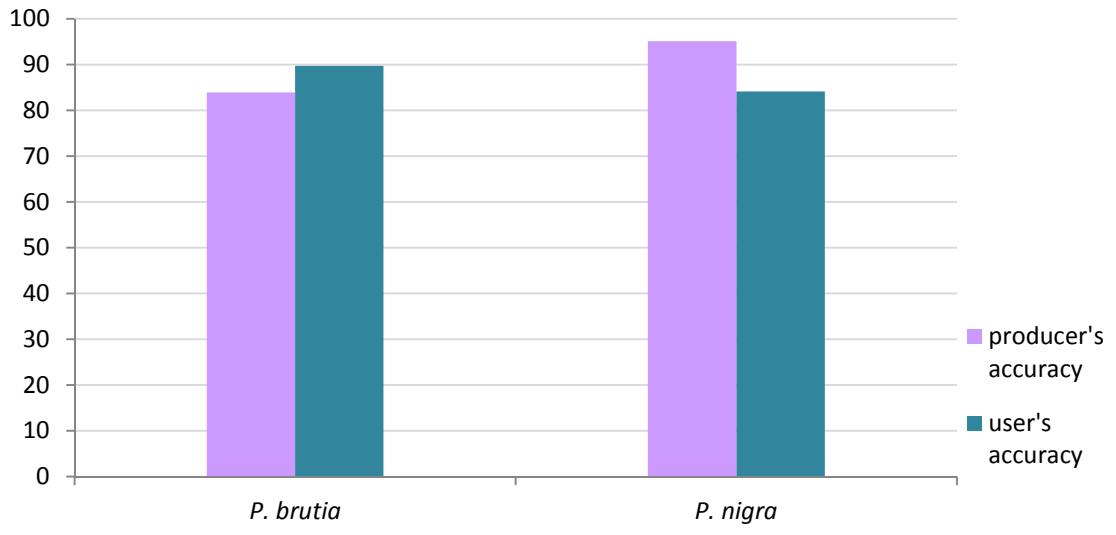

Figure 6.6 Producer's and user's accuracy of SVM classification map for the two *Pinus* species of Thassos.

It is interesting to note that although the SVM methodology was more laborious than the SAM methodology, the resulted maps were of comparable but lower accuracy.

6.3.2 Taxiarchis

The influence of the complexity of the landscape in the case of Taxiarchis is already discussed in sections 5.3 and 5.3.2 and is not repeated in this section.

Field reference data, collected in 172 locations, were used to assess the accuracy of the map and the efficacy of the methodology. SVM proved to be efficient in mapping the four forest species, achieving OA of 81% and KIA equal to 0.757. This level of accuracy is very close to what is considered operational according to literature.

The lower producer's accuracy (80.3%) indicates that *Q. frainetto* class was underestimated, specifically against maquis and *F. sylvatica* classes. The user's accuracy was higher (86%), indicating that fewer areas were erroneously assigned the *Q. frainetto* label, with bare land being the most common between them.

SVM mapped *F. sylvatica* with low accuracy, however considerably higher than in the case of SAM classification. Producer's accuracy (72.7%) was higher than user's (61.5%) indicating that this class was overestimated rather than underestimated. The confusion was between *F. sylvatica* and *Q. frainetto*, the two deciduous species of the study area. As discussed in section 5.3.2, the low accuracy of classifying *F. sylvatica* can be attributed to the small extent and lengthy boarders with other landcover and especially *Q. frainetto*.

P. nigra was again very accurately mapped with both user's and producer's accuracy higher than 90%, and minimal confusion with maquis and *F. sylvatica*. As already discussed, the overestimation of P. nigra is evident as the P. nigra label has also been assigned to several pixels that are covered with small fields with fir trees, for which a separate class was not included in the classification scheme.

P. brutia was rather overestimated as reference data indicated that some maquis pixels were erroneously assigned the *P. brutia* label.

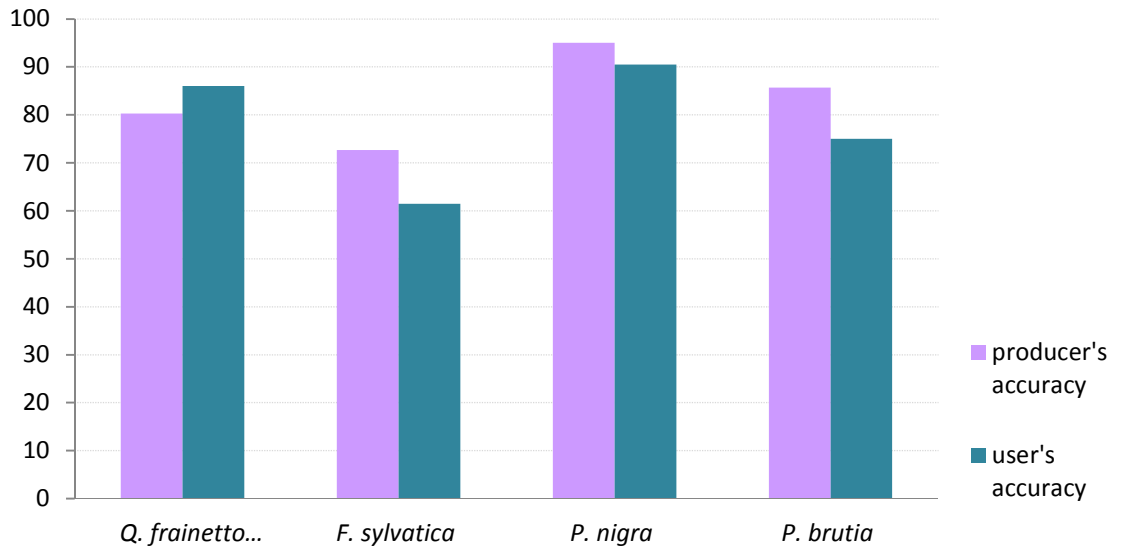

Figure 6.7 Producer's and user's accuracy of SVM classification map for the species of Taxiarchis.

As apparent in Figure 6.7, SVM more accurately classified *P. nigra*, with *Q. frainetto*, *P brutia* and *F. sylvatica* following in the mentioned order (Figure 6.7).

As explained in section 5.3.1 bare land overestimation is given, affecting the overall appearance of the map.

It is interesting to note that in the case of the more complex classification problem of Taxiarchis, SVM out performed SAM, especially in the case of the *F. sylvatica* class, which in the case of SAM was classified with accuracy less than 50% while with SVM achieved accuracies were between 60 and 70%.

6.4 CHAPTER CONCLUSIONS

The following points summarize the key points discussed in chapter 6:

- SVM is an advanced classification technique that has been recently introduced with success in the remote sensing community. It was investigated in this study following the investigation of a SAM based methodology, to examine whether the use of a novel technique allows for advanced results in Mediterranean forest species mapping. Thassos Island, where the spatial distribution of the forest species is simpler, was the first study

area to be analyzed, while image analysis of the more complex Taxiarchis study area followed.

- The classification schemes developed for the investigation of SAM and related nomenclatures were also used in this investigation.
- Image spectra, as opposed to library spectra, were used to train the classifier. As training samples collected for SAM were not adequate to train SVM, more spectra were collected to form a larger training set.
- An OAO approach was used to address the multiclass scheme, and an RBF kernel was chosen to project the data to a higher dimensional feature space. A custom 5-fold cross-validation application was used to indicate the optimal combination of margin parameter C and kernel parameter γ.
- In the case of Thassos, the achieved OA was 89% and the respective KIA was 0.821. Both species, namely *P. brutia* and *P. nigra*, were mapped with very high user's and producer's accuracy (>88%) and minimal confusion was noted between them. This was almost certainly facilitated by the simple distribution pattern of the two species.
- In the case of Taxiarchis, the resulting map was of lower OA (82.6%) and KIA (0.765) than in the Thassos study area. The lower accuracy compared to Thassos could be attributed to the higher complexity of the problem (more species, complex pattern) and the fewer preprocessing steps applied on the image.
- The investigation of SVM in two study areas revealed that the proposed methodology is efficient to map forest species in a regional level. The implementation of the methodology was considerable more laborious than the SAM based methodology, both in training and parameterizing context. Although it provided no improvement over the Thassos map produced with SAM, it increased the accuracy of the more complex Taxiarchis map. Notable is the substantial increase in the classification accuracy of *F. sylvatica*, which was not possible with SAM.

7

GEOGRAPHIC OBJECT BASED IMAGE APPROACH IN MEDITERRANEAN FOREST SPECIES MAPPING

Chapter 5 and 6 investigated the use of a traditional and an advanced pixel based technique, and demonstrated their efficiency and limitations in mapping Mediterranean forest species. This chapter discusses describes the investigation of the GEOBIA methodology developed for the species level classification of the study areas. Along with the presentation of the methodology and the acquired results, this chapter also discusses the various aspects that influence the efficiency of the methodology, and the value of the produced maps.

7.1 METHODOLOGY

As discussed in detail in section 2.3.8, GEOBIA is technically and theoretically different to pixel based image processing approach, and includes processes which transform image data from the remotely sensed physical reality to the human conceptualization of the geographic objects.

Driven by the concept that important information necessary to interpret an image is not represented in single pixels, but in meaningful image objects and their mutual relationships, GEOBIA classifies image objects which are extracted in a previous image segmentation step.

In order to guide the segmentation process to create meaningful objects, visual interpretation of the segmentation results is fundamental. In this sense it is not rational to use the MNF components image, as it is not comprehensible by the analyst for visual interpretation. Adding to that, because MNF transformation is solely depended on the image in hand, it deprives the possibility for model transferability, one of GEOBIA's advantages. Because of these, it was decided that the **original spectral bands** would be used as input data in this investigation.

Two different classification models were developed to map the forest species of the two study areas. Although the two methodologies differ, they both use the same segmentation algorithm and make use of the Nearest Neighbor classifier. Sections 7.1.1 and 7.1.2, describe these two

model components, while sections 7.1.3 and 7.1.4 describe the two classification models, further describing the uncommon parts.

7.1.1 Segmentation

The development of the classification model starts with the segmentation of the image into image objects. The multiresolution segmentation algorithm (Baatz and Schape, 2000) was used in this study. The multiresolution segmentation algorithm is a bottom-up segmentation algorithm, based on a pairwise region merging technique; consecutively merges pixels or existing image objects. The segmentation procedure starts with single image objects of one pixel and repeatedly merges them in several loops in pairs to larger units, as long as an upper threshold of homogeneity is not exceeded locally. This homogeneity criterion is defined as a combination of spectral and shape homogeneity and is controlled by the scale parameter.

Setting the scale parameter and finding a useful segmentation level is a trial and error procedure (Blaschke and Hay, 2001) that represents one of the main limitations of GEOBIA (Hay et al., 2003) and decidedly affect the subsequent analysis.

In order to determine the size of the objects, which should be as large as possible and as fine as necessary, during segmentation several **parameters** need to be defined.

- **Layer weights.** Layer weights determine the degree to which information provided by each layer is used during the process of the object generation. Their values range from 0 to 1.

- **Scale parameter.** The scale parameter is a unitless abstract term that determines the maximum allowed heterogeneity for the resulting image objects throughout the segmentation process. It defines the maximum standard deviation of the homogeneity criteria in regard to the weighted image layers for resulting image objects. Thus, the higher the value of the scale parameter is, the larger the resulting objects. Its values range from 1 to infinity. Eventually a large scale factor will prevent multiple objects to be generated.

- **Homogeneity** is composed by 4 criteria, which define the total relative homogeneity attributes of the resulting image objects to be minimized as a result of a segmentation run.
    - **Color** refers to the digital value (reflectance) of the resulting image object.

- **Shape** refers to the textural homogeneity of the resulting object.
- **Smoothness** refers to the smoothness of borders between the resulting objects.
- **Compactness** refers to the overall compactness of the resulting object.

The relations of these criteria as shown in Figure 7.1 are:

- color + shape = 1
- smoothness + compactness = 1

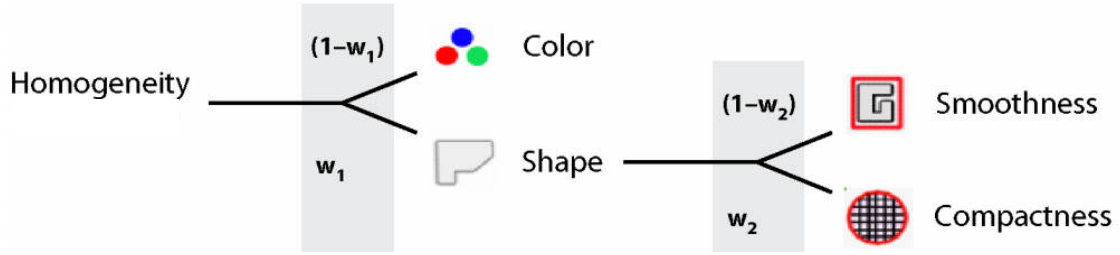

Figure 7.1 Homogeneity with its 4 criteria and the relationships between them.

7.1.2 Nearest Neighbor

The Nearest Neighbor is a non-parametric rule, thus operates without a priori assumptions about the distributions from which the training examples are drawn. It involves a training set of both positive and negative cases. A new sample is classified by calculating the distance to the nearest training case; the label of that point then determines the classification of the sample (Figure 7.1).

NN classifies objects based on **given sample objects** within a **defined feature space.** Feature space may comprise of a variety of class describing features such as spectral values, shape, texture and class related features, between other. These features can be combined in an arbitrary manner to span the feature space for nearest neighbor classifier. A Feature Space Optimization (FSO) tool is available to determine the most descriptive features for each class, which may vary between classes.

NN classifier has a fuzzy logic basis. Fuzzy classification delivers not only the assignment of one class to an image object, but the degree of assignment to all considered classes. This degree of assignment or membership function may be perceived as indicating mixture of landcover classes

or as probability of the class assignment accuracy. In both contexts, this information gives useful insights for the model development and the value of the map.

An optimal NN training routine starts with one training object per class and adds objects until the classification result is regarded adequate. This routine was followed in this investigation, but as the number of objects was increasing it was considered rational to use the training samples collected in the SAM based methodology.

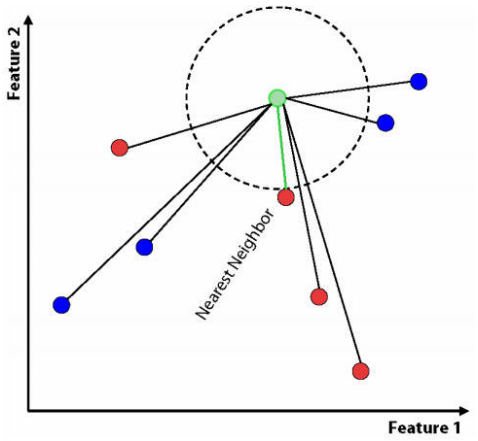

$$d = \sqrt{\sum_f \left(\frac{v_f^{(s)} - v_f^o}{\sigma_f} \right)^2}$$

d is the distance between the training object s and the test object o

$v_f^{(s)}$ is the value of feature f of the training object

v_f^o is the value of feature f of the test object

σ_f is the standard deviation of the values of feature f

Figure 7.2 The principle of NN and the formula ogf the distance measurment between training and test object.

Training pixels and image objects were imported in a GIS to implement their spatial matching. The center coordinates of the training pixels were used to create a point vector layer with the class label assigned, which was then spatially joint to the image object vector layer. The objects that acquired a class label were exported and converted to a test and training mask (TTA mask) to be used to train the NN classifier. Care was taken to identify the occasions where more than one training samples fell within the same object and verify the absence of any conflict. This routine essentially extrapolates the class information of a point based measurement in a polygon object; however this assumption was regarded appropriate implying confidence on the segmentation result.

7.1.3 Thassos classification model

A single level classification model was developed, because a second level was not required in the sense that there is no land caver or function that operates in a different scale (i.e. lakes). This is

also in agreement with Blaschke (2010), who argues that **medium resolution imagery** does not support multi-level segmentation.

For the creation of this level the segmentation parameters have been chosen through an imperative process, which was finalized when the generated objects **best delineated the landscape features**, as confirmed by visual inspection (figure 7.3).

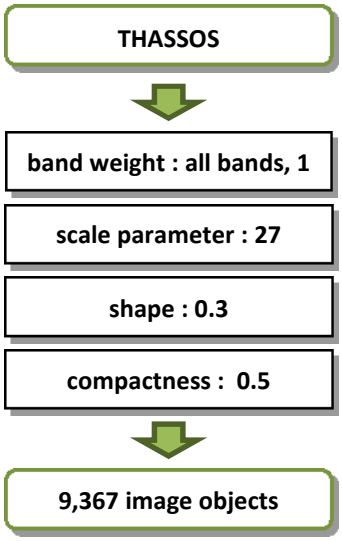

Figure 7.3 Segmentation parameters of Thassos segmentation.

Since, in this study there was no prior band selection or evaluation technique applied, all spectral bands were weighted equally.

While color is usually given full importance, in this study the shape factor was given a factor of 0.3 to acknowledge the fact that certain shape compactness applies to the concept of spatial objects.

Three secondary landcover classes were considered and described using means of spectral bands.

- bare land: meanB5 > 863
- deciduous species: meanB5 ≤ 863 AND meanB25 ≤ 864 AND meanB40 > 3,275
- non forest vegetation: mean B5 ≤ 863 AND meanB25 ≥ 863

In the case of the two *Pinus* species, feature evaluation did not make it possible to create discriminating membership functions that could accurately classify them. This is because of the

common spectral characteristics of the two species, which are not distinct in a limited, manageable by the analyst feature space. To overcome this, the feature space was increased, and NN classifier was used, on the unclassified objects, to manage this multidimensional space and provide complex class descriptions of the two *Pinus* classes.

Training objects were selected as described in section 7.1.2. The FSO was used based on these training samples, to demonstrate the most valuable features for the separation of the two classes. The features used for evaluation comprised of 141 mean band values and the respective 141 mean ration values. FSO indicated that the best separation distance (1.627) was achieved using 70 features, the majority of which were ratio features (Figure 7.3, table 7.1).

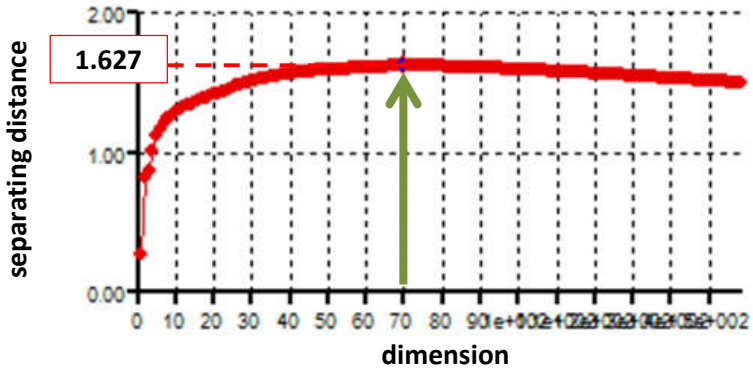

Figure 7.4 Graph showing the increase of separation distance with the increase of features used (Thassos).

Table 7.1 Features that comprise the optimal feature space for implementation of NN in Thassos.

Mean B39	Ratio B11	Ratio B15	Ratio B67	Ratio B87
Mean B47	Ratio B110	Ratio B2	Ratio B68	Ratio B88
Mean B48	Ratio B111	Ratio B27	Ratio B69	Ratio B89
Mean B57	Ratio B112	Ratio B28	Ratio B7	Ratio B9
Mean B58	Ratio B113	Ratio B29	Ratio B70	Ratio B90
Mean B60	Ratio B114	Ratio B39	Ratio B71	Ratio B91
Mean B61	Ratio B115	Ratio B47	Ratio B72	Ratio B92
Mean B62	Ratio B12	Ratio B48	Ratio B74	Ratio B93
Ratio B10	Ratio B13	Ratio B49	Ratio B75	Ratio B94
Ratio B100	Ratio B137	Ratio B5	Ratio B78	Ratio B95
Ratio B101	Ratio B138	Ratio B61	Ratio B79	Ratio B96
Ratio B102	Ratio B14	Ratio B62	Ratio B8	Ratio B97
Ratio B108	Ratio B140	Ratio B63	Ratio B80	Ratio B98
Ratio B109	Ratio B141	Ratio B66	Ratio B81	Ratio B99

Once the classification of the complete image was finished, there were obvious misclassifications; mostly overestimating *P. nigra*. These could be addressed, as GEOBIA allows for knowledge based post-classification manipulation.

The classification model was extended to further refine the classification result. Misclassified objects were identified using class related and topological features, and assigned new class labels. The rules developed were:

- *P. nigra* enclosed by *P. brutia* → *P. brutia*
- *P. nigra* with border to *P. nigra* = 0 → low vegetation
- *P. nigra* with Rel. border to brutia 1 ≥ 0.3 AND Rel. border to *P. brutia* ≤ 0.66 → *P. brutia*
- *P. brutia* with Rel. border to low vegetation = 1 → low vegetation

7.1.4 Taxiarchis classification model

As in the case of Thassos, a single level classification model was developed, because a second level was not required, in the sense that there is no land caver or function that operates in a different scale (i.e. lakes).

For the creation of this level the segmentation parameters have been chosen through an imperative process, which was finalized when the generated objects **best delineated the landscape features**, as confirmed by visual inspection.

Again, in this study there was no prior band selection or evaluation technique applied, consequently all spectral bands were weighted equally.

While color is usually given full importance, in this study the shape factor was given a factor of 0.3 to acknowledge the fact that certain shape compactness applies to the concept of spatial objects.

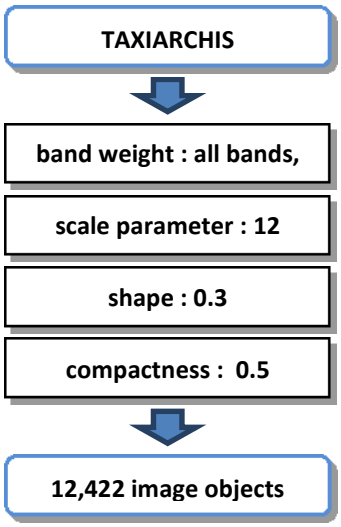

Figure 7.5 Segmentation parameters of Taxiarchis segmentation.

As demonstrated by previous investigations of this study, Taxiarchis forest classification is very challenging. Adding to that, almost all of the landcover classes are classes of forest species, which in the case of Thassos were identified with the use of NN classifier. Because of these, the NN classifier was used in this classification and no class was described using membership functions.

Training objects were selected as described in section 7.1.2. The FSO was used based on these training samples, to demonstrate the most valuable features for the separation of the two classes. The features used for evaluation comprised of 131 mean band values and the respective 131 mean ration values. FSO indicated that 209 features were necessary to achieve the maximum separating distance, which was 1.595. However, even this combination did not provide adequate mapping, so the MNF component image was considered for classification. Five MNF components selected by the FSO achieved separating distance 2.05 and thus were used for classification.

The classification model was extended to further refine the classification result. Misclassified objects were identified using class related and topological features, and assigned new class labels. The rules developed were:

- *P. brutia* with Rel. border to 3 *P. nigra* > 0.3 → *P. nigra*
- *F. sylvatica* enclosed by *Q. frainetto* → *Q. frainetto*
- *P. nigra* enclosed by *P. brutia* → *P. brutia*

- *P. brutia* with Border to *P. brutia* = 0 pixel → *Q. frainetto*

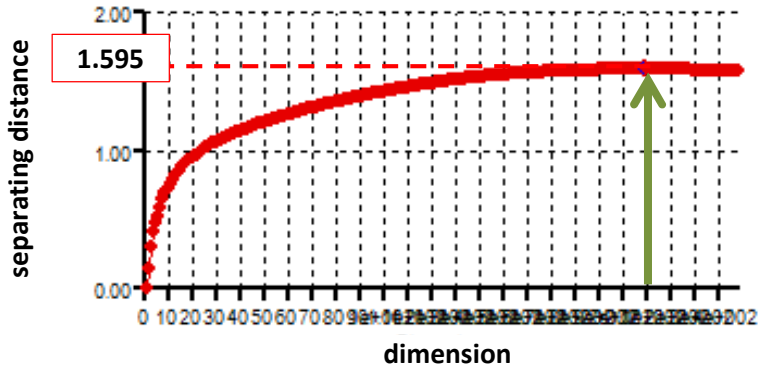

Figure 7.6 Graph showing the increase of separation distance with the increase of features used (Taxiarchis).

Table 7.2 Features that comprise the optimal feature space for implementation of NN in Taxiarchis.

Ratio B19	Ratio B75	Mean B63	Ratio B61	Mean B85	Mean B91
Mean B42	Ratio B23	Mean B77	Mean B37	Mean B82	Mean B88
Ratio B40	Mean B52	Mean B28	Mean B5	Ratio B83	Mean B94
Ratio B78	Mean B2	Mean B45	Mean B30	Ratio B118	Mean B104
Mean B20	Ratio B25	Ratio B31	Ratio B73	Ratio B7	Mean B9
Ratio B77	Ratio B66	Mean B115	Ratio B35	Mean B103	Mean B95
Ratio B20	Mean B56	Ratio B27	Mean B68	Mean B7	Ratio B80
Mean B39	Mean B3	Mean B59	Ratio B51	Ratio B105	Ratio B34
Ratio B18	Mean B24	Mean B27	Mean B29	Mean B120	Mean B79
Ratio B64	Mean B73	Ratio B58	Mean B64	Mean B93	Ratio B84
Ratio B39	Ratio B26	Mean B70	Mean B83	Ratio B43	Mean B122
Mean B44	Ratio B71	Ratio B52	Ratio B69	Mean B90	Ratio B122
Ratio B57	Ratio B56	Ratio B74	Mean B65	Mean B97	Ratio B82
Mean B19	Mean B22	Ratio B79	Ratio B37	Mean B81	Mean B121
Ratio B21	Mean B53	Ratio B53	Mean B35	Ratio B8	Mean B101
Mean B43	Mean B114	Mean B47	Ratio B17	Mean B87	Ratio B50
Mean B41	Mean B46	Mean B34	Mean B32	Ratio B60	Mean B109
Ratio B76	Ratio B4	Mean B54	Mean B105	Ratio B32	Ratio B121
Mean B55	Ratio B30	Mean B58	Ratio B116	Ratio B120	Ratio B11
Ratio B59	Mean B76	Mean B36	Ratio B72	Ratio B47	Ratio B42
Ratio B63	Max. diff.	Mean B75	Mean B118	Mean B86	Mean B11
Ratio B1	Ratio B29	Mean B74	Mean B62	Mean B100	Mean B98
Ratio B24	Mean B51	Mean B26	Ratio B85	Mean B89	Mean B113

Mean B50	Mean B18	Ratio B68	Mean B17	Mean B92	Ratio B49
Mean B40	Ratio B28	Ratio B38	Ratio B45	Mean B102	Mean B119
Ratio B22	Mean B23	Mean B67	Ratio B6	Ratio B89	Mean B99
Ratio B3	Ratio B62	Mean B60	Mean B31	Mean B123	Mean B10
Ratio B67	Ratio B55	Mean B61	Mean B80	Ratio B48	Ratio B10
Mean B57	Mean B66	Mean B48	Ratio B70	Mean B8	Ratio B117
Mean B1	Mean B38	Mean B71	Ratio B46	Ratio B44	Ratio B109
Mean B21	Mean B78	Ratio B65	Mean B116	Mean B84	Ratio B87
Ratio B2	Mean B4	Ratio B5	Mean B6	Ratio B123	Mean B108
Ratio B36	Ratio B115	Mean B33	Ratio B33	Ratio B9	Mean B112
Mean B49	Mean B25	Mean B69	Brightness	Mean B96	Ratio B81
Ratio B114	Ratio B54	Mean B72	Ratio B41	Mean B117	

7.2 RESULTS

7.2.1 Thassos

The GEOBIA classification model for the Hyperion image of Thassos as described above resulted in the map shown in Figure 7.7, excluding the area covered by clouds and their shadow. On this investigation the secondary landcover was grouped in three classes, namely ‘agricultural land’, ‘low vegetation’ and ‘bare land’, with the intention to separate them from the forest species classes, but not necessarily between them; thus, they are all mapped as “other’.

According to these maps 2,222 ha of the study area are covered by *P. brutia*, and 1,270 ha are covered by *P. nigra*.

To estimate the accuracy of the map and refer the value of the product, reference data collected during field surveys were used. Reference data which were collected and stored in vector point format were conveyed to image polygons using the routine described in section 7.1.2.

Because secondary landcover was grouped differently than the way it was recorded during field survey, there was no correspondence between the landcover classes and the field collected references. In order to report the accuracy of the resulted map they were grouped into the class ‘other’.

A confusion matrix (table 7.3) was populated by labels assigned to objects by the classification model, and labels assigned to the respective reference data; cross-tabulated, using geographic

location as key. The matrix was analyzed with four measures of agreement, namely KIA, OA, user's and producer's accuracy. The OA of the map was **85.3%**, and the KIA was **0.765**.

According to these maps 2,220 ha of the study area are covered by *P. brutia*, and 1,270 ha are covered by *P. nigra*.

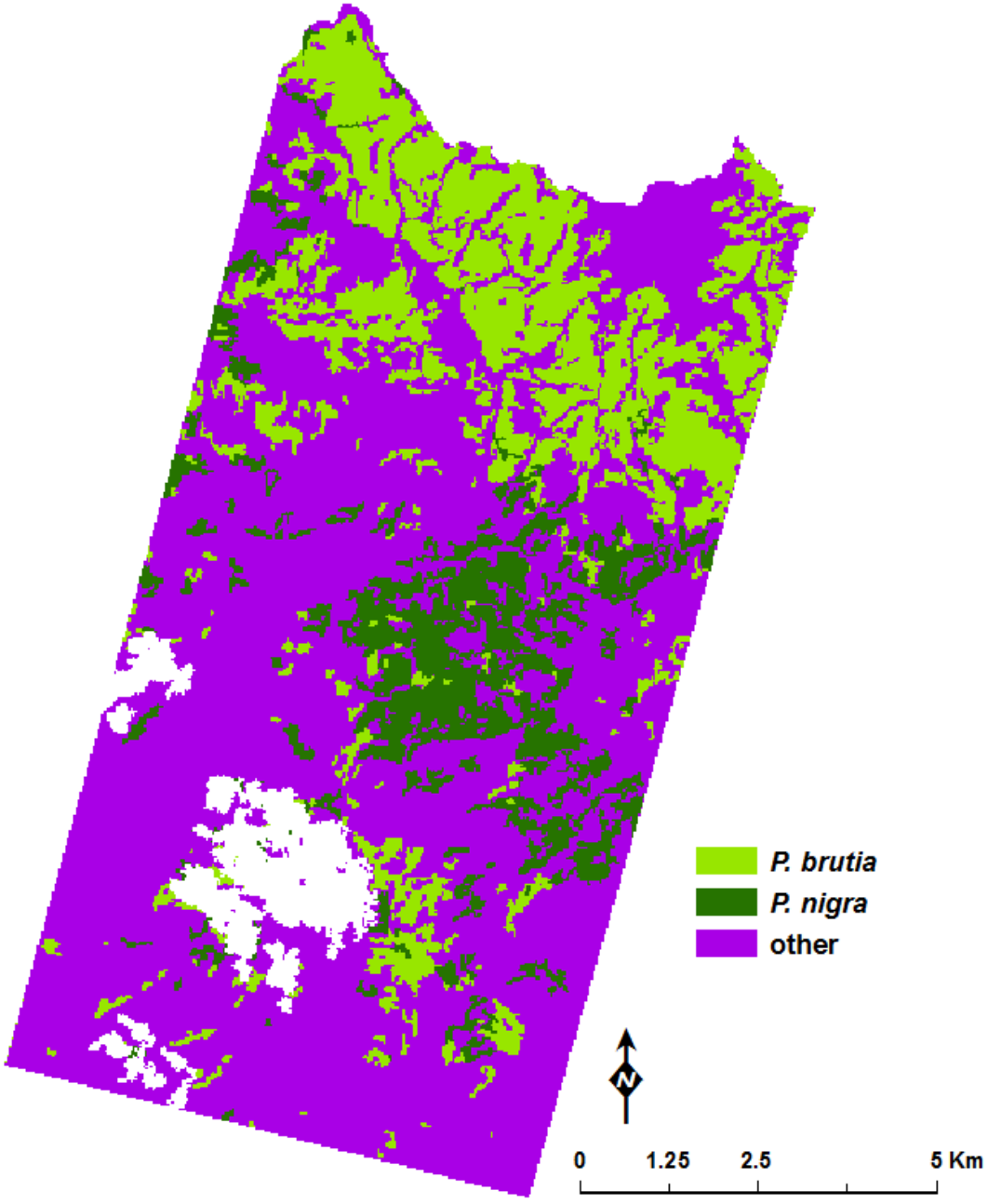

Figure 7.7 Thassos species map produced by GEOBIA (other classes grouped).

Table 7.3 Confusion matrix of the implementation of GEOBIA in Thassos.

Reference / Classification	*P. brutia*	*P. nigra*	other	producer's accuracy %	user's accuracy %
P. brutia	2164	163	204	86.4	85.5
P. nigra	100	1139	81	69.2	86.3
other	240	345	3270	92.0	84.8
TOTAL	2504	1647	3555		

7.2.2 Taxiarchis

The GEOBIA classification model for the Hyperion image of Taxiarchis as described above resulted in the map shown in Figure 7.8, excluding the area covered by clouds and their shadow. On this investigation the secondary landcover, namely 'maquis', 'agricultural land' and 'bare land', were grouped into a new class, namely 'other'. According to this map, 1,840 ha of the study area are covered *Q. frainetto*, 290 ha are covered *F. sylvatica*, 360 ha are covered by *P. nigra* and 520 ha are covered by *P. brutia*.

To estimate the accuracy of the map and refer the value of the product, reference data collected during field surveys were used. Reference data which were collected and stored in vector point format were conveyed to image polygons using the routine described in section 7.1.2.

The confusion matrix is shown in table 6.3, together with the user's and producer's accuracy of each class. The OA of the complete classification scheme map was 72.8%, and the KIA was 0.658. When the rest of the cover classes are grouped into one 'other' class, the OA of the map increased to 74.1% and KIA to 0.662.

According to this map, 1,840 ha of the study area are covered *Q. frainetto*, 290 ha are covered *F. sylvatica*, 360 ha are covered by *P. nigra* and 520 ha are covered by *P. brutia*.

Table 7.4 Confusion matrix of the implementation of GEOBIA in Taxiarchis.

Reference / Classification	*Q. frainetto*	*F. sylvatica*	*P. nigra*	*P. brutia*	maquis	bare land	producer's accuracy %	user's accuracy %
Q. frainneto	1452	97	23	0	45	17	77.3	88.9
F. sylvatica	171	265	124	0	0	25	70.5	45.3
P. nigra	0	0	524	79	82	28	71.7	73.5
P. brutia	72	0	0	621	134	0	62.6	75.1
maquis	162	14	0	292	873	72	77.0	61.8
bare land	21	0	60	0	0	339	70.5	80.7
TOTAL	1878	376	731	992	1134	481		

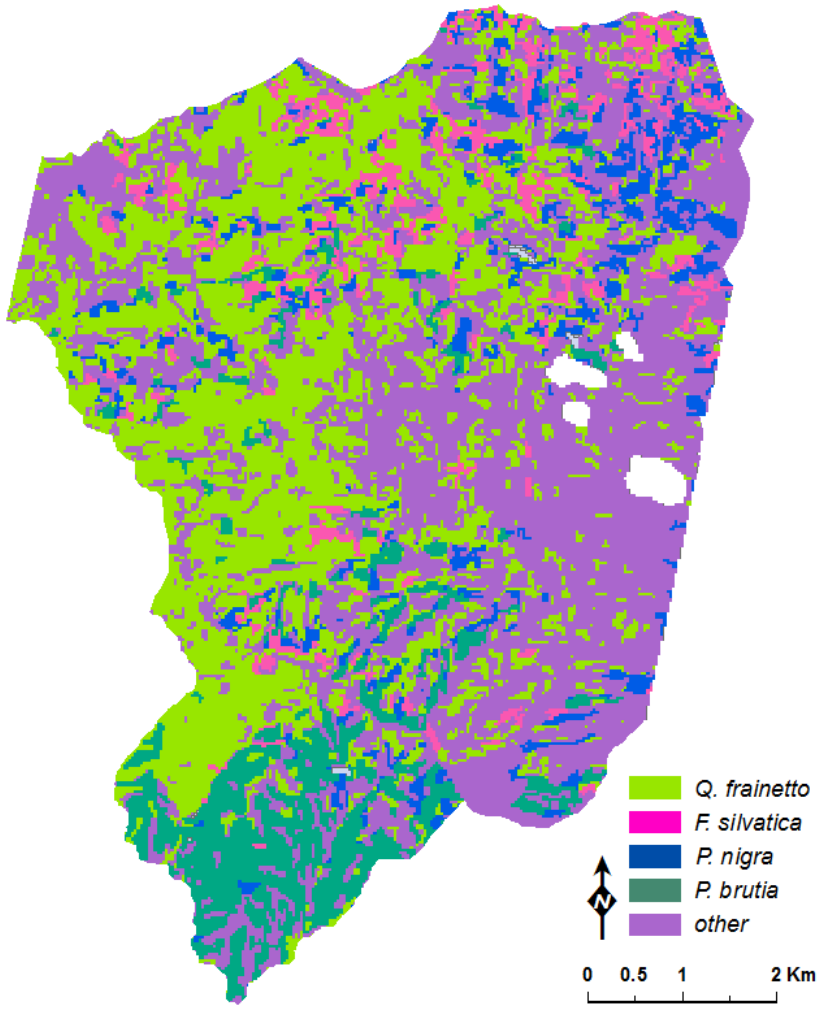

Figure 7.8 Taxiarchis species map produced by GEOBIA (other classes grouped).

7.3 DISCUSSION

Issues related to the influence of high spectral dimensionality on the different GEOBIA components remain to be investigated. Properly planned case studies can facilitate an appropriate statistical design and hypothesis testing. Such endeavor was out of the scopes of this study.

Fuzzy concepts make it possible for objects to belong to several classes but with different degrees of membership. Although, the main aim of each classification is to define classes as unambiguously as possible, these ambiguity measures were used at a later phase to provide further refinement of the classification.

7.3.1 Thassos

As with previous investigations, Thassos study area was the first to be examined because of the simpler distribution pattern of the forest species.

Because of the visual interpretation that is needed in order to guide the segmentation process and the lack of model transferability that the MNF transformation introduces (see section 7.1) the original spectral bands were used as input in this analysis.

The multiresolution segmentation algorithm was used to create one level of image objects, and segmentation parameters were chosen so that image objects best delineated the landscape features. Since in this study there was no prior band selection or evaluation technique applied, all spectral bands were weighted equally. While color is usually given full importance, in this study the shape factor was given a value of 0.3 to acknowledge the fact that certain shape compactness applies to the concept of spatial objects.

To classify the secondary landcover classes, the classification model was developed using membership functions and bands with centers in 0.477μm, 0.681 μm and 0.833 μm, in the blue, red and near infrared region of the electromagnetic spectrum respectively.

However, a feature space of higher dimensionality was necessary to separate *P. nigra* and *P. brutia*, thus the NN classifier was used. In order to increase feature space, a broad range of features was computed for each object. Among several features that were evaluated for their usefulness to discriminate between these species, band ratios showed most prominence. It was interesting that although the use of original spectral bands proved unsatisfactory in mapping the

species and preserving their spatial pattern, the use of band ratios dramatically increased the classification accuracy. A 70 dimensional feature space was indicated by FSO tool for the NN.

Once the classification of the complete image was finished, there were obvious misclassifications; mostly overestimating *P. nigra*. These could be addressed, as GEOBIA allows for knowledge based post-classification manipulation. Misclassified objects were identified using class related and topological features, and assigned new class labels.

The OA classification of the produced map was **85.3%** and the KIA was **0.765**, a level of accuracy considered operational according to literature.

A closer look of the confusion matrix reveals that the majority of misclassifications were between the forest species and the rest of the landcover, as opposed to misclassification between the two forest species, which was also the case in the previous investigations.

In particular, *P. brutia* was classified with equal user's and producer's accuracy (86%), while In the case of *P. nigra* there were more omission than commission errors leading to underestimation of this class. As indicated by the class statistics, *P. brutia* was more accurately mapped by *P. nigra* (Figure 7.9).

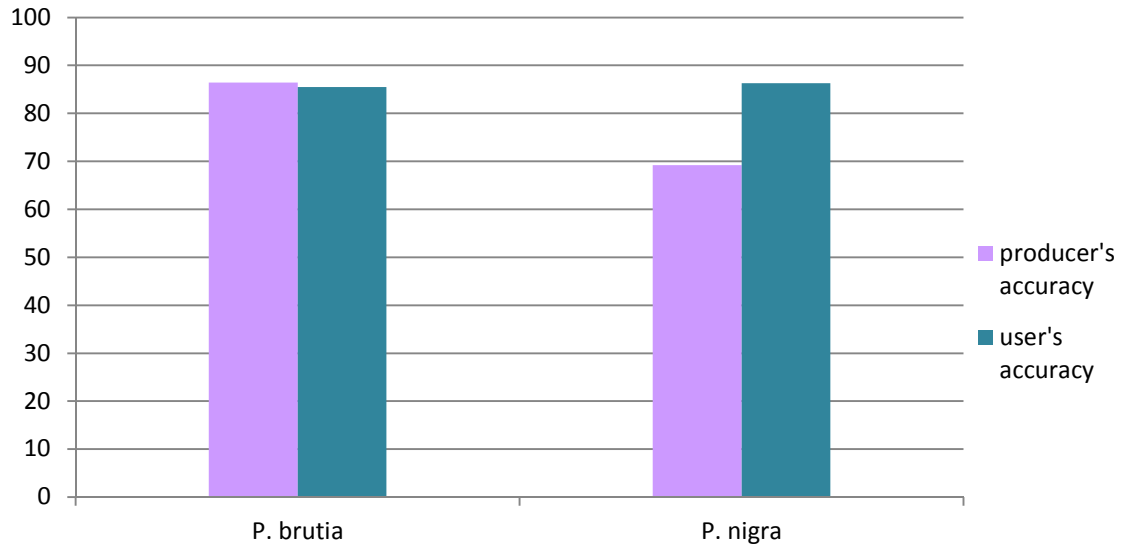

Figure 7.9 Producer's and user's accuracy of GEOBIA classification map for the two *Pinus* species of Thassos.

The lower performance of this methodology, compared to the performance of the SAM and SVM methodologies may be attributed to several issues. The main consideration is that in a difficult problem when the objects or features that need to be distinguished have very similar spectral properties, which is the case with species mapping, grouping spectral responses may be a drawback. Adding to that, it is still not clear which is the most adequate way of assessing the accuracy of a map delivered by an object based methodology, thus variation in accuracy may be the result of the accuracy assessment method. Further, especially in the case of medium spatial resolution imagery, there is the issue of mixture and how this is addressed in image objects.

On the other hand, the GIS functionalities that GEOBIA provides are a very significant advantage that adds value to the map. More specifically, when the scale of a study is regional and data management is a key issue, organizing data in vector format and allowing for topological relations is a critical factor that may lead to successful applications.

7.3.2 Taxiarchis

Mapping forest species in Taxiarchis has already been demonstrated that is a challenging task, both because of the presence of more species and because of their complex distribution pattern.

Although using the original spectral bands was initially planned, the low accuracy map provided led to the decision to incorporate the MNF component band in the analysis.

The multiresolution segmentation algorithm was used to create one level of image objects, and segmentation parameters were chosen so that image objects best delineated the landscape features. All spectral bands were weighted equally and shape factor was given a value of 0.3 to acknowledge the fact that certain shape compactness applies to the concept of spatial objects.

The NN classifier was used in a feature space of five MNF components identified by the FSO tool to classify the entire scene and no class was described using membership functions.

After the NN classification, the classification model was extended to further refine the classification result. Misclassified objects were identified using class related and topological features, and assigned new class labels.

The OA classification of the produced map was **74.1%** and the KIA was **0.662**, a level of accuracy not considered operational according to literature.

In particular, *P. brutia* and *P. nigra* were adequately mapped there with limited omission and commission errors. As indicated by the class statistics, *P. brutia* was more accurately mapped by *P. nigra*.

The lower producer's accuracy (77.3%) indicates that *Q. frainetto* class was underestimated, specifically against *F. sylvatica* class. The user's accuracy was higher (88.9%), indicating that fewer areas were erroneously assigned the *Q. frainetto* label, with maquis and *F. sylvatica* being the most common between them.

In the case of *F. sylvatica* the classification model achieved very low user's (45.3%) but higher producer's (70.5%) accuracy. The confusion was between *F. sylvatica* and *Q. frainetto*, the two deciduous species of the study area and between *F. sylvatica* and *P. nigra* that grow in the same region and share lengthy borders. As discussed in section 5.3.2, the low accuracy of classifying *F. sylvatica* can be attributed to the small extent of this class that increased the difficulty in classifier training.

P. nigra was mapped with user's and producer's accuracy 73.5% and 71.7% respectively. Although the achieved accuracy was considerably lower than what was achieved by the other methodologies, in this case it was possible to correct the misclassifications that resulted from the presence of agricultural fields of *Abies* species, as it was possible to identify them by means of relationship to neighbor objects.

P. brutia was mapped with user's and producer's accuracy 75.1% and 62.6% respectively being once more confused mainly with maquis (Figure 7.10).

As pointed out in section 7.3.1, the lower performance of this methodology may be attributed to the grouping of spectral responses. Although in theory image objects provide a significantly increased signal-to-noise ratio compared to single pixels as to the attributes to be used for classification, in the case of attributes with subtle spectral differences this may not be beneficial.

On the other hand, the GIS functionalities that GEOBIA provides are a very significant advantage that adds value to the map. Especially, when the scale of a study is regional and data management is a key issue, organizing data in vector format and allowing for topological relations is a critical factor that may lead to successful applications.

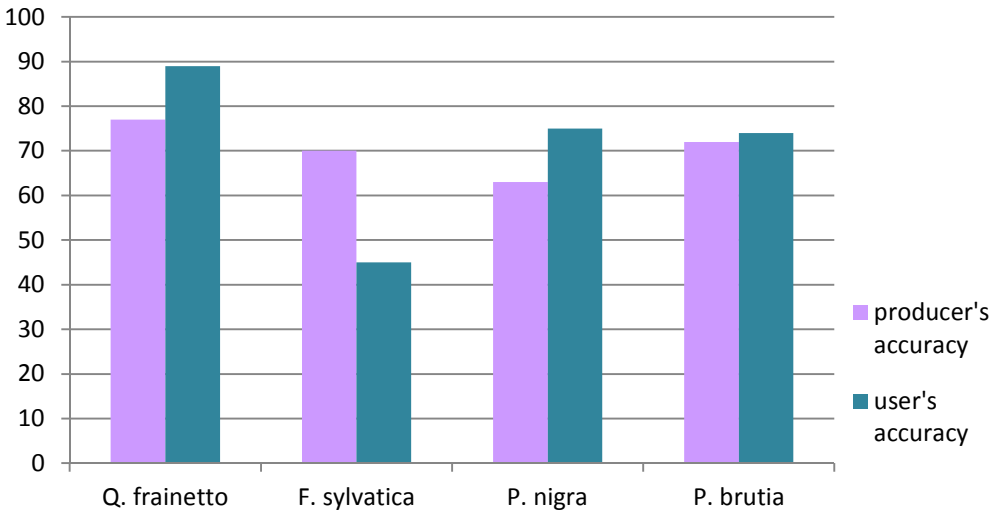

Figure 7.10 Producer's and user's accuracy of GEOBIA classification map for the species of Taxiarchis.

7.4 CHAPTER CONCLUSIONS

The key points discussed in this chapter are summarized below.

- The multiresolution segmentation algorithm (Baatz and Schape, 2000) was used in this study. The multiresolution segmentation algorithm is a bottom-up segmentation algorithm, based on a pairwise region merging technique; consecutively merges pixels or existing image objects.

- A single level classification model was developed for both study areas, because a second level was not required in the sense that there is no landcover or function that operates in a different scale. Segmentation parameters have been chosen through an imperative process, which was finalized when the generated objects **best delineated the landscape features**, as confirmed by visual inspection.

- In the case of Thassos the classification model included membership functions to map bare land, deciduous species and non forest vegetation, while the NN classifier was used to map the two *Pinus* species. The later was chosen because a feature space of higher dimensionality was necessary in order for the two species to be separated. The FSO tool was used to identify a 70 feature dimensional space, comprised by spectral and ratio features, where the separation distance was optimal. The classification model was

further extended to refine the classification result, using topological and class related features.

- The OA classification of the produced map for Thassos was **85.3%** and the KIA was **0.765**, a level of accuracy considered operational according to literature. As indicated by the class statistics, *P. brutia* was more accurately mapped than *P. nigra*.

- In the case of Taxiarchis, the NN classifier was used to map all classes (the majority of which were forest species classes), as it was already demonstrated that classification of this study area was very challenging. The MNF component image was used as the use of the original spectral image did not provide sufficient results. The classification model was further extended to refine the classification result, using topological and class related features.

- The OA classification of the produced map for Taxiarchis was **74.1%** and the KIA was **0.662**, a level of accuracy not considered operational according to literature. However, in this case it was possible to address the overestimation of *P. nigra* that resulted from the presence of agricultural fields of *Abies* species, as it was possible to identify them by means of relationship to neighbor objects.

- Issues related to the influence of high spectral dimensionality on the different GEOBIA components remain to be investigated. Properly planned case studies can facilitate an appropriate statistical design and hypothesis testing. Such endeavor was out of the scopes of this study.

8

CONCLUSIONS AND SUGGESTIONS FOR FURTHER RESEARCH

8.1 CONCLUSIONS

This study aimed to investigate the potential of employing EO1 Hyperion satellite hyperspectral imagery in Mediterranean forest species mapping, in two typical Greek forests.

It was demonstrated that accurate forest species mapping is feasible, as the proposed methodologies produced maps that described the species distribution of the study areas with accuracies, which in most cases may be considered equivalent of that found in most forest inventory systems. Attained maps could provide valuable information for regional and national planning and policy making, as well as serve as an intermediate tier in obtaining essential biomass and carbon sequestration estimates, for national reporting obligations towards national and international policies. They would also provide valuable basemaps for a broad range of applications, which could gainfully use this information, although producing it would be out of their scopes.

The conclusions of this study, in relation to each of the three specific objectives, are the following:

I. **The first objective was to investigate the performance of Spectral Angle Mapper (SAM), a traditional remote sensing classification technique used with hyperspectral data, in Mediterranean forest species mapping and, assess the accuracy of the produced maps with field survey data.**

The investigation of the SAM based methodology showed that this straightforward technique is adequate for accurate mapping of forest species, in both study areas. In the case of Thassos both species, namely P. brutia and P. nigra, were mapped with very high user's and producer's accuracy (>88%). It is noteworthy that no confusion was observed between the forest species, and all misclassifications occurred between forest and other landcover. This may be attributed

to the inevitable landcover mix in pixels, particularly prominent in imagery of the versatile Mediterranean region. In the case of Taxiarchis, species mapping was also successful, however achieving lower accuracies (overall accuracy = 80%). The complex distribution pattern of forest species was very influential, both in locating adequate training samples and in the increased proportion of mixed pixels, leading in the case of F. sylvatica in unacceptable accuracies (>50%).

II. **The second objective was to investigate the performance of Support Vector Machines (SVM), an advanced supervised learning technique, in Mediterranean forest species mapping and, assess the accuracy of the produced maps with field survey data.**

SVM is an auspicious advanced technique, recently adopted by the remote sensing community. The implementation of this technique was considerable more laborious, both in training and parameterizing context, and required tools that are not available in commercial remote sensing software. The proposed methodology resulted in maps with overall accuracies higher than 82%. Although the SVM based methodology provided no improvement over the Thassos species map produced with SAM, it increased the accuracy of the more complex Taxiarchis map. Noteworthy was the substantial increase in the classification accuracy of F. sylvatica, which was unacceptable in the case of SAM.

III. **The third objective was to investigate the potential of a geographic object based image approach (GEOBIA), which considers geographic object as a unit of analysis, in Mediterranean forest species mapping and, assess the accuracy of the produced maps with field survey data.**

GEOBIA is technically and theoretically different to pixel based image processing approach, and includes processes which transform image data from the remotely sensed physical reality to the human conceptualization of the geographic objects. This methodology achieved lower overall accuracies, 85.3% and 74.1% for Thassos and Taxiarchis respectively. This could be possibly attributed to the fact that when the geographic features under mapping have subtle spectral differences and get grouped in objects, some part of the variability is lost, impeding accurate classification. Regardless, user's and producer's accuracies of the forest species exhibited the same patterns, with F. sylvatica being gain the most problematic species for mapping. On the other hand, the GIS functionalities that GEOBIA provides are a very significant advantage that adds value to the map. More specifically, when the scale of a study is regional and data

management is a key issue, organizing data in vector format and allowing for topological relations is a critical factor that may lead to successful applications.

A key observation of this study was that preprocessing of Hyperion imagery was very laborious but also a decisive factor for the success of the proposed methodologies. Poorer preprocessing of the Taxiarchis image may be responsible for lower accuracies achieved in this study area, compared to Thassos study area of which the image was further preprocessed for the removal of spectral smile and topographic effect.

Another finding was that confusion and misclassification mostly occurred as a result of landcover mix, within the boundaries of the 30 by 30 meters pixel. This was evident in both study areas, but most prominently in the case of Taxiarchis where the complex distribution pattern creates lengthy boarders between forest species or other landcover, increasing the number of mixed misclassified pixels. This was an anticipated challenge in mapping the diverse, disturbed and fragmented Mediterranean forest.

It was also noted that detection and mapping of conifer species was superior to that of deciduous, across study areas and methodologies. *P. nigra* was mapped with higher accuracy in all cases, while *F. sylvatica* was systematically the most problematic, possibly because it was the species with the lesser extent. These findings show that species mapping is species specific, and are accordant to other aforementioned published studies.

8.2 SUGGESTIONS FOR FURTHER RESEARCH

The overall conclusion of this study is that EO1 Hyperion satellite hyperspectral imagery is valuable for Mediterranean forest species mapping, therefore further research should explore additional available techniques and data, and develop robust methodologies, in anticipation of forest species mapping being considered a mainstream remote sensing task.

In particular, if this study was to continue, it would more thoroughly address the phase of image preprocessing, examining novel proposed techniques for radiometric effect removal as well as data dimensionality reduction.

Further study would also examine the parallel use of other remote sensing data, such as high spatial resolution imagery, radar or LiDAR, to provide more spatially explicit or structural information for identifying and handling the aforementioned transitional zones. The forthcoming

satellite hyperspectral sensors (EnMAP, HERO) will also provide further opportunities. In this sense, GEOBIA provides an excellent framework for multisensor approach implementation.

To address this difficulty of deciduous species mapping, multitemporal analysis or image acquisition guided by species phenology would be considered in future investigation. The use of other classification techniques may also prove advantageous.

It has been demonstrated throughout this study that forest species mapping is significantly important, as it provides means for understanding and managing forest ecosystems. Satellite hyperspectral technology, which appears to be the only candidate to address regional forest species mapping in a viable, cost effective and repetitive manner, was found to be of great value.

9

REFERENCES

Abe, S., (2010). *Support Vector Machines for Pattern Classification*. Springer

Adler-Golden, S., Matthew, M., Bernstein, L., Levine, R., Berk, A., Richtsmeier, S., Acharya, P., Anderson, G., Felde, G., Gardner, J., Hoke, M., Jeong, L., Pukall, B., Ratkowski, A. and Burke, H. (1999). Atmospheric Correction for Shortwave Spectral Imagery Based on MODTRAN4. *In: SPIE proceedings Imaging Spectrometry*. pp. 61-69.

Aguirre-Gutiérrez, J., Seijmonsbergen, A. C., Duivenvoorden, J. F., (2012). Optimizing land cover classification accuracy for change detection, a combined pixel-based and object-based approach in a mountainous area in Mexico. *Applied Geography*, Volume 34, Pages 29-37.

Aizerman, A., Braverman, E.M., and Rozoner, L.I. , (1964). Theoretical founda-tions of the potential function method in pattern recognition learning. *Automat. Remote Contro*l, vol. 25, pp. 821–837, 1964.

Albrecht, F., Lang, S., Hölbling, D., (2010). Spatial accuracy assessment of object boundaries for object-based image analysis. *The International Archives of the Photogrammetry, Remote Sensing and Spatial Information Sciences*, Vol. XXXVIII-4/C7

Anderson, J.E., Plourde, L.C., Martin, M.E., Braswell, B.H., Smith, M.L., Dubayah, R.O., Hofton, M.O., Blair, J.B., (2008). Integrating waveform lidar with hyperspectral imagery for inventory of a northern temperate forest. *Remote Sensing of Environment*, 112(4,15), 1856-1870.

Archibold, O.W., (1995). *Ecology of World Vegetation*. Chapman and Hall, London, UK.

Arianoutsou, M., (2001). Landscape changes in Mediterranean Ecosystems of Greece: implications for Fire and Biodiversity issues. *Journal of Mediterranean Ecology*, 2, 165-178.

Arroyo, L.A., Healey, S.P., Cohen, W.B., Cocero, D., Manzanera, J.A., (2006).Using object-oriented classification and high-resolution imagery to map fuel types in a Mediterranean region. *Journal of Geophysical Research G: Biogeosciences*, 111(4), art. no. G04S04.

Asner, G. P., & Heidebrecht, K.B. (2003). Imaging spectroscopy for desertification studies: Comparing AVIRIS and EO-1 Hyperion in Argentina drylands. *IEEE Transactions on Geoscience and Remote Sensing, 41*, 1283−1296.

Asner, G.P., Martin, R.E., (2008). Spectral and chemical analysis of tropical forests: Scaling from

leaf to canopy levels, *Remote Sensing of Environment,* 112, 3958–3970.

Asner, G. P., Palace, M., Keller, M., Pereira, R., Silva, J. N. M., and Zweede, J. C., (2002). Estimating canopy structure in an Amazon Forest from laser range finder and IKONOS satellite observations. *Biotropica*, 34 (4), 483-492.

Asner, G.P., Knapp, D.E., Kennedy-Bowdoin, T., Jones, M.O., Martin, R.E., Boardman, J., Hughes, R.F., (2008). Invasive species detection in Hawaiian rainforests using airborne imaging spectroscopy and LiDAR. *Remote Sensing of Environment*, 112(5), 1942-1955.

Asner, G.P., Knapp, D., Balaji, E., Páez-Acosta, A.G., (2009). Automated mapping of tropical deforestation and forest degradation: CLASlite. *Journal of Applied Remote Sensing* 3, 1–23.

Asner, G.P., (1998). Biophysical and biochemical sources of variability in canopy reflectance. *Remote Sensing of Environment* 64,134-153.

Asner, G.P., (2008).Hyperspectral Remote Sensing of Tropical and Sub-Tropical Forests Edited by Margaret Kalacska and G. Arturo Sanchez-Azofeifa CRC Press (*Chapter 12. Hyperspectral Remote Sensing of Canopy Chemistry, Physiology, and Biodiversity in Tropical Rainforests* Gregory P. Asner)

Aspinall, R.J., (2002, November). Use of logistic regression for validation of maps of the spatial distribution of vegetation species derived from high spatial resolution hyperspectral remotely sensed data, *Ecological Modelling*, 157(2–3), 301-312.

Athanasiadis, N.H., (1986). *Forest botany*. *Trees and bushes of the forests in Greece*, Giahoudi Giapouli, 1st Edn. Thessaloniki, Greece, 309 p. In Greek.

Atkinson, P.M., (2004). Resolution manipulation and sub-pixel mapping. In: de Jong, S.M., van der Meer, F.D. (Eds.), Remote Sensing and Digital Image Analysis. Including the Spatial Domain. Book Series: Remote Sensing and Digital Image Processing, vol. 5Kluwer Academic Publishers, Dordrecht, pp. 51–70(Chapter 4).

Baatz, M., & Schape, A., (1999). *Object-Oriented and Multi-Scale Image Analysis in Semantic Networks*. In*: 2nd International Symposium on Operationalization of Remote Sensing*, 15-20.

Baatz, M. and Chape, A., (2000). Multiresolution Segmentation: an optimization approach for high quality multi-scale image segmentation. (J. Strobl, T. Blaschke, & G. Greisebener, Eds.)*Journal of Photogrammetry and Remote Sensing*, 58(3-4), 12-23. Herbert Wichmann Verlag.

Baker, P.J., & Robinson, A., (2010). *Review and comparison of tree- and stand-based forest growth models for potential integration into EnSym* https://ensym.dse.vic.gov.au/docs/EnSymForestModellingReport_2.pdf

Ball, D.W., (1995). Defining Terms, Spectroscopy, 10, 16-18.

Barbero, M., Loisel, R., Quezel, P., Richardson, D., Romane, F., (1998). *Pines of the Mediterranean Basin*. In: Richardson, D.M. (Ed.), *Ecology and Biogeography of Pinus*. Cambridge University Press, Cambridge, pp. 153–170.

Beck, P.S.A., Atzberger, C., Høgda, K.A., Johansen, B., Skidmore, A.K., (2006). Improved monitoring of vegetation dynamics at very high latitudes: A new method using MODIS NDVI. *Remote Sensing of Environment*, 100(3), *pp. 321-334.*

Bell, I.E., and Baranoski, G.V.G., (2004), Reducing the dimensionality of plant spectral database. IEEE Trans. *Geoscience and Remote Sensing*, 42(3), pp 570-576.

Belousov, A. I., Verzakov, S. A., &von Frese, J. (2002). A flexible classification approach with optimal generalisation performance: Support vector machines.Chemometrics and Intelligent Laboratory Systems, 64, 15−25.

Benz, U.C., Hofmann, P., Willhauck, G., Lingenfelder, I., Heynen, M., (2004). Multi-resolution, object oriented fuzzy analysis of remote sensing data for GIS-ready information. *ISPRS Journal of Photogrammetry and Remote Sensing 58* (3-4), 239-258

Berberoglu, S., Akin, A., (2009). Assessing different remote sensing techniques to detect land use/cover changes in the eastern Mediterranean. *International Journal of Applied Earth Observation and Geoinformation*, 11(1), 46-53.

Bergeron, M., Hollinger, A., Staenz, K., Maszkiewicz, M., Neville, R.A., Qian, S., Goodenough, D.G., (2008). Hyperspectral Environment and Resource Observer (HERO) mission. *Canadian Journal of Remote Sensing*, 34(S1): S1-S11, 10.5589/m07-071

Bergmeier E., & Dimopoulos P., (2008): *Identifying plant communities of thermophilous deciduous forest in Greece: Species composition, distribution, ecology and syntaxonomy, Plant Biosystems - An International Journal Dealing with all Aspects of Plant Biology.* Official Journal of the Societa Botanica Italiana, 142:2, 228-254

Bergmeier E., (1990). Walder und Gebusche des Niederen Olymp (Kato Olimbos, NO-Thessalien). Ein Beitrag zur systematischen und orographischen Vegetationsgliederung Griechenlands. *Phytocoenologia* 18:161–342.

Berk, A., Adler-Golden, S.M., (2002). Exploiting MODTRAN radiation transport for atmospheric correction: the FLAASH algorithm. In: *Fifth International Conference on Information Fusion, Annapolis*. pp. 798–803.

Berk, A., Bernstein, L. S., Anderson, G. P., Acharya, P. K., Robertson, D. C., (1998). MODTRAN cloud and multiple scattering upgrades wit application to AVIRIS. *Remote Sensing of Environment, 65*, 367−375.

Biging, G.S., Congalton, R.G. and Murphy, E.C., (1991). *A comparison of photointerpre-tation and ground measurements of forest structure*. InProceedings of the 57th Annual Meeting of American Society for Photogrammetry and Remote Sensing, Baltimore, MD, pp. 6–15

(Bethesda, MD: American Society for Photogrammetry and Remote Sensing).

Blackburn, G.A., Ferwerda, J.G., (2008). Retrieval of chlorophyll concentration from leaf reflectance spectra using wavelet analysis. *Remote Sensing of Environment*, 112 (4), 1614-1632.

Blackburn, G.A., (1999). Relationships between spectral reflectance and pigment concentrations in stacks of deciduous broadleaves. *Remote Sensing of Environment*, 70(2), 224–237.

Blaschke, T. and G. J. Hay, (2001). Object-oriented image analysis and scale-space: Theory and methods for modeling and evaluating multi-scale landscape structure. *Proceedings of the International Archives of Photogrammetry and Remote Sensing*, vol. 34, part 4/W5, 22-29. Challenges in Geospatial Analysis, Integration and Visualization. October 29 - 31, University of Georgia. Athens, Georgia.

Blaschke, T., Strobl, J., (2001). What's wrong with pixels? Some recent developments interfacing remote sensing and GIS. GIS - Zeitschrift für Geoinformationssys-teme 14 (6), 12-17

Blaschke, T., (2010). Object based image analysis for remote sensing. *ISPRS Journal of Photogrammetry and Remote Sensing, 65* (1), 2 16

Blondel J., Aronson J., (1999). *Biology and wildlife of the Mediterranean region*. Oxford University Press, Oxford, UK

Boardman, J. W., & Kruse, F. A. (1994). Automated spectral analysis: A geologic example using AVIRIS data, north Grapevine Mountains, Nevada. *Proceedings, tenth thematic conference on geologic remote sensing* (pp. I − 407-I-418). Ann Arbor, MI.: Environmental Research Institute of Michigan.

Boardman, J.W., 1998. Leveraging the high dimensionality of AVIRIS data f or improved sub-pixel target unmixing and rejection of false positives: Mixture Tuned Matched Filtering. *AVIRIS 1998 Proceedings*, JPL, California, p. 6.

Boardman, B. (2005). Renewable Iceland. *Geography review* (4): 40-41.

Boggs, G.S. Assessment of SPOT 5 and QuickBird remotely sensed imagery for mapping tree cover in savannas (2010). *International Journal of Applied Earth Observation and Geoinformation*, 12 (4), pp. 217-224

Bernhard E. Boser, Isabelle M. Guyon, Vladimir N. Vapnik, (1992). A Training Algorithm for Optimal Margin Classifiers. *Proceedings of the 5th Annual ACM Workshop on Computational Learning Theory*, p144-152

Boudreau, J., Nelson, R.F., Margolis, H.A., Beaudoin, A., Guindon, L., Kimes, D.S., (2008). Regional aboveground forest biomass using airborne and spaceborne LiDAR in Québec. *Remote Sensing of Environment*, 112 (10), 3876-3890.

Boydak, M., (2004). Silvicultural characteristics and natural regeneration of Pinus brutia Ten. *A review Plant Ecology*, 171 (1-2), 153-163.

Braun-Blanquet, J. (1952). The groupements végétaux de la France Méditerranéenne. - CNRS, Paris

Broge, N.H., Leblanc, E., (2001). Comparing prediction power and stability of broadband and hyperspectral vegetation indices for estimation of green leaf area index and canopy chlorophyll density. *Remote Sensing of Environment*, 76 (2), 156-172.

Brown de Colstoun, E. C., Story, M. H., Thompson, C., Commisso, K., Smith, T. G., & Irons, J. R. (2003). National Park vegetation mapping using multitemporal Landsat 7 data and a decision tree classifier. *Remote Sensing of Environment, 85*, 316−327.

Brown, M., Lewis, H. G., & Gunn, S. R. (2000). Linear spectral mixture models and support vector machines for remote sensing. *IEEE Transactions on Geoscience and Remote Sensing*, 38, 2346−2360.

Bruzzone, L., Carlin, L., (2006). A multilevel context-based system for classifiaction of very high spatial resolution images. *IEEE Transactions on Geoscience and Remote Sensing 44*, 2587–2600.

Bruzzone, L., Chi, M., Marconcini, M., (2006). A Novel Transductive SVM for the Semisupervised Classification of Remote-Sensing Images. *IEEE Transactions on Geoscience and Remote Sensing, Vol. 44*, No. 11, pp. 3363-3373.

Buddenbaum, H., Schlerf, M., Hill, J., (2005). Classification of coniferous tree species and age classes using hyperspectral data and geostatistical methods. *International Journal of Remote Sensing,* 26, 5453–5465.

Bunting, P., Lucas, R.(2006). The delineation of tree crowns in Australian mixed species forests using hyperspectral Compact Airborne Spectrographic Imager (CASI) data, *Remote Sensing of Environment*, Volume 101, Issue 2Pages 230-248.

Burges, C.J.C., 1998. A tutorial on Support Vector Machines for pattern recognition. *Data Mining and Knowledge Discovery 2*, 121–167.

Campbell, P., Entcheva, K., Rock, B.N., Martin, M.E., Neefus, C.D., Irons, J.R., Middleton, E.M., Albrechtova, J., (2004). 'Detection of initial damage in Norway spruce canopies using hyperspectral airborne data', *International Journal of Remote Sensing*, 25: 24, 5557-5584

Campbell, J. B. (1996). *Introduction to remote sensing* (2nd ed.). London: Taylor and Francis.

Camps-Valls, G., Bruzzone, L., (2005). Kernel-based methods for hyperspectral image classification. IEEE Transactions on Geoscience and Remote Sensing 43, 1351–1362.

Caravello, G.U., Giacomin, F., (1993). Landscape ecology aspects in a territory centuriated in

Roman times. *Landscape and Urban Planning,* 24, 77-85.

Carleer, A. and Wolff, E., (2004). Exploition of very high resolution satellite data for tree species identification. *Photogrammetric Engineering and Remote Sensing, 70(1*), 135-140.

Carlson, K.M., Asner, G.P., Hughes. R., Ostertag R., Martin R.E., (2007). Hyperspectral remote sensing of canopy biodiversity in Hawaiian lowland rainforests, NY, *Print. Ecosystems,* 10,536–549.

Chang, C.C., and Lin, C.J., (2010). LIBSVM: a library for support vector machines. *ACM Transactions on Intelligent Systems and Technology*, 2:27:1--27:27.

Chavez Jr., P.S., (1988). An improved dark-object subtraction technique for atmospheric scattering correction of multispectral data. *Remote Sensing of Environment*, 24 (3), pp. 459-479

Chelle, M., Andrieu, B., and Bouatouch, K., (1998). Nested radiosity for plant canopies. **Vis. Comput., 14**(3). pp 109-125

Chen, X. and Vierling, L, (2006). Spectral mixture analyses of hyperspectral data acquired using a tethered balloon. *Remote Sensing of Environment*, Volume 103, Issue 3, Pages 338-350,

Chen C-M. (2000). Comparisonof Principal Components Analysis and Minimum Noise Fraction Transformation for reducing the dimensionality of Hyperspectral imagery. *Geographical Research,* 33, 163- 178.

Chmiel, J., Fijałkowska, A., (2010). Thematic accuracy assessment for object based classification in agricultural areas: comparative analysis of selected approaches. In (Eds) E.A. Addink and F.M.B. Van Coillie. The International Archives of the Photogrammetry, Remote Sensing and Spatial Information Sciences, Vol. XXXVIII-4/C7.

Cho, M.A., Debba, P., Mathieu, R., Naidoo, L., Van Aardt, J., Asner, G.P., (2010). Improving discrimination of savanna tree species through a multiple-endmember spectral angle mapper approach: Canopy-level analysis. *IEEE Transactions on Geoscience and Remote Sensing*, 48(11), 4133-4142.

Chuvieco, E., Opazo, S., Sione, W., Del Valle, H., Anaya, J., Di Bella, C., Cruz, I., Manzo, L., López, G., Mari, N., González-Alonso, F., Morelli, F., mSetzer, A., Csiszar, I., Kanpandegi, J.A., Bastarrika, A., Libonati, R., (2008). Global burned-land estimation in Latin America using MODIS composite data. *Ecological Applications*, 18 (1), pp. 64-79.

Cingolani, A.M., Renison, D., Zak, M.R. and Cabido, M.R., (2004). Mapping vegetation in a heterogeneous mountain rangeland using Landsat data: an alternative method to define and classify land-cover units*. Remote Sensing of Environment*, 92, pp. 84–97.

Clark, M.L., Roberts, D.A., Clark, D.B., (2005). Hyperspectral discrimination of tropical rain forest tree species at leaf to crown scales. *Remote Sensing of Environment,* 96, 375–398.

Cochrane, M.A., (2000).Using vegetation reflectance variability for species level classification of hyperspectral data. *International Journal of Remote Sensing*, 21(10), 2075-208

Cohen, J. (1960). A coefficient of agreement with provision for scaled disagreement or partial credit. *Phychological Bulletin*, 70, 213-220.

Coleman T.L., Gudapati L., Derrington J., (1990), Monitoring Forest Plantations Using Landsat Thematic Mapper Data. *Remote Sensing of Environment,* 33, 211-221.

Congalton, R.G., Green, K., (1999). *Assessing the accuracy of remotely sensed data: principles and practices. Boca Raton*, FL: Lewis Publishers. 137 p.

Congalton, R.G., (1991). A review of assessing the accuracy of classifications of remotely sensed data. *Remote Sensing of Environment*, 37, 35−46.

Cooley, T., Anderson, G.P., Felde, G.W., Hoke, M.L., Ratkowski, A.J., Chetwynd, J.H., Gardner, J.A., Adler-Golden, S.M., Matthew, M.W., Berk, A., Bernstein, L.S., Acharya, P.K., Miller, D., Lewis, P., (2002). FLAASH, a MODTRAN4-based atmospheric correction algorithm, its applications and validation. *International Geoscience and Remote Sensing Symposium* (IGARSS), 3, pp. 1414-1418.

Corona, P., Mariano, A., (1992). Naturalistic afforestation for the improvement of a peri-urban area under Mediterranean conditions. In: Teller, A. (Ed.), *Responses of Forest Ecosystems to Environmental Changes*. Elsevier Applied Science, Barking, 981-982

Cortes, C. and Vapnik, V., (1995). *Support-vector network*. Machine Learning, 20:273, 297.

Cowling, R.M., Rundel P.W., Lamont, B.B., Arroyo, M.K., Arianoutsou, M., (1996). Plant diversity in mediterranean-climate regions. *Trends in Ecology and Evolution*, 11,362-366.

Dadon, A., Karnieli, A., Ben-Dor, E., (2010). Detecting and correcting the curvature effect (smile) in Hyperion images by use of MNF. Proc. *Hyperspectral 2010 Workshop*, Frascati, Italy.

Dafis, S., Kakouros P., (2006). Guidelines for rehabilitation of degraded oak forests. *Greek Biotope/Wetland Centre*. Thermi. 40p

Dafis, S., (1976). Classification of forest vegetation of Greece. *Ministry of Agriculture. General Directorate of Forests*. Publication No. 36.

Dafis, S., (1982). The present state of the forests in our country. *Scientific Bulletin Geotechnica*, 18–22

Dafis, Sp., (1997). The Mediterranean Forest and its protection. *Sci. Ann. Dept. For. Natural Environ*, 37, 159-170.

Dalponte, M., Bruzzone, L., Gianelle, D., (2008). Fusion of hyperspectral and LIDAR remote sensing data for classification of complex forest areas. *IEEE Transactions on Geoscience and*

Remote Sensing, 46 (5), 1416-1427.

Dalponte, M., Bruzzone, L., Vescovo, L., Gianelle, D., (2009). The role of spectral resolution and classifier complexity in the analysis of hyperspectral images of forest areas. *Remote Sensing of Environment*, 113(11), 2345-2355,

Dalponte, M., Ørka, H.O., Gobakken, T., Gianelle, D., Næsset, E., (2012). Tree Species Classification in Boreal Forests With Hyperspectral Data. *IEEE Transactions on Geoscience and Remote Sensing*, Article in Press.

Darvishzadeh, R., Skidmore, A., Schlerf, M., Atzberger, C., (2008). Inversion of a radiative transfer model for estimating vegetation LAI and chlorophyll in heterogeneous grassland. *Remote Sensing of Environment*, 112(5), 2592-2604.

Datt, B., McVicar, T. R., Van Niel, T. G., Jupp, D. L. B., Pearlman, J. S. (2003). Preprocessing EO-1 hyperion hyperspectral data to support the application of agricultural indexes. *IEEE Transactions on Geoscience and Remote Sensing*, 41(6 PART I), 1246-1259.

Davis, F.W., Brown, R.W., Buyan, B. and Kealy, J., (1995). *Vegetation change in blue oak and blue oak/foothill pine woodland*. Contract Report of Forest and Rangeland Resources Assessment Program, California Department of Forestry and Fire Protection, Sacramento, California.

de Dios, V.R., Fischer, C.,Colinas, C.., (2007). Climate change effects on Mediterranean forests and preventive measures, *New Forests*, 33, 29–40

di Castri, F., (1981). Mediterranean type shrublands of the world. In di Castri, F., Goodall, D.W., Specht, R.C. (Eds.). *Mediterranean Type Shrublands, series: Ecosystems of the World*, Vol. 11. Elsevier Scientific Publishing Company, Amsterdam–Oxford–New York, pp. 1–52.

Dong, P., & Liu, J. (2011). Hyperspectral image classification using support vector machines with an efficient principal component analysis scheme. Wang, Y., and Li, T., (Eds.): *Foundations of Intelligent Systems, AISC* 122, and pp. 131–140. Springer-Verlag, Berlin Heidelberg.

Dong, J., Kaufmann, R.K., Myneni, R.B., Tucker, C.J., Kauppi, P.E., Liski, J., Buermann, W., Alexeyev, V., Hughes, M.K., (2003). Remote sensing estimates of boreal and temperate forest woody biomass: Carbon pools, sources, and sinks. *Remote Sensing of Environment*, 84(3), 393-410.

Dragan, M., Sahsuvaroglu, T., Gitas, I., Feoli, E., (2005). Application and validation of a desertification risk index using data for Lebanon. *Management of Environmental Quality*, 16(4), 309-326.

Dragozi E., Tompoulidou M., Gitas I.G., (2012). *Forest mapping and forest cover change detection in a Mediterranean area, using coarse resolution data and advanced image analysis techniques*. 32nd EARSeL Symposium and 36th General Assembly, Mykonos

Duveiller, G., Defourny, P., Desclée, B., Mayaux, P., (2008). Deforestation in Central Africa: Estimates at regional, national and landscape levels by advanced processing of systematically-distributed Landsat extracts. *Remote Sensing of Environment,* 112 (5), 1969-1981.

Eckert, S., Kneubühler, M., (2004). Application of Hyperion Data to Agricultural Land Classification and Vegetation Properties Estimation in Switzerland. *Proc. XXth Congress ISPRS*, July 12-23, 2004, Istanbul, pp: 866-872.

Emberger, L. 1955. Une classification biogéographique des climats. *Rec. Trav. Lab. Bot. Geol.* Montpellier 7: 3-43.

Falkowski, M.J., Evans, J.S., Martinuzzi, S., Gessler, P.E., Hudak, A.T., (2009). Characterizing forest succession with lidar data: An evaluation for the Inland Northwest, USA. Remote Sensing of Environment, 113 (5), pp. 946-956.

Feret, J.-B., Asner, G.P. (2013). Tree species discrimination in tropical forests using airborne imaging spectroscopy. *IEEE Transactions on Geoscience and Remote Sensing*, 51 (1), art. No. 6241414, pp. 73-84.

Finley, C. D., & Glenn, N. F. (2010). Fire and vegetation type effects on soil hydrophobicity and infiltration in the sagebrush-steppe: II. Hyperspectral analysis. *Journal of Arid Environments, 74*(6), 660-666.

Fitzpatrick-Lins, K., (1981). Comparison of sampling procedures and data analysis for a land-use and land-cover map. *Photogrammetric Engineering and Remote Sensing. 47(3*): 343-351.

Foody, G.M., Hill, R. A., (1996). Classification of tropical forest classes from Landsat TM data. *International Journal of Remote Sensing,* 17, 2353-2368.

Foody, G.M. and Mathur A. (2004). Toward intelligent training of supervised image classifications: Directing training data acquisition for SVM classification. *Remote Sens. Environ., 93*: 107-117.

Foody, G.M., Mathur, A., Sanchez-Hernandez, C. and Boyd, D.S., (2006). Training set size requirements for the classification of a specific class. *Remote Sensing of Environment*, 104 (1), 1-14.

Foody, G.M., (2002). Status of land cover classification accuracy assessment. *Remote Sensing of Environment,* 81, 185–201.

Foody, G.M., (2004). Supervised image classification by MLP and RBF neural networks with and without an exhaustively defined set of classes. *International Journal of Remote Sensing 25*, 3091–3104.

Formaggio, A. R., Vieira, M. A., Rennó, C. D., Aguiar, D. A., Mello, M. P., (2010). Object based image analysis and data mining for mapping sugarcane with Landsat imagery in Brazil. The

International Archives of the Photogrammetry. *Remote Sensing and Spatial Information Sciences,* Vol. XXXVIII-4/C7

Frankenberg, C., Meirink, J.F., Van Weele, M., Platt, U., Wagner, T., (2005). Assessing methane emissions from global space-borne observations. *Science*, 308 (5724), 1010-1014.

Franklin, S.E., (1994). Discrimination of subalpine forest species and canopy density using digital CASI, SPOT PLA and Landsat TM data. *Photogrammetric Engineering & Remote Sensing*, 60, 1233–1241

Franklin, S.E., (2001). *Remote Sensing for Sustainable Forest Management*. CRC Press

Fyllas, N.M., Dimitrakopoulos, P.G., Troumbis, A.Y., (2008). Regeneration dynamics of a mixed Mediterranean pine forest in the absence of fire. *Forest Ecology and Management*, 256(8), 1552-1559.

Galvão, L.S., Formaggio, A.R., Tisot, D.A., (2005). Discrimination of sugarcane varieties in Southeastern Brazil with EO-1 Hyperion data. *Remote Sensing of Environment, Volume 94*, Issue 4, 28 Pages 523-534,

Gao, Y. and J.F. Mas, (2008). A comparison of the performance of pixel-based and object-based classifications over images with various spatial resolutions. In (Eds) E.A. Addink and F.M.B. Van Coillie. *The International Archives of the Photogrammetry, Remote Sensing and Spatial Information Sciences*, Vol. XXXVIII-4/C7.

Gao, B.C., Heidebrecht, K.B. and Goetz, A.F.H., (1993). Derivation of Scaled Surface Reflectances from AVIRIS Data, *Remote Sensing of Environment*, vol. 44, 165–178.

Gausman, H. W. (1985).*Plant leaf optical properties in visible and near-infrared light*. Lubbock, Texas' Texas Tech Press.

Gaussen H., (1993). Heywood V.H. and Chater A.O. Pinus L. Tutin et al. (eds), Flora Europeaeae, Second Edition, Cambridge University Press, 1: 40-44.

Gehler, V., and Schölkpf, (2009). An introduction to kernel learning algorithms. In Camps-Valls, G. and Bruzzone, L. (Eds.), *Kernel Methods for Remote Sensing Data Analysis*. UK

Georghiou K., Delipetrou P., (2000). *Electronic Database 'Chloris' on the Endemic. Sub-endemic. Rare. Threatened and Protected plants of Greece: Taxonomy, Distribution, Conservation status, Protection status, Biology, Ecology and iterature*. University of Athens

Ghanbari, F., Shataee, S., (2008). *Capability investigation of ASTER imagery for mixed hardwood forest types classification*. *29th Asian Conference on Remote Sensing 2008, ACRS 2008, 3,* 1710-1715.

Gibbs, H.K., Brown, S., Niles, J.O., Foley, J.A., (2007). Monitoring and estimating tropical forest carbon stocks: Making REDD a reality. *Environmental Research Letters*, 2 (4), art. no.

045023, .

Gitas I.Z. and Devereux B.J. (2006). The role of topographic correction in mapping recently burned Mediterranean forest areas from LANDSAT TM images. *International Journal of Remote Sensing*. Vol.27, No.1, 41-54.

Gitas, I., Radoglou, K., Devereux, B. & Spanos, I. (2000). *Comparative study of post-fire ecosystem recovery by using field plots and geographical information sysytems.* Ed. V. Tsihrintzis. Proceedings of the International Conference on the Protection and Restoration of the Environment, V: pp: 651-658. University of Thrace.

Gitas, I.Z., Mitri, G.H., Ventura, G., (2004). Object-based image classification for burned area mapping of Creus Cape, Spain, using NOAA-AVHRR imagery. *Remote Sensing of Environment*, 92 (3), 409-413.

Gitas, I.Z., (1999). Geographical Information Systems and Remote Sensing in mapping and monitoring fire-altered forest landscapes. Ph.D. Dissertation Department of Geography, University of Cambridge.

Goetz, A. F. H., Ferri, M., Kindel, B., & Qu, Z. (2002). Atmospheric correction of Hyperion data and techniques for dynamic scene correc-tion. In 2002 *IEEE International Geoscience and Remote Sensing Symposium and the 24th Canadian Symposium on Remote Sensing*, Toronto, Canada, June 24–28, 2002

Goetz, S.J., Baccini, A., Laporte, N.T., Johns, T., Walker, W., Kellndorfer, J., Houghton, R.A., Sun, M. (2009). Mapping and monitoring carbon stocks with satellite observations: A comparison of methods. *Carbon Balance and Management*, 4, art. no. 2, .

Gong, P. and Yu, B., (2001). 'Conifer species recognition: effects of data transformation'. *International Journal of Remote Sensing*, 22(17), 3471 — 3481.

Gong, P., Pu, R., Yu, B., (1997). Conifer species recognition: An exploratory analysis of in situ hyperspectral data, *Remote Sensing of Environment*, 62(2), 189-200.

Gong, P., Pu, R., Biging, G.S., Larrieu, M.R. (2003). Estimation of forest leaf area index using vegetation indices derived from Hyperion hyperspectral data. *IEEE Transactions on Geoscience and Remote Sensing*, 41 (6 PART I), 1355-1362.

Goodenough, D.G., Bhogall, A.S., Chen, H., Dyk A., (2001). *Comparison of methods for estimation of Kyoto Protocol products of forests from multitemporal LANDSAT*. Proc. of the intern. geosc. and rem. sens. symp., IGARSS '01, 2, University of California, Santa Barbara, 764–767

Goodenough, D.G., Bhogal, A.S., Dyk, A., Hollinger, A., Mah, Z., Niemaann, K.O., Pearlman, J., Chen, H., Tan, T., Love, J. and McdonaldD, S., (2002). Monitoring forest with Hyperion and ALI. *IEEE International Geoscience and Remote Sensing Symposium and the 24th Canadian Symposium on Remote Sensing*, Toronto, Canada, 24–28 June 2002 (Piscataway, NJ: IEEE), II,

pp. 882–885.

Goodenough, D. G., Dyk, A., Niemann, K. O., Pearlman, J. S., Chen, H., Han, T., (2003). Processing hyperion and ALI for forest classification. *IEEE Transactions on Geoscience and Remote Sensing*, 41(6 PART I), 1321-1331.

Goodenough , D.G., J ay , P.S., Hao , C., Duk , A., Tian , H., Jingyang , L., J ohn , M. and N Iemann , K.O., (2004). Forest information from hyperspectral sensing*. IEEE International Geoscience and Remote Sensing Symposium, 4*, pp. 2585–2589.

Goodenough, D. G., Chen, H., Han, D. T., & Li, J. Y. (2005). Multisensor Data fusion for aboveground carbon estimation. Proceedings of XXVIIIth *General Assembly of the International Union of Radio Science (URSI*), October, 23–29, 2005, New Delhi, India (pp. 1–4).

Goodenough, D.G., Li, J.Y., Asner, G.P., Schaepman, M.E., Ustin, S.L., Dyk, A., (2006). Combining hyperspectral remote sensing and physical modeling for applications in land ecosystems. *International Geoscience and Remote Sensing Symposium*, art. no. 4241665, 2000-2004.

Govender, M., Dye, P.J., Weiersbye, I.M., Witkowski, E.T.F., Ahmed, F., (2009). Review of commonly used remote sensing and ground-based technologies to measure plant water stress. *Water SA*, 35 (5), 741-752.

Grant, L., (1987). Diffuse and specular characteristics of leaf reflectance. *Remote Sensing of Environment*, 22, 309–322

Green, A.A., Berman, M., Switzer, P. and Craig, M.D., (1988). A transformation for ordering multispectral data in terms of image quality with implications for noise removal. *IEEE Transactions on Geoscience and Remote Sensing, 26*, pp. 65–74.

Gualtieri, J. A., & Cromp, R. F. (1998). Support vector machines for hyperspectral remote sensing classification. *Proceedings of SPIE*, 3584, 221–232

Guo, G., Li, S.Z., Chan, K.L., (2001). Support vector machines for face recognition. *Image and Vision Computing, 19* (9-10), pp. 631-638.

Guo, G., Fu, Y., Dyer, C.R., Huang, T.S., (2008). Image-based human age estimation by manifold learning and locally adjusted robust regression. *IEEE Transactions on Image Processing, 17* (7), pp. 1178-1188.

Haest, B., Thoonen, G., Vanden Borre, J., Spanhove, T., Delalieux, S., Bertels, L., Kooistra, L., Mücher, C.A., Scheunders, P., (2010). An object-based approach to quantity and quality assessment of heathland habitats in the framework of Natura 2000 using hyperspectral airborne AHS images. In: Addink, E.A. et al. (Ed*.). Proceedings of GEOBIA 2010-Geographic Object-Based Image Analysis*, Ghent, Belgium.

Hall, O., Hay, G.J., (2003). A multiscale object-specific approach to digital change detection. *Int.*

J. Appl. Earth Observ. Geoinf. 4/4, 311–327.

Hamada, Y., Stow, D.A., Coulter, L.L., Jafolla, J.C., Hendricks, L.W., (2007). Detecting Tamarisk species (Tamarix spp.) in riparian habitats of Southern California using high spatial resolution hyperspectral imagery. *Remote Sensing of Environment, 109* (2), pp. 237-248.

Han, T., Goodenough, D. G., Dyk, A., & Love, L. (2002). Detection and correction of abnormal pixels in Hyperion images. Proceedings of the *IEEE International Geoscience and Remote Sensing Symposium* (IGARSS'02), Toronto (Ontario), Canada, Vol. 3. (pp. 1327−1330)

Han, Y., and Yu, L., (2010). A Variance Reduction Framework for Stable Feature Selection: 2010 *IEEE International Conference on Data Mining*.

Hagner, O., Rigina, O., (1998). Detection of forest decline in Monchegorsk area. *Remote Sensing of Environment*, 63 (1), 11-23.

Hanley, M.E., Fenner, M., (1997). Seedling growth of four fire-following Mediterranean plant species deprived of single mineral nutrients. *Funct. Ecol.* 11, 398–405.

Hansen, P.M., Schjoerring, J.K., (2003). Reflectance measurement of canopy biomass and nitrogen status in wheat crops using normalized difference vegetation indices and partial least squares regression. *Remote Sensing of Environment*, 86 (4), 542-553**.**

Hassan, N., Hashim, M., (2011). *Decomposition of mixed pixels of ASTER satellite data for mapping Chengal (Neobalanocarpus heimii sp) tree*. Proceedings - 2011 IEEE International Conference on Control System, Computing and Engineering, ICCSCE 2011, art. no. 6190499, 74-79.

Hatala, J.A., Crabtree, R.L., Halligan, K.Q., Moorcroft, P.R., (2010). Landscape-scale patterns of forest pest and pathogen damage in the Greater Yellowstone Ecosystem. *Remote Sensing of Environment,* 114 (2010), 375–384

Hay, G., and Castilla, G. (2008). Geographic Object-Based Image Analysis (GEOBIA): A new name for a new discipline. In Blaschke, T, Lang, S., Hay, G. (Eds.), *Object-based image analysis: spatial concepts for knowledge-driven remote sensing applications*. Berlin; London: Springer, 2008.

Hay, G.J., Dube, P., Bouchard, A., Marceau, D.J., (2002). A scale-space primer for exploring and quantifying complex landscapes. *Ecological Modeling* 153 (1–2), 27–49

Hay, G.J., Blaschke, T., Marceau, D.J., Bouchard, A., (2003). A comparison of three image-object methods for the multiscale analysis of landscape structure. *ISPRS Journal of Photogrammetry and Remote Sensing 57* (5–6), 327–345.

Hay, G.J., Castilla, G., Wulder, M.A., Ruiz, J.R., (2005). An automated object-based approach for the multiscale image segmentation of forest scenes*. International Journal of Applied Earth Observation and Geoinformation, 7 (4)*, pp. 339-359.

Haykin, S., (1999). Neural Networks: A Comprehensive Foun-dation, 2nd edition, Prentice Hall, New Jersey, 842 pp.

Helmer, E.H.S., Brown, S., Cohen, W.B., (2000). Mapping montane tropical successional stage and land use with multi-date Landsat imagery. *International Journal of Remote Sensing,* 21, 2163–2183.

Hernando, A., Tiede, D., Albrecht, F., Lang, S. (2012). Spatial and thematic assessment of object-based forest stand delineation using an OFA-matrix. *International Journal of Applied Earth Observation and Geoinformation*, 19, 214-225.

Hestir, E. L., Khanna, S., Andrew, M. E., Santos, M. J., Viers, J. H., Greenberg, J. A., et al. (2008). Identification of invasive vegetation using hyperspectral remote sensing in the california delta ecosystem. Remote Sensing of Environment, 112(11), 4034-4047.

Heumann, B.W., (2011). Satellite remote sensing of mangrove forests: Recent advances and future opportunities. *Progress in Physical Geography*, 35 (1), 87-108.

Heumann, B.W., (2011). An Object-Based Classification of Mangroves Using a Hybrid Decision Tree—Support Vector Machine Approach. Remote Sensing 3, no. 11: 2440-2460.

Heywood V.H., (1999). The Mediterranean region: a major centre of plant diversity. *Options Mediterr,* 38,1–15

Hill, R.A., Thomson, A.G. (2005). Mapping woodland species composition and structure using airborne spectral and LiDAR data. *International Journal of Remote Sensing*, 26 (17), 3763-3779

Hobbs, R.J., Richardson, D.M., Davis, G.W., (1995). Mediterranean-type ecosystems. Opportunities and constraints for studying the fundion of biodiversity, in Mediterranean-Type Ecosystems. *The Function of Biodiversity*, l-42.

Houborg, R., Soegaard, H., Boegh, E., (2007). Combining vegetation index and model inversion methods for the extraction of key vegetation biophysical parameters using Terra and Aqua MODIS reflectance data. *Remote Sensing of Environment*, 106 (1), 39-58.

Horvat, I., Glavač, V. & Ellenberg, H. (1974). *Vegetation Südosteuropas*. G. Fischer, Stuttgart, DE

Huang, C., &Townsend, J. R. G. (2003). A stepwise regression tree for nonlinear approximation: Applications to estimating subpixel land cover. *International Journal of Remote Sensing*, 24, 75−90.

Huber, S., Kneubühler, M., Psomas, A., Itten, K., Zimmermann, N.E., (2008). Estimating foliar biochemistry from hyperspectral data in mixed forest canopy. *Forest Ecology and Management, 256 (3)*, pp. 491-501.

Hudak, A.T., Lefsky, M.A., Cohen, W.B., Berterretche, M., (2002). Integration of lidar and Landsat ETM+ data for estimating and mapping forest canopy height. *Remote Sensing of*

Environment, 82 (2-3), 397-416.

Hughes, G.F., (1968). On the mean accuracy of statistical pattern recognizers. *IEEE Transactions on Information Theory*, IT-14:55-63.

Huson, D., (2007). *Algorithms in Bioinformatics II*, SoSe'07, ZBIT

Hyde, P., Dubayah, R., Peterson, B., Blair, J.B., Hofton, M., Hunsaker, C., Knox, R., Walker, W., (2005). Mapping forest structure for wildlife habitat analysis using waveform lidar: Validation of montane ecosystems. *Remote Sensing of Environment*, 96 (3-4), 427-437

Hyde, P., Dubayah, R., Walker, W., Blair, J.B., Hofton, M., Hunsaker, C., (2006). Mapping forest structure for wildlife habitat analysis using multi-sensor (LiDAR, SAR/InSAR, ETM+, and Quickbird) synergy. *Remote Sensing of Environment*, 102 (1-2), 63-73.

Hyyppä, J., Hyyppä, H., Inkinen, M., Engdahl, M., Linko, S., Zhu, Y.-H., (2000). Accuracy comparison of various remote sensing data sources in the retrieval of forest stand attributes. *Forest Ecology and Management*, 128 (1-2), 109-120.

Jensen, J. R., (2005). *Introductory Digital Image Processing*, 3rd Ed., Upper Saddle River, NJ: Prentice Hall.

Jia, G.J., Burke, I.C., Kaufmann, M.R., Goetz, A.F.H., Kindel, B.C., Pu, Y., (2006). Estimates of forest canopy fuel attributes using hyperspectral data. *Forest Ecology and Management,* 229, 27–38

Jimenez-Rodriguez, L. O., Arzuaga-Cruz, E. & Velez-Reyes, M. (2007). Unsupervised linear feature-extraction methods and their effects in the classification of high-dimensional data, IEEE Trans. Geosci. *Remote Sensing*, Issue: 2: 469–483.

Johansen, K. and Phinn, S., (2006). Mapping structural parameters and species composition of riparian vegetation using IKONOS and Landsat ETM plus data in Australian tropical savannahs. *Photogrammetric Engineering and Remote Sensing*, 72 (1), 71-80.

Jollineau, M. Y. and Howarth, P. J. (2008) 'Mapping inland wetland complex using hyperspectral imagery'. *International Journal of Remote Sensing*, 29: 12, 3609 — 3631.

Jones, T.G., Coops, N.C., Sharma, T., (2010). Assessing the utility of airborne hyperspectral and LiDAR data for species distribution mapping in the coastal Pacific Northwest. *Remote Sensing of Environment*, 114 (12), 2841-2852.

Jupp, D. L. B. & Datt, B. (Eds.). (2004). Evaluation of the EO-1 Hyperion hyperspectral instrument and its applications at Australian validation sites, 2001–2003 (pp. 20−23). Canberra, Australia: CSIRO Earth Observation Centre.

Jyothi, B.N., G.R. Babu, and I.V.M. Krishna. (2008). Object oriented and multi-scale image analysis: strengths, weaknesses, opportunities, and threats – a review. *J. of Computer*

Science 4(9): 706-712.

Kamal, M., Phinn, S., (2011). Hyperspectral Data for Mangrove Species Mapping: A Comparison of Pixel-Based and Object-Based Approach. *Remote Sens*. 3, 2222-2242.

Karimi, Y., Prasher, S.O., Patel, R.M., KIMB, S.H., (2006). Application of support vector machine technology for weed and nitrogen stress detection in corn. *Computers and Electronics in Agriculture 51* (1–2), 99–109.

Karteris, M.A., Meliadis, I.M., Kritikos, G.S. and Nikolaidis, A., (1992). *Forest classification and mapping of Mediterranean forests and maquis with satellite data*, Mediterranean Agronomic Institute of Chania, Chania, Greece.

Ke, Y., Quackenbush, L.J., Im, J., (2010). Synergistic use of QuickBird multispectral imagery and LIDAR data for object-based forest species classification. *Remote Sensing of Environment*, 114(6, 15), 1141-1154.

Keeley, J.E., Zedler, P.H., (1998). *Evolution of life histories in Pinus. In: Richardson, D.M. (Ed.), Ecology and Biogeography of Pinus*. Cambridge University Press, Cambridge, pp. 219–250.

Kennedy R.E., Cohen W.B., Takao G., (1997). Empirical methods to compensate for a view-angle-dependent brightness gradient in AVIRIS imagery. *Remote Sensing of Environment,* 62, 277-291.

Keramitsoglou, I., Kontoes, C., Koutroumbas, K., Sykioti, O., Sifakis, N., (2005). *Mapping of forest species and tree density using new Earth Observation sensors for wildfire applications*. Proceedings of SPIE - The International Society for Optical Engineering, 5976, art. No. 59760G,.

Keramitsoglou, I., Kontoes, C., Sykioti, O., Sifakis, N., Xofis, P., (2008). Reliable, accurate and timely forest mapping for wildfire management using ASTER and Hyperion satellite imagery. *Forest Ecology and Management,* 255, 3556–3562

Key, T., Warner, T.A., McGraw, J.B., Fajvan, M.A., (2001). A Comparison of Multispectral and Multitemporal Information in High Spatial Resolution Imagery for Classification of Individual Tree Species in a Temperate Hardwood Forest. *Remote Sensing of Environment*, 75(1), 100-112.

Khurshid, K. S., Staenz, K., Sun, L., Neville, R., White, H. P., Bannari, A., et al. (2006). Preprocessing of EO-1 Hyperion data. Canadian Journal of Remote Sensing, 32, 84–97.

Kim, M., Madden, M., Warner, T.A., (2009). Forest type mapping using object-specific texture measures from multispectral Ikonos imagery: Segmentation quality and image classification issues. *Photogrammetric Engineering and Remote Sensing,* 75 (7), 819-829.

Knerr, S., Personnaz, L. and Dreyfus, G., (1990). Single-layer learning revisited: a stepwise procedure for building and training neural networks. *Neurocomputing: Algorithms,*

Architectures and Applications, NATO ASI (Berlin: Springer-Verlag).

Knorn, J., Rabe, A., Volker, C., Radeloff, C.V., Kuemmerl, T., Kozak, J., Hostert, P., (2009). Land cover mapping of large areas using chain classification of neighboring Landsat satellite images. *Remote Sensing of Environment,* 113, 957–964.

Koetz, B., Morsdorf, F., van der Linden, S., Curt, T., Allgower, B., (2008). Multi-source land cover classification for forest fire management based on imaging spectrometry and LiDAR data. *Forest Ecology and Management,* 256 263–271

Kokaly, R.F., Despain, D.G., Clark, R.N., Livo, K.E. (2003). Mapping vegetation in yellow stone national park using spectral feature analysis of AVIRIS data. *Remote Sensing of Environment*, 84(3), 437-456.

Kokaly, R.F., Asner, G.P., Ollinger, S.V., Martin, M.E., Wessman, C.A., (2009). Characterizing canopy biochemistry from imaging spectroscopy and its application to ecosystem studies. *Remote Sensing of Environment,* 113, S78–S91

Kokkoris, Y., Arianoutsou, M., (2001). *The ecological profile of endemic plants in the fire prone environments of the Mediterranean ecosystems of Greece.* Proceedings of the 8' Congress of the Hellenic Botanical Society. In Greek with an English Summary. 204-207.

Koppen, W., (1931). Grundriss der Klimakunde, Walter de Gruyter & Co.

Kötz, B., Schaepman, M., Morsdorf, F., Bowyer, P., Itten, K., Allgöwer, B. (2004). Radiative transfer modeling within a heterogeneous canopy for estimation of forest fire fuel properties. *Remote Sensing of Environment*, 92 (3), 332-344.

Kovacs, J.M., Wang, J., Flores-Verdugo, F., (2005). Mapping mangrove leaf area index at the species level using IKONOS and LAI-2000 sensors for the Agua Brava Lagoon, Mexican Pacific. *Estuarine, Coastal and Shelf Science*, 62 (1-2), 377-384.

Kruse, F.A., Lefkoff, A.B., Boardman, J.B., Heidebrecht, K.B., Shapiro, A.T., Barloon, P.J., Goetz, A.F.H., (1993). The Spectral Image Processing System (SIPS) – interactive visualization and analysis of imaging spectrometer data. Remote Sensing Environment 44, 145–163.

Kumar, S., Ghosh, J., Crawford, M. (2001). Best-Bases Feature Extraction Algorithms for Classification of Hyperspectral Data. *IEEE Transactions on geoscience and remote sensing, vol. 39*, no. 7, 1368-1379.

Laliberte, A.S., Fredrickson, E.L, and Rango, A., (2007), Object-oriented Image Analysis for Mapping Arid Rangelands. *Photogrammetric Engineering & Remote Sensing, Vol. 73*, No. 2, February 2007, pp. 197–207.

Lampropoulos, A.S., Lampropoulou, P.S., Tsihrintzis, G.A., (2011). A movie recommender system based on ensemble of transductive SVM classifiers. *NCTA 2011 - Proceedings of the International Conference on Neural Computation Theory and Applications*, pp. 242-247.

Landgrebe, D., (2003*). Signal Theory Methods in Multispectral Remote Sensing*, John Wiley & Sons, 2003.

Lang, S., Albrecht, F., Kienberger, S., Tiede, D., (2010). Object validity for operational tasks in a policy context. *Journal of Spatial Science*, 55(1).

Lang, S., (2008). Object-based image analysis for remote sensing applications: Modeling reality Dealing with complexity. In: Blaschke, T., Lang, S., Hay, G.J. (Eds.), Object Based Image Analysis. Springer, Heidelberg, Berlin, New York, pp. 1-25.

Le Houerou, H.N., (1981). Impact of man and his animals on mediterranean vegetation. pp. 479-521. In: di Cashi, F., Goodall. D.W. & R.L. Specht. (Eds). *Mediterranean-type shrublands*. Elsevier, Amsterdam.

Lee, C., & Landgrebe, D. A. (1993). Decision boundary feature extraction for nonparametric classification. *IEEE Transactions on Systems, Man and Cybernetics*, 23, 433–444.

Lee, K.S., Cohen, W.B., Kennedy, R.E., Maiersperger, T.K., Gower, S.T., (2004). Hyperspectral versus multispectral data for estimating leaf area index in four different biomes. *Remote sensing of environment*, 91(4), 508-520.

Lefsky, M.A., Hudak, A.T., Cohen, W.B., Acker, S.A., (2005). Geographic variability in lidar predictions of forest stand structure in the Pacific Northwest. *Remote Sensing of Environment*, 95 (4), 532-548.

Leisz, D.R., (1982). Concerns and costs of managing Mediterranean-type ecosystems, 3–5. In C. E. Conrad and W. C. Oechel [eds.], *Proceedings of the symposium on dynamics and management of Mediterranean-type ecosystems*, 22–26 Jun 1981, San Diego, CA. USDA, Forest Service, General Technical Report PSW-58, Pacific Southwest Forest and Range xperiment Station, Berkeley, CA.

Leutner, B.F., Reineking, B., Müller, J., Bachmann, M., Beierkuhnlein, C., Dech, S., Wegmann, M., (2012). Modelling forest α-diversity and floristic composition - on the added value of LiDAR plus hyperspectral remote sensing. *Remote Sensing*, 4 (9), 2818-2845.

Li, X., Jiang, W., Sheng, S., & Chen, Q. (2009). Research on wetland classification approaches based on hyperion hyperspectral image. Paper presented at the *Proceedings of SPIE - the International Society for Optical Engineering.*

Liarikos, K., Maragkou, P., Papagiannis, T., (2012). *Greece now and then: Multitempotal mapping of land cover*, 1987-2007. WWF, Grecce.

Liu, W., Gopal, S. Woodcock, C.E., (2004). Uncertainty and confidence in land cover classification using a hybrid classifier approach. *Photogrammetric Engineering and Remote Sensing*, 70, 963–972.

Lizarazo I. & Elsner P. (2008). From pixels to grixels: A unified functional model for Geographic

Object-Based Image Analysis. *GEOBIA 2008: Pixels, Object, Intelligence*. Calgary (Canada).

Loveland, T.R., (2000). The patterns and characteristics of global land cover. In: Hill, M.J., Aspinall, R.J. (Eds.), *Spatial Information and Land Use Management*. Gordon and Breach, Reading, pp. 13 /24

Lu, D. & Weng, Q., (2007). A survey of image classification methods and techniques for improving classification performance. *International Journal of Remote Sensing*, 28:5, 823-870

Lucas, R. M., Lee, A. C., Bunting, P. J., (2008). 'Retrieving forest biomass through integration of CASI and LiDAR data', *International Journal of Remote Sensing*, 29(5), 1553-157.

Lucas, R., Bunting, P., Paterson, M., Chisholm, L., (2008). Classification of Australian forest communities using aerial photography, CASI and HyMap data. *Remote Sensing of Environment*, 112, 2088−2103.

Lumme, J. H. (2004). Classification of vegetation and soil using imaging spectrometer data. XXth ISPRS Congress, Commission 7, Istanbul, Turkey, ISPRS, Vol.XXXV, Part B7.

MacDonald, D., Crabtree, J.R., Wiesinger, G., Dax, T., Stamou, N., Fleury, P., Gutierrex Lazpita, J., Gibon, A., (2000). Agriculture abandonment in mountain areas of Europe: environmental consequences and policy response. *J Environ Manage,* 59,47–69

Makedos, I., (1987). *The Pinus brutia forest of Thasos, In Pinus halepensis and Pinus brutia forests* (Ecology, management and development), (Ed, Papanastasis, V.), Hellenic Association of Foresters, Chalkida, Greece, pp. 153-160.

Mallinis, G., Koutsias, N., (2012). Comparing ten classification methods for burned area mapping in a Mediterranean environment using Landsat TM satellite data. *International Journal of Remote Sensing*, 33 (14), 4408-4433.

Mallinis, G., Koutsias, N., Makras, A., Karteris, M., (2004). Forest parameters estimation in a European Mediterranean landscape using remotely sensed data. *Forest Science*, 50 (4), 450-460.

Mallinis, G., Koutsias, N., Tsakiri-Strati, M., Karteris, M., (2008). Object-based classification using Quickbird imagery for delineating forest vegetation polygons in a Mediterranean test site. *ISPRS Journal of Photogrammetry and Remote Sensing*, 63 (2), 237-250.

Mallinis, G., Maris, F., Kalinderis, I., Koutsias, N., (2009). Assessment of post-fire soil erosion risk in fire-affected watersheds using remote sensing and GIS. *GIScience and Remote Sensing*, 46 (4), 388-410.

Marceau, D.J., Hay, G.J., (1999). Remote sensing contributions to the scale issue. *Canadian Journal of Remote Sensing. 25* (4), 357–366.

Marceau, D.J., (1999). The scale issue in the social and natural sciences. *Canadian Journal of Remote Sensing. 25* (4), 347–356.

Martin, M.E., Newman, S.D., Aber, J.D., Congalton, R.G., (1998). Determining forest species composition using high spectral resolution remote sensing data. *Remote Sensing of Environment*, 65(3), 249-254.

Martin, M.E., Plourde, L.C., Ollinger, S.V., Smith, M.L., McNeil, B.E., (2008). A generalizable method for remote sensing of canopy nitrogen across a wide range of forest ecosystems. *Remote Sensing of Environment,* 112, 3511–3519

Maselli, F., Chiesi, M., (2006). Evaluation of statistical methods to estimate forest volume in a Mediterranean region. *IEEE Trans. Geosci. Remote Sens.,* 44(8), 2239–2250.

Matthew, M., Adler-Golden, S., Berk, A., Richtsmeier, S., Levine, R., Bernstein, L., Acharya, P., Anderson, G., Felde, G., Hoke, M., Ratkowski, A., Burke, H., Kaiser, R. and Miller, D. (2000). Status of Atmospheric Correction Using a MODTRAN4-based Algorithm. In: *SPIE Proceedings, Algorithms for Multispectral, Hyperspectral, and Ultraspectral Imagery* pp. 199-207.

Mciver, D.K., Friedl, M.A., (2001). Estimating pixel-scale land cover classification confidence using nonparametric machine learning methods. *IEEE Transactions on Geoscience and Remote Sensing*, 39, 1959–1968.

McRoberts, R.E., Tomppo, E.O., (2007). Remote sensing support for national forest inventories Remote Sensing of Environment, 110 (4), pp. 412-419.

McRoberts, R.E., Tomppo, E.O., (2007). Remote sensing support for national forest inventories. *Remote Sensing of Environment*, 110 (4), 412-419.

Melgani, F., Bruzzone, L., (2004). Classification of hyperspectral remote sensing images with support vector machines. *IEEE Transactions on Geoscience and Remote Sensing 42*, 1778–1790.

Meroni, M., Colombo, R., Panigada, C., (2004). Inversion of a radiative transfer model with hyperspectral observations for LAI mapping in poplar plantations. *Remote Sensing of Environment*, 92 (2), 195-206.

Miao, X., Gong, P., Swope, S., Pu, R., Carruthers, R., Anderson, G. L., (2006). Estimation of yellow starthistle abundance through CASI-2 hyperspectral imagery using linear spectral mixture models. *Remote Sensing of Environment*, 101(3), 329-341.

Miao, X., Patil, R., Heaton, J. S., Tracy, R. C., (2011). Detection and classification of invasive saltcedar through high spatial resolution airborne hyperspectral imagery. *International Journal of Remote Sensing*, 32(8), 2131-2150.

Michelson, D.B., Lilieberg, B.M., Pilesjo, P., (2000). Comparison of algorithms for classifying

Swedish land cover using Landsat TM and ERS-1 SAR data. *Remote Sensing of Environment,* 71, 1–15.

Miller, C. J., 2002, Performance assessment of ACORN atmospheric correction algorithm, Proceedings. *SPIE Algorithms and Technologies for Multispectral, Hyperspectral, and Ultraspectral Imagery* VIII,v. 4725, pp. 438–449.

Mitri, G., Gitas, I., (2010). Mapping post-fire vegetation regeneration using EO-1 Hyperion. *IEEE Transactions on Geoscience and Remote Sensing,* 48 (3), 1613–1618.

Mohd Hasmadi, I., Kamaruzaman, J., & Nurul Hidayah, M. A. (2010). Analysis of crown spectral characteristic and tree species mapping of tropical forest using hyperspectral imaging. *Journal of Tropical Forest Science*, 22(1), 67-73.

Mountrakis, D., M. (1985). *Geology of Greece*, University Studio Press, Thessaloniki.

Mountrakis, G., Im, J., Ogole, C., (2011). Support vector machines in remote sensing: A review. ISPRS Journal of Photogrammetry and Remote Sensing, 66(3):247-259.

Moustakidis, S., and Theocharis, J. (2010): SVM-FuzCoC: A novel SVM-based feature selection method using a fuzzy complementary criterion. *Pattern Recognition 43*(11): 3712-3729

Mücher, C.A., Kooistra, L., Vermeulen, M., Haest, B., Spanhove, T., Delalieux, S., Vanden Borre, J., Schmidt, A. (2010). Object identification and characterization with hyperspectral imagery to identify structure and function of Natura 2000 habitats. In: Addink, E.A. et al. (Ed.) (2010). *Proceedings of GEOBIA 2010-Geographic Object-Based Image Analysis*, Ghent, Belgium.

Muinonen, E., Tokola, T., (1990). *An application of remote sensing for communal forest inventory*, Proceedings from S/IUFRO Workshop in Umeå, 26–28 February, Remote Sensing Laboratory, Swedish University of Agricultural Sciences, Report 4:35–42.

Muller-Landau, H., Wright, S.J., Calderon, O., Hubbell, S.P. & Foster, R.B., (2002). Assessing recruitment limitation: concepts, methods and examples fortropical foresttrees. In: *Seed Dispersal and Frugivory: Ecology, Evolution and Conservation* (eds: Levey, J., Silva, W.R. & Galetti, M.). CAB International, Oxfordshire, UK, pp. 33–53.

Mundt, J. T., Glenn, N. F., Weber, K. T., Prather, T. S., Lass, L. W., & Pettingill, J. (2005). Discrimination of hoary cress and determination of its detection limits via hyperspectral image processing and accuracy assessment techniques. *Remote Sensing of Environment*, 96 (3-4), 509-517.

Myneni, R.B., Dong, J., Tucker, C.J., Kaufmann, R.K., Kauppi, P.E., Liski, J., Zhou, L., Alexeyev, V., Hughes, M.K., (2001). *A large carbon sink in the woody biomass of northern forests*. Proceedings of the National Academy of Sciences of the United States of America, 98 (26), 14784-14789.

Myers, N., Mittermeier, R.A., Mittermeier, C.G., da Fonseca G.A.B., Kent, J., (2000). Biodiversity

hotspots for conservation priorities, *Nature,* 403, 853-858.

Nagendra, H., Rocchini, D., (2008). High resolution satellite imagery for tropical biodiversity studies: The devil is in the detail. Biodiversity and Conservation, 17 (14), pp. 3431-3442.

Nagendra, H., (2001). Using remote sensing to assess biodiversity. *International Journal of Remote Sensing*, 22:2377–2400.

Nahal, I., (1983). Le pin brutia (*Pinus brutia* Ten. subsp. brutia), Premiere partie. *Forest Mediterranee,* 5, 165-172.

Nakos, G., (1995). *Desertification in the Mediterranean Area: A Decision Support System for the prevention of desertification resulting from forest fires.* Institute of Mediterranean Forest Ecosystems, Athens.

Narumalani, Sunil, Mishra, Deepak R., Burkholder, Jared, Merani, Paul B. T. and Willson, Gary(2006), 'A Comparative Evaluation of ISODATA and Spectral Angle Mapping for the Detection of Saltcedar Using Airborne Hyperspectral Imagery', *Geocarto International*, 21: 2, 59 — 66

Naveh, Z., Dan. J., (1973). The human deeradation of mediterranean landscapes in Israel. pp. 371-390. In: di Cashi, F. & Mooney, H.A. (eds). *Mediterranean - type ecosystems: origin and structure*. Springer. Berlin- Heidelberg - New York

Naveh, Z., Lieberman, S., (1993). *Landscape Ecology Theory and Applications*. Second Edition. Springer-Ver- lag, New York.

Naveh, Z., (1998). From Biodiversity to Ecodiversity - Holistic Conservation of the Biological and Cultural Diversity of Mediterranean Landscapes. pp. 23-54. In: Rundel, P. W., Montenegro, G., Jaksic, F. (eds). *Landscape degradation in Mediterranean-Type Ecosystems. Ecological Studies* 136. Springer-Verlag. Berlin/ Heidelberg.

Nelson, R.E., Kimes, D.S., Salas, W.A., Routhier, M., (2000). Secondary forest age and tropical forest biomass estimation using Thematic Mapper imagery. *Bioscience,* 50, 419–437.

Neumann, M., Ferro-Famil, L., Reigber, A., (2010). Estimation of forest structure, ground, and canopy layer characteristics from multibaseline polarimetric interferometric SAR data. IEEE Transactions on Geoscience and Remote Sensing, 48 (3 PART 1), art. no. 2031101, pp. 1086-1104.

Neville R.A., Sun L., Staenz K., (2003). Detection of spectral line curvaturein imaging spectrometer data. *SPIE, 2003: Algorithms and Technologies for Multispectral, Hyperspectral, and Ultraspectral Imagery IX.,*144-154

Neville, R. A., Sun, S., Staenz, K., (2008). Spectral calibration of imaging spectrometers by atmospheric absorption feature matching, *Can. J. Remote Sens.*, 34(29–42).

Nidamanuri, R. R., and Zbell, B., (2011). Transferring spectral libraries of canopy reflectance for crop classification using hyperspectral remote sensing data. *Biosystems Engineering*, Volume 110, Issue 3, Pages 231-246.

Oldeland, J., Dorigo, W., Lieckfeld, L., Lucieer, A., Jürgens, N., (2010). Combining vegetation indices, constrained ordination and fuzzy classification for mapping semi-natural vegetation units from hyperspectral imagery. *Remote Sensing of Environment*, 114(6), 1155-1166.

Pal, M., Mather, P.M. (2003). An assessment of the effectiveness of decision tree methods for land cover classification. *Remote Sensing of Environment*, 86 (4), 554-565.

Pal, M., and Mather, P.M., (2004). Assessment of the effectiveness of support vector machines for hyperspectral data. *Future Generation Computer Systems*, Volume 20, Issue 7, 1 Pages 1215-1225,

Pal, M., & Mather, P. M. (2006). Some issues in the classification of DAIS hyperspectral data. *International Journal of Remote Sensing*, 27(14), 2895-2916.

Panetsos, K. P. (1981). Monograph of *Pinus halepensis* (Mill.) and *Pinus brutia* (Ten.), *Annales Forestales, Zagreb,* **9,** 39-77

Papageorgiou, A.C., Vidalis, A., Gailing, O., Tsiripidis, I., Hatziskakis, S., Boutsios, S., Galatsidas, S., Finkeldey, R., (2008). Genetic variation of beech (Fagus sylvatica L.) in Rodopi (N.E. Greece). European Journal of Forest Research, 127 (1), pp. 81-88.

Papathanassiou, K.P., Cloude, S.R., (2001). Single-baseline polarimetric SAR interferometry. *IEEE Transactions on Geoscience and Remote Sensing, 39* (11), pp. 2352-2363.

Papavassiliou, V., Stafylakis, T., Katsouros, V., Carayannis, G., (2010). Handwritten document image segmentation into text lines and words. Pattern Recognition, 43 (1), pp. 369-377.

Papeş, M., Tupayachi, R., Martínez, P., Peterson, A.T., Powell, G.V.N., (2010). Using hyperspectral satellite imagery for regional inventories: A test with tropical emergent trees in the Amazon Basin. *Journal of Vegetation Science*, 21 (2), pp. 342-354.

Parker Williams, A., & Hunt Jr., E. R. (2002). Estimation of leafy spurge cover from hyperspectral imagery using mixture tuned matched filtering. Remote Sensing of Environment, 82(2-3), 446-456.

Pearlman, J.S., Barry, P.S., Segal, C.C., Shepanski J., Beiso, D., and. Carman, .S. L (2003).Hyperion, a space-based imaging spectrometer. *IEEE Trans. Geosci. Remote Sens*., vol. 41, no. 4, pp. 1160–1173.

Peña, M.A. and Altmann, S.H., (2009). Use of satellite-derived hyperspectral indices to identify stress symptoms in an Austrocedrus chilensisforest infested by the aphid Cinara cupressi. International Journal of Pest Management, 55: 3, 197 — 206

Pengra, B. W., Johnston, C. A., & Loveland, T. R. (2007). Mapping an invasive plant, phragmites australis, in coastal wetlands using the EO-1 hyperion hyperspectral sensor. *Remote Sensing of Environment, 108*(1), 74-81.

Petropoulos, G. P., Kalaitzidis, C., & Prasad Vadrevu, K. (2011). Support vector machines and object-based classification for obtaining land-use/cover cartography from hyperion hyperspectral imagery. *Computers and Geosciences*, 41, 99-107.

Petropoulos, G.P., Arvanitis, K., Sigrimis, N., (2012). Hyperion hyperspectral imagery analysis combined with machine learning classifiers for land use/cover mapping. *Expert Systems with Applications* , Volume 39 (3)

Peuhkurinen, J., Maltamo, M., Vesa, L., Packalén, P., (2008). Estimation of forest stand characteristics using spectral histograms derived from an Ikonos satellite image. *Photogrammetric Engineering and Remote Sensing, 74* (11), pp. 1335-1341.

Pignatti, S., Cavalli, R. M., Cuomo, V., Fusilli, L., Pascucci, S., Poscolieri, M., et al. (2009). Evaluating hyperion capability for land cover mapping in a fragmented ecosystem: Pollino national park, italy. *Remote Sensing of Environment, 113*(3), 622-634.

Piscini, A., Amici, S., & Fieri, D. (2010). Spectral analysis of aster and hyperion data for geological classification of volcano teide. Paper presented at *the International Geoscience and Remote Sensing Symposium (IGARSS)*, 2267-2270.

Plaza, A., Benediktsson, J.A., Boardman, J.W., Brazile, J., Bruzzone, L., Camps-valls, G., Chanussot, J., Fauvel, M., Gamba, P., Gualtieri, A., Marconcini, M., Tilton, J.C., TriannI, G., (2009). Recent advances in techniques for hyperspectral image processing. *Remote Sensing of Environment 113* (1), S110–S122

Polychronaki, A., Gitas, I.Z., (2010). The development of an operational procedure for burned-area mapping using object-based classification and ASTER imagery. *International Journal of Remote Sensing, 31* (4), pp. 1113-1120.

Poorter, L., Oberbauer, S. F., & Clark, D. B. (1995). Leaf optical-properties along a vertical gradient in a tropical rain-forest canopy in Costa-Rica. *American Journal of Botany*, 82(10), 1257–1263.

Portigal, F., Holasek, R., Mooradian, G., Owensby, P., Dicksion, M., Fene, M., Elliot, M., Hall, E., and Driggett, D., (1997). Vegetation classification using red-edge first derivative and green peak statistical moment indices with the Advanced Airborne Hyperspectral Imaging System (AAHIS). *Third International Airborne Remote Sensing Conference and Exhibition*, Copenhagen , Denmark, 7 – 10 July 1997 , vol. II (Ann Arbor, MI: ERIM), pp. 789–797.

Preiss E, Martin JL, Debussche M (1997) Rural depopulation and recent landscape changes in a Mediterranean region: consequences to the breeding avifauna. Landscape Ecology 12:51–61

Pu, R., Gong, P., (2004). Wavelet transform applied to EO-1 hyperspectral data for forest LAI and crown closure mapping. *Remote Sensing of Environment, 91* (2), pp. 212-224.

Pu, Q. Yu, P. Gong, G. S. Biging (2005). EO-1 Hyperion, ALI and Landsat 7 ETM+data comparison for estimating forest crown closure and leaf area index. *International Journal of Remote Sensing Vol. 26*, No. 3, 457–474

Pu, R., 2009, Broadleaf species recognition within situ hyperspectral data. *International Journal of Remote Sensing Vol. 30*, No. 11, pp. 2759–2779.

Qu, Z., Kindel, B.C., Goetz, A.F.H. (2003). The High Accuracy Atmospheric Correction for Hyperspectral Data (HATCH) Model. *IEEE Transactions on Geoscience and Remote Sensing, vol.41*, 1223-1231.

Quezel, P., 1977. Forests of the Mediterranean basin. MAB Technical notes. *Mediterranean forests and maquis: ecology, conservation and management. UNESCO*, Paris, pp. 9–32

Radoglou, K.M. (1996). Environmental control of CO 2 assimilation rates and stomatal conductance in five oak species growing in field conditions in Greece. *Annals of Forest Science*, 53:269–278.

Radoux, J., Bogaert, P., Fasbender, D., Defourny P. (2011).Thematic accuracy assessment of geographic object-based image classification International. *Journal of Geographical Information Science, Vol. 25*, Iss. 6.

Rafieyan, O., Darvishsefat, A. A., Babaii, S., Mataji, A., (2010) Object based classification using ULTRACAM-D images for tree species discrimination. Case study: Hyrcanian forest, Iran. In (Eds) E.A. Addink and F.M.B. Van Coillie. *The International Archives of the Photogrammetry, Remote Sensing and Spatial Information Sciences*, Vol. XXXVIII-4/C7.

Ramsey III, E., Rangoonwala, A., Nelson, G., Ehrlich, R. and Martella, K.(2005) 'Generation and validation of characteristic spectra from EO1 Hyperion image data for detecting the occurrence of the invasive species, Chinese tallow'. *International Journal of Remote Sensing*, 26: 8, 1611 — 1636

Ranson, K.J, Sun, G., (1994). Mapping biomass of a northen forest using multifrequency SAR data. *IEEE Transactions on Geoscience and Remote Sensing, 32* (2), pp. 388-396.

Rao, R.N. (2008). Development of a crop-specific spectral library and discrimination of various agricultural crop varieties using hyperspectral imagery. *International Journal of Remote Sensing, 29*: 1, 131 — 144.

Rautiainen, M., Lang, M., Mõttus, M., Kuusk, A., Nilson, T., Kuusk, J., Lükk, T. , (2008). Multi-angular reflectance properties of a hemiboreal forest: An analysis using CHRIS PROBA data. *Remote Sensing of Environment, 112* (5), pp. 2627-2642.

Remmel, T.K., Csillag, F., Mitchell, S., Wulder, M.A., (2005). Integration of forest inventory and

satellite imagery: A Canadian status assessment and research issues. *Forest Ecology and Management, 207* (3), pp. 405-428.

Riano, D., Chuvieco, E., Salas, J., Palacios-Orueta, A., Bastarrika, A., (2002). Generation of fuel type maps from Landsat TM images and ancillary data in Mediterranean ecosystems. *Canadian Journal of Forest Research*, 32, 1301–1315

Richards, J., (1999*). Error correction and registration of image data. In Remote Sensing Digital Image Analysis: An Introduction*, pp. 313–337 (Berlin: Springer).

Richardson, D.M., Rundel, P.W., (1998). Ecology and biogeography of Pinus: an introduction. In: Richardson, D.M. (Ed.), *Ecology and Biogeography of Pinus.* Cambridge University Press, Cambridge, pp. 3–4

Richter, R. (1998). Correction of satellite imagery over mountainous terrain.*Applied Optics*, 37, 4004−4015.

Roberts, D. A., Gardner, M., Church, R., Ustin, S., Scheer, G., & Green, R. O. (1998). Mapping chaparral in the santa monica mountains using multiple endmember spectral mixture models. *Remote Sensing of Environment,* 65(3), 267-279.

Roberts, D.A., Dennison, P.E., Gardner, M.E., Hetzel, Y., Ustin, S.L., Lee, C.T., (2003). Evaluation of the potential of Hyperion for fire danger assessment by comparison to the airborne visible/infrared imaging spectrometer. *IEEE Transactions on Geoscience and Remote Sensing, 41* (6 PART I), pp. 1297-1310.

Roberts, D.A., Keller, M., Soares, J.V., (2003). Studies of land-cover, land-use, and biophysical properties of vegetation in the Large Scale Biosphere Atmosphere experiment in Amazônia. *Remote Sensing of Environment, 87* (4), pp. 377-388.

Roberts, D. A., Ustin, S. L., Ogunjemiyo, S., Greenberg, J., Dobrowski, S.Z., Chen, J., et al. (2004). Spectral and structural measures of Northwest forest vegetation at leaf to landscape scales. *Ecosystems*, 7(5), 545–562.

Rodriguez, W., Feller, I.C., (2004). Mangrove landscape characterization and change in Twin Cays, Belize using aerial photography and IKONOS satellite data. *Atoll Research Bulletin*, (509-530), pp. 1-22.

Rogan, J., Franklin, J., Roberts, D.A., (2002). A comparison of methods for monitoring multi temporal vegetation change using Thematic Mapper imagery. *Remote Sensing of Environment 80*, 143–156.

Rosenqvist, Å., Shimada, M., Chapman, B., Freeman, A., De Grandi, G., Saatchi, S., Rauste, Y., (2000). The global rain forest mapping project-a review. *International Journal of Remote Sensing, 21* (6-7), pp. 1375-1387.

Rosenqvist, Å., Milne, A., Lucas, R., Imhoff, M., Dobson, C. (2003). A review of remote sensing

technology in support of the Kyoto Protocol. *Environmental Science and Policy, 6* (5), pp. 441-455.

RSI. (2001). *ENVI FLAASH User's guide*. Boulder, CO' Research Systems, Inc.

Running, S.W., and Coughlan, J.C., (1988). A general model for forest ecosystem processes for regional applications. I. Hydrologic balance, canopy gas exchange and primary production processes. *Ecological Modeling*, 42, pp. 125–154

Saito, H., Bellan, M.F., Al-Habshi, A., Aizpuru, M., Blasco, F., (2003). Mangrove research and coastal ecosystem studies with SPOT-4 HRVIR and TERRA ASTER in the Arabian Gulf. *International Journal of Remote Sensing, 24* (21), pp. 4073-4092.

San, B.T. & M.L. Süzen, (2011). Evaluation of cross-track illumination in EO-1 Hyperion imagery for lithological mapping. *International Journal of Remote Sensing*, 32:22, 7873-7889

Scarascia-Mugnozza, G., Oswald, H., Piussi, P., Radoglou, K., (2000). Forests of the Mediterranean region: gaps in knowledge and research needs. *Forest Ecology and Management,* Volume 132, Issue 1, Pages 97-109,

Secretariat of the Convention on Biological Diversity (2001). *The Value of Forest Ecosystems. Montreal,* SCBD, 67p. (CBD Technical Series no. 4).

Schiewe, J., (2002). Segmentationof high-resolution remotely senseddata concepts, applications and problems. In: *Joint ISPRS Commission IV Symposium: Geospatial Theory, Processing and Applications*, 9 12 July 2002 (on CDROM).

Schimper A. F. W. (1903). *Plant-geography upon a physiological basis*. Clarendon Press, Oxford, UK.

Schlerf, M., Atzberger, C., Hill, J. (2005). Remote sensing of forest biophysical variables using HyMap imaging spectrometer data. *Remote Sensing of Environment*, 95 177–194

Schlerf, M., Atzberger, C., Hill, J., (2005). Remote sensing of forest biophysical variables using HyMap imaging spectrometer data. *Remote Sensing of Environment*, 95 (2), pp. 177-194.

Schlerf, M., Atzberger, C., (2012). Vegetation structure retrieval in beech and spruce forests using spectrodirectional satellite data. *IEEE Journal of Selected Topics in Applied Earth Observations and Remote Sensing*, 5 (1), art. No. 6151222, pp. 8-17.

Schmidt, K.S., & Skidmore, A.K. (2001). Exploring spectral discrimination of grass species in african rangelands*. International Journal of Remote Sensing, 22*(17), 3421-3434.

Schmidtlein, S., Sassin, J., (2004). Mapping of continuous floristic gradients in grasslands using hyperspectral imagery. *Remote Sensing of Environment, Volume 92*, Issue 1, Pages 126-138,

Schneider, W., Steinwender, J., (1999). Landcover mapping by inter-related segmentation and classification of satellite images. *International Archives of Photogrammetry and Remote*

Sensing, 32, Part 7-4-3 W6.

Scholes, R.J., Kendall, J., Justice, C.O., (1996). The quantity of biomass burned in southern Africa. *Journal of Geophysical Research D. Atmospheres*, 101 (19), pp. 23667-23676

Sedano, F., Gong, P., Ferrao, M., (2005). Land cover assessment with MODIS imagery in southern African Miombo ecosystems. *Remote Sensing of Environment*, 98,429–441.

Serpico, S., and Buzzone, L. (2001). A new search algorithm for feature selection in hyperspectral remote sensing images*: IEEE Transactions on geoscience and remote sensing*, vol. 39, no. 7, 1360-1367.

Settle J.J., Drake, N.A., (1993). Linear mixing and the estima-tion of ground cover proportions. *International Journal of Remote Sensing*, 14, 1159 – 1177.

Shafri, H.Z.M., Suhaili, A., Mansor, S., 2007. The performance of maximum likeli-hood, spectral angle mapper, neural network and decision tree classifiers in hyperspectral image analysis. *Journal of Computer Science 3*, 419–423.

Sharma, B.D., Clevers, J., De Graaf, R., Chapagain, N.R. (2004). Mapping Equus kiang (Tibetan wild ass) habitat in Surkhang, Upper Mustang, *Nepal Mountain Research and Development*, 24 (2), pp. 149-156.

Shoshany, M. (2000). Satellite remote sensing of natural Mediterranean vegetation: A review within an ecological context. *Progress in Physical Geography, 24* (2), pp. 153-178.

Smith, G. and Milton, E., (1999). The use of empirical line method to calibrate remotely sensed data to reflectance. *International Journal of Remote Sensing, 57*, pp. 194–203.

Smith J.A., Tzeu Lie Lin, Ranson, K.J., 1980. The Lambertian Assumption and Landsat Data. Photogrammetric Eng. and Rem. Sensing, 46(9), pp.1183-1189

Smith, J. H., Wickham, J. D., Stehman, S. V., & Yang, L. (2002). Impacts of patch size and land cover heterogeneity on thematic image classification accuracy. *Photogrammetric Engineering and Remote Sensing, 68*, 65−70.

Smith, J. H., Stehman, S. V., Wickham, J. D., & Yang, L. (2003). Effects of landscape characteristics on land-cover class accuracy. *Remote Sensing of Environment, 84*, 342−349.

Smith, M.-L., Martin, M.E., Plourde, L., Ollinger, S.V. Analysis of hyperspectral data for estimation of temperate forest canopy nitrogen concentration: Comparison between an airborne (AVIRIS) and a spaceborne (Hyperion) sensor(2003) *IEEE Transactions on Geoscience and Remote Sensing, 41* (6 PART I), pp. 1332-1337.

Somers, B., Asner, G.P., (2012). Hyperspectral time series analysis of native and invasive species in Hawaiian rainforests. *Remote Sensing, 4* (9), pp. 2510-2529.

Song, C., Dickinson, M.B., Su, L., Zhang, S., Yaussey, D., (2010). Estimating average tree crown size using spatial information from Ikonos and QuickBird images: Across-sensor and across-site comparisons. *Remote Sensing of Environment, 114* (5), pp. 1099-1107.

Spanos, I.A., Radoglou, K.M. & Raftoyannis, Y. 2001. Site quality effects on post-fire regeneration of *Pinus brutia* forest on a Greek island. *Applied Vegetation Science,* **4**: 229-236.

Spanos, I., (1992). Structure and regeneration of Pinus brutia in Thassos island. PhD Thesis. Aristotle University of Thesssaloniki, Vol.ΛΓ/1990, pp.180. Thessaloniki.

Spanos, I., (1994). Natural regeneration of the Pinus brutia forest in the northwestern Thasos after the fire of 1989, *Geotechnic scientific issue*, 4, 33-39.

Staenz, K., Neville R.A., Clavette, S., Landry, R., White, H.P., (2002). Retrieval of Surface Reflectance from Hyperion Radiance Data. *IEEE Geoscience and remote sensing letters* 2002; 1; 1419-1421.

Stafylakis, T., Papavassiliou, V., Katsouros, V., Carayannis, G., (2008). Robust text-line and word segmentation for handwritten documents images ICASSP, *IEEE International Conference on Acoustics, Speech and Signal Processing - Proceedings*, art. no. 4518379, pp. 3393-3396.

Stavrakoudis, D. G., Galidaki, G. N., Gitas, I. Z., & Theocharis, J. B. (2012). A genetic fuzzy-rule-based classifier for land cover classification from hyperspectral imagery. *IEEE Transactions on Geoscience and Remote Sensing, 50* (1), pp. 130-148.

Stavrakoudis, D.G., Galidaki, G.N., Gitas, I.Z., Theocharis, J.B., (2012). Reducing the complexity of genetic fuzzy classifiers in highly-dimensional classification problems*. International Journal of Computational Intelligence Systems*, 5 (2), pp. 254-275.

Stehman, S. V., Wickham, J. D., Smith, J. H., & Yang, L. (2003). Thematic accuracy of the 1992 National Land-Cover Data (NLCD) for the eastern United States: statistical methodology and regional results. *Remote Sensing of Environment*, 86, 500−516.

Story, M.; Congalton, R.G. 1986. Accuracy assessment: a user's perspective. *Photogrammetric Engineering and Remote Sensing. 52*: 397-399.

Sun, G., Ranson, K.J., Kimes, D.S., Blair, J.B., Kovacs, K., (2008). Forest vertical structure from GLAS: An evaluation using LVIS and SRTM data. *Remote Sensing of Environment, 112 (1*), pp. 107-117.

Thenkabail, P. S., Smith, R. B., & De Pauw, E. (2000). Hyperspectral vegetation indices and their relationships with agricultural crop charac-teristics. *Remote Sensing of Environment, 71*, 158–182.

Thenkabail, P. S., Enclona,E.A., Ashton, M.S., Legg, C., De Dieu, M. J. (2004). Hyperion, IKONOS, ALI, and ETM+ sensors in the study of African rainforests. *Remote Sensing of Environment,*

90 23–43.

Thirgood, J.V., (1981). *Man and the Mediterranean forest*. Academic Press, New York.

Thomlinson, J. R., Bolstad, P. V., & Cohen, W. B. (1999). Coordinating methodologies for scaling landcover classifications from site-specific to global: steps toward validating global map products. *Remote Sensing of Environment*, 70, 16–28.

Tokola, T., Sarkeala, J. and van der Linden,M., (2001). Use of topographic correction in Landsat TM-based forest interpretation in Nepal. *International Journal of Remote Sensing*, 22:551–563

Tomppo, E., Olsson, H., Ståhl, G., Nilsson, M., Hagner, O., Katila, M., (2008). Combining national forest inventory field plots and remote sensing data for forest databases. *Remote Sensing of Environment, Volume 112*, and Issue 5.

Tomppo, E., (1993). Multi-source national forest inventory of Finland, *Proceedings of Ilvessalo Symposium on National Forest Inventories*, Finland, 17–21 August, The Finnish Forest Research Institute, Research Papers, 444:52–60.

Townsend, P. and Foster, J., (2003). Mapping forest composition in the Appalachians using data from EO-1 Hyperion, Landsat, and AVIRIS. Available online at: *http://eo1.gsfc.nasa.gov/new/validationReport/index.html*

Townsend, P.A., Foster, J.R., Chastain Jr., R.A., Currie, W.S., (2003). Application of imaging spectroscopy to mapping canopy nitrogen in the forest of the central Appalachian mountains using hyperion and AVIRIS. *IEEE Transactions on Geoscience and Remote Sensing, 41* (6 PART I), pp. 1347-1354.

Trabaud, L., Campant, C., (1991). Problems of natural recolonisation of the Salzmann pine, Pinus nigra Arn. ssp. salzmannii (Dunal) Franco, after fire. *Biological Conservation* 58, 329–34

Tsai, F., Lin, E.K. and Yoshino, K. (2007). Spectrally segmented principal component analysis of hyperspectral imagery for mapping invasive plant species. International Journal of Remote Sensing, 28: 5, 1023 — 1039.

Tucker, C. J., and Garrett, M. W., (1977). Leaf optical system modeled as a stochastic process. Applied Optics, 16, 1151–1157.

Tucker, C.J., Townsend, J.R.G., and Goff, T.E., (1985). African Land Cover Classification Using Satellite Data. *Science*, 227:369-375.

Turner, W., E.J. Sterling, and A.C. Janetos (eds.). (2001). Special section on contributions of remote sensing to biodiversity conservation: A NASA approach. *Conservation Biology*, 15(4):832-953.

Underwood, E., Ustin, S., & DiPietro, D. (2003). Mapping nonnative plants using hyperspectral

imagery. *Remote Sensing of Environment*, 86(2), 150-161.

Ustin, S. L., & Xiao, Q. F. (2001). Mapping successional boreal forests in interior central alaska. *International Journal of Remote Sensing, 22*(9), 1779-1797.

Ustin, S. L., DiPietro, D., Olmstead, K., Underwood, E., & Scheer, G. J. (2002). Hyperspectral remote sensing for invasive species detection and mapping. *Proceedings of the IEEE International Geoscience and Remote Sensing Symposium* (IGARSS'02), Toronto, Ontario, Canada, Vol. 3 pp. 1658–1660).

Valentini, R., G. Scarascia Mugnozza, E. Giordano and A. Vannini. 1992. Water relations of Mediterranean oaks. Possible influences on their dieback. *Proc. Int. Congr. Recent Advances in Studies on Decline*. Selva di Fasano, Brindisi, pp 439–446.

van Aardt, J.A.N. and Wynne, R.H., 2001, Spectral separability among six southern tree species. *Photogrammetric Engineering & Remote Sensing*, 67, pp. 1367–1375.

van der Werff, H.M.A., van der Meer, F.D., (2008). Shape-based classification of spectrally identical objects. *ISPRS Journal of Photogrammetry and Remote Sensing 63* (2), 251-258.

Van Gestel, T., Suykens, J.A.K., Baestaens, D.-E., Lambrechts, A., Lanckriet, G., Vandaele, B., De Moor, B., Vandewalle, J., (2001). Financial time series prediction using least squares support vector machines within the evidence framework. *IEEE Transactions on Neural Networks*, 12 (4), pp. 809-821.

Vanhuysse, S., Ippoliti, C., Conte, A., Goffredo, M., De Clercq, E., De Pus, C., Gilbert, M., Wolff, E., (2010). Object based classification of SPOT and ASTER data complemented with data derived from MODIS vegetation indices time series in a Mediterranean test site. In (Eds) E.A. Addink and F.M.B. Van Coillie. *The International Archives of the Photogrammetry, Remote Sensing and Spatial Information Sciences*, Vol. XXXVIII-4/C7.

Vapnik, V., and Chervonenkis, A., (1964). A note on one class of perceptrons. *Automation and Remote Control*, 25.

Vapnik, V., and Lerner, A., (1963). Pattern recognition using generalized portrait method. *Automation and Remote Control*, 24, 1963.

V. Vapnik, S. Golowich, and A. Smola. Support vector method for function approximation, regression estimation, and signal processing. In M. Mozer, M. Jordan, and T. Petsche, editors, *Advances in Neural Information Processing Systems* 9, pages 281– 287, Cambridge, MA, 1997. MIT Press.

Vapnik, V., 1995. *The Nature of Statistical Learning Theory*. Springer-Verlag, New York, 188 pp.

Veraverbeke, S., Somers, B., Gitas, I., Katagis, T., Polychronaki, A., Goossens, R., (2012). Spectral mixture analysis to assess post-fire vegetation regeneration using Landsat Thematic Mapper imagery: Accounting for soil brightness variation International. *Journal of Applied Earth*

Observation and Geoinformation, 14 (1), pp. 1-11.

Vieira, I. G., Silva de Almeida, A., Davidson, E. A., Stone, T. A., Reis de Carvalho, C. J., & Guerrero, J. B. (2003). Classifying successional forests using Landsat spectral properties and ecological characteristics in eastern Amazonia. *Remote Sensing of Environment*, 87, 470−481

Vyas, D., Krishnayya, N. S. R., Manjunath, K. R., Ray, S. S., & Panigrahy, S. (2011). Evaluation of classifiers for processing hyperion (EO-1) data of tropical vegetation. *International Journal of Applied Earth Observation and Geoinformation, 13*(2), 228-235.

Walsh, S. J., McCleary, A. L., Mena, C. F., Shao, Y., Tuttle, J. P., González, A., et al. (2008). QuickBird and hyperion data analysis of an invasive plant species in the galapagos islands of ecuador: Implications for control and land use management. *Remote Sensing of Environment, 112*(5), 1927-1941.

Walsh, S. J. (1980). Coniferous tree species mapping using Landsat data. *Remote Sensing of Environment, 9*, 11−26.

Williams, P., Geladi, P., Fox, G., Manley, M., (2009). Maize kernel hardness classification by near infrared (NIR) hyperspectral imaging and multivariate data analysis. *Analytica Chimica Acta*, 653 (2), pp. 121-130.

Wittenberg, L., Malkinson, D., Beeri, O., Halutzy, A., Tesler, N., (2007). Spatial and temporal patterns of vegetation recovery following sequences of forest fires in a Mediterranean landscape, Mt. Carmel Israel Catena, 71 (1), pp. 76-83.

Wolter, P. T., Host, G. E., Mladenoff, D. J., & Crow, T. R. (1995). Improved forest classification in the northern Lake States using multi-temporal Landsat imager. *Photogrammetric Engineering & Remote Sensing, 61*, 1129−1143.

Woolley, J. T. (1971). Reflectance and transmittance of light by leaves. *Plant Physiology, 47*, 656–662.

Wu, J., Peng, D.-L. (2011). Advances in researches on hyperspectral remote sensing forestry information-extracting technology. *Spectroscopy and Spectral Analysis, 31* (9), pp. 2305-2312.

Wulder, M.A.; White, J.C.; Hay, G.J.; Castilla, G., (2008). Towards automated segmentation of forest inventory polygons on high spatial resolution satellite imagery. *The Forestry Chronicle 84*(2): 221-230.

Wulder, M.A., Dechka, J.A., Gillis, M.A., Luther, J.E., Hall, R.J., Beaudoin, A., Franklin, S.E., (2003). Operational mapping of the land cover of the forested area of Canada with Landsat data: *EOSD land cover program Forestry Chronicle, 79* (6), pp. 1075-1083.

Youngentob, K.N., Roberts, D.A., Held, A.A., Dennison, P.E., Jia, X., Lindenmayer, D.B., (2011). Mapping two Eucalyptus subgenera using multiple endmember spectral mixture analysis

and continuum-removed imaging spectrometry data. *Remote Sensing of Environment, 115* (5), pp. 1115-1128.

Yu, S., Berthod, M., and Giraudon, G. (1999). Toward robust analysis of satellite images using map information-Application to urban area detection. *IEEE 7hns. On Geoscience and Remote Sensing, 37*(4):1925-1939.

Zammit, O., Descombes, X., Zerubia, J., (2006). Burnt area mapping using support vector machines. *Forest Ecology and Management*, 234(1 S 240):15.

Zarco-Tejada, P., Miller, J., Harron, J., Hu, B., Noland, T., Goel, N., et al. (2004). Needle chlorophyll estimation through model inversion using hyperspectral data for boreal conifer forest canopies. *Remote Sensing of Environment, 89*, 189−199

Zarco-Tejada, P.J., Miller, J.R., Morales, A., Berjón, A., Agüera, J., (2004). Hyperspectral indices and model simulation for chlorophyll estimation in open-canopy tree crops. *Remote Sensing of Environment, 90* (4), pp. 463-476.

Zhang, C., Xie, Z., (2013). Object-based Vegetation Mapping in the Kissimmee River Watershed Using HyMap Data and Machine Learning Techniques. *Wetlands,* pp. 1-12.